Università
della
Svizzera
italiana

**Faculty
of Economics**

Institute of Finance

*Thesis submitted in partial fulfillment of the requirements
for the degree of*

Doctor of Philosophy in Economics

The Electricity price modelling and derivatives pricing in the Nord Pool market

Author:
Valeria Volpe

Supervisor:
Prof. Giovanni Barone-Adesi

Jury:
Prof. Enrico De Giorgi
Prof. Didier Sornette

Presented and defended publicly
November 27, 2009

"... there is one elementary truth that ignorance of which kills countless ideas and splendid plans: that the moment one definitely commits oneself, then Providence moves too. All sorts of things occur to help one that would never otherwise have occurred. A whole stream of events issues from the decision, raising in one's favor all manner of unforeseen incidents and meetings and material assistance, which no man could have dreamed would have come his way. Whatever you can do, or dream you can do, begin it. Boldness has genius, power, and magic in it. Begin it now."

W. H. Murray

This thesis is dedicated to my parents
for all their support, love and care.

Contents

List of Figures

List of Tables

Acknowledgement

This thesis represents the conclusion of an amazing journey through the knowledge of nance and myself.
It goes without saying that this work has been dependent on the help and support of numerous people: I would like to thank them for all their inputs and aids.
I would like to show my heart-felt gratitude to my supervisor, Professor Giovanni Barone-Adesi, for his encouragement, guidance and support.
BSI Gamma Foundation and the Swiss National Science Foundation are gratefully acknowledged for the funding they provided in support of this work.
Naturally, this research would have not been possible without quality data and I am grateful to the NordPool for assisting and providing me with all their available data.
My endless gratitude goes to my parents that with their love and unyielding support, when things looked bleak, made this all possible.
Finally, I would like to thank the love of my life, Giovanni. His love, endless patience and constant support were invaluable.
Now, it is time for further steps!

Chapter 1

Introduction

1.1 Motivation and structure of the thesis

Since the last decade, the electricity markets are constantly growing in importance all around the world. The shift to competition, from a vertically integrated and monopolistic structure, is still quite recent and in many countries not completed yet. However, looking at the pioneering and old tradition electricity marketplaces, the time series data start to be quite relevant. This, together with the inapplicability of the main results of other well established financial and commodity markets, has enormously stimulated and challenged the research. Many open issues are still present however, and no unanimous consensus has been still achieved in literature.

The main purpose of the following research is the attempt to answer to these open questions. The chosen market to retrieve data from and to test the proposed modelling features, is the Nord Pool, the Scandinavian electricity market, the oldest and largest European deregulated electricity marketplace.

In this first introductory chapter, a general overview of the nature of the electricity as a very special and unique commodity is given together with a more detailed insight of the Nord Pool market.

In the second chapter we deal with the spike feature, which is the crucial and distinguishing aspect we observe in the electricity price time series. Complex to model, spikes have to be first clearly defined and detected. We borrow wavelet methodologies from signal processing and we propose an 'ad hoc 'algorithm to automatically detect the electricity spikes.

In the third chapter we propose a partially parametric regime switching model for

the spot price. Exploiting the spike detection algorithm, we manage to preserve Markovianity.
In the fourth chapter we deal with the American option pricing.
In the fifth chapter we investigate the existence and the nature of the Futures risk premium in the Nord Pool market. This in-depth analysis lead us to observe the inadequacy of the Futures price definition commonly accepted in the financial literature. Hence we propose a new Futures pricing model coherent with the spot price dynamic already described, which takes into account the physical peculiarities of the Scandinavian electricity production system.
Concluding remarks and hints for further research follow in the sixth chapter.

1.2 The electricity in the financial markets

The act of offering electricity to the end-user requires an integrated electricity system constituted by *generation*, *transmission* and *distribution* facilities. Because of the huge amount of fix investments to make the whole system work, the electricity sector was ever since considered a natural monopoly, and so relegated to vertical integrated structure usually owned by the central authority. This held all the generating plants, decided which ones had to operate to meet load requirements and fixed how much consumers had to pay for power and physically distributed the electricity.
In the last twenty years, several deregulation experiences have been carried on worldwide. To allow and ease the entrance of multiple private competitors in the system production, the three main sectors of generation, transmission and distribution, were split. A supporting regulation, which ensures the free admission to the transmission line, completed the creation of a competitive electricity generation market. Whereas before the central planning aimed to match the required load to the total minimum cost of the entire production system, now the individual producers' maximization profit criterion is leading to the competition. In deregulated markets the producers offer specific amount of electricity to the wholesale market at a specific cost per unit; then, an independent system operator equilibrates the aggregate market supply with the total demand, setting a spot price that clears the market. All those who offer to generate electricity at or below the spot price, are partially or fully dispatched and they receive the same spot price for each generated unit.
From a price point of view this transformation process has brought to an extraordinary

increase in volatility, which implies an increase in risk for all the market participants. Hence follows the key role, played by the electricity spot price evolution for every one who deals with the electricity market.
The generating-companies profit equation relies on spot price. In the short run, for instance, they have to make decisions regarding unit commitment: they only want their generators to be dispatched if it is going to be profitable and, as these decisions are often required hours or days in advance, spot price evolution is the starting point. Again, plants need periodic maintenance and in order to determine the minimum impact time, relatively to profit level, to take off-line plants, spot price knowledge is crucial.
Potential investors in new or existing power plants also need to model the spot price evolution to determine their own profitability. Many industries use and pay for electricity as an important input for their operations; their risk management decision cannot preclude from spot price modelling.
Aside from generators, investors and consumers, also the regulatory bodies, require models for the spot price. Due to unavoidable characteristics such as market segmentation and fragmentation because of transmission constraints, electricity markets are subject to the risk of exercising of market power, that is the ability of a firm to offer its generation for sale at a price above its marginal cost, yet still be dispatched. So, these markets need to be scrutinized regarding imperfect competition. Once again, in order to test hypothesis regarding market behaviour, a model that is able to mimic market price accurately is the key requirement.
Last but not least, all the pricing of financial derivatives written on electricity, relays on a good price modelling.
Summing up, the liberalization process has opened the doors of financial markets to electricity, transforming it in a very special traded commodity. Commodity price modelling is not a new area of research. However as it is explained in the sequel, electricity spot price exhibits a range of characteristics that renders the traditional pricing models unsuitable.

1.3 The electricity price features

Before tackling with any kind of modelling ambition we have to clearly understand the nature of this commodity and consequently the implication for its price behaviour.

Non-storability

The crucial aspect of electricity is undoubtedly the fact that it cannot be stored. The main implication is that electricity has to be consumed as soon as it is produced. This is a total novelty in the financial trading markets and the consequences are remarkable. No inventories, no storage, but a hour by hour perfect match of load and generation has to be planned. Here, the complexity of the market organization mechanisms arises too. Among differently generated types of electricity however, some distinction may be outlined. For instance, any unit of water in the reservoirs, is electricity waiting to be generated. Also large availability of a given fuel or a gas storage represent potential electricity. Nevertheless, the limit of the generating capacity and the time required to generate it has to be considered. Further, if a sort of storage, in terms of means to produce, is feasible, this is expensive, logistically complex and moreover not accessible to everyone. A net asymmetry, which is not present in other financial markets, is unavoidable.

All the distinguishing features that will be analysed in the sequel may be seen as consequences of this physical limit.

Multiple prices

If the goods cannot be stored, neither can they be easily transported. So, not only electricity has to be consumed and produced simultaneously, but in order to receive a unit of electricity from a given generator, one has to be connected to the physical distribution grid, otherwise there is no means to receive such unit of electricity exactly from that producer. Hence a MWh delivered in France is physically the same MWh delivered in Finland, or in California, but their prices are not expected to be equal; they are different prices for what are actually different goods, as no arbitrage, in space, can be performed. Therefore, there are several geographical regions between which moving electricity is either physically impossible or non-economical when feasible. This is a unique feature of the electricity, not shared with other financial markets nor other commodity market: an ounce of gold, regardless market frictions, has essentially the same price wherever. Not surprisingly, substantial price differences in electricity prices are observed in different regions. Electricity is a localized market.

Spikes

One of the most pronounced features of electricity markets are the abrupt and generally unanticipated extreme changes in the spot prices known as spikes. Within a very short period of time, the price can increase substantially and then drop back to

the previous level. Regulation however, plays a major role as, for instance, spikes are almost absent in UK and in Italy as well.

The spiky nature of spot prices is once again an effect of non-storability of electricity. Electricity to be delivered at a specific hour cannot be substituted for electricity available shortly after or before. As currently there is no efficient technology (at a reasonable price) for storing vast amounts of power, it has to be consumed at the same time as it is produced. Hence spikes frequently occur during high consumption periods of the year and, in between these, during on-peak hours of business days. Extreme load fluctuations indeed, caused by severe weather conditions often in combination with generation outages or transmission failures, can easily lead to price spikes. However, they are usually quite short-lived, and as soon as the weather phenomenon or outage is over, prices fall back to a normal level. These temporary price escalations account for a large part of the total variation of spot prices changes, driving the price series volatility to extraordinary high level with respect to other commodity and financial markets. Tremendous are the implications in terms of risk burden: firms that are not prepared to manage the risk arising from price spikes can see their earnings for the whole year evaporate in a few hours. There are also cases of power companies having to file for bankruptcy after having underestimated the risks related to price spikes. A textbook example is the bankruptcy of the Power Company of America, a well established power-trading company, in 1998. So, despite their rarity, price spikes are the very reason for designing insurance protection against electricity price movements.

Obviously, the increase in the horizon at which the price data are aggregated, may easily smooth away the spikes. For weekly or monthly averages, the effects of price spikes are less and less apparent and eventually neutralized. One should refrain to follow these easy shortcut, as the smoothing is just apparent, due to the 'convenient' representation of the time series. Neither a producer, nor an investor, nor a consumer and not even a speculator, who really operate in the electricity markets, may profit of this 'smoothing'. Only derivatives instruments conveniently written on electricity price may offer a sort of smoothing, but their pricing once again have to refer to the spiked price series to be reliable.

Inelastic demand

Customers reaction to pricing signals, or stated differently, 'demand response ' is an economic-financial standard. Efficiency in markets increases when customers can ad-

equately react to price changes that result from resource scarcity and market power. The liberalization process has gone in this direction increasing the competition. However the essential nature of the electricity for our society, makes almost inelastic its demand curve. This, in conjunction with the other aforementioned reasons, may be seen as another cause to spikes formation. Put it differently, if the demand for electricity were highly elastic, in presence of shortages and congestion grid for instance, when the price quickly rises, no one would accept such a price, preferring to wait. But basically no one can refrain from consuming electricity on a short notice: everything in everyday life works with electricity; business activity, factories cannot stop working just to wait for a better price, as the economic cost to stop the production is extremely high, hence whatever price is accepted in the short run. This inelastic demand is not so common to other financial activities and cooperate to make electricity a very special commodity.

Negative Prices

Even if rarely observed, negative price cannot be excluded. Once again this possibility is closely related to the nature of the electricity and is also particulary sensible to the kind of generated electricity. Some generators have high start-up and shut-down costs, and are slow to rump up. This is the case of coal-fuelled, natural gas steam turbine or nuclear plants, for instance. Therefore in order to ensure to be dispatched in peak periods, taking advantage of high spot prices, they must also ensure to generate in off-peak periods. If there is enough competition among producers to be dispatched, it can be economically rational to offer negative prices. So, when energy load is very low or near zero, negative prices can truly result with consumers (at least at the wholesale level) that are getting paid for using power, and the more power consumers use the more they get paid.

Just to refer to a real market, in the first half of 2008, prices at ERCOT[1] market were below zero nearly 20% of the time; during March, when negative prices were most frequent, the 33% of the time. After mostly taking the summer off, negative power prices were back to near 10% in October. The Texas case is reported also because it offers the witness of how negative prices may arise also for different and new reasons each time. The Texas negative prices indeed, appear to be the result of the large installed capacity of wind generation. Wind generators face very small costs of shutting down and starting back up, but they do face another cost when shutting

[1]The Electric Reliability Council of Texas

down: loss of the Production Tax Credit and state Renewable Energy Credit revenue which depend upon generator output. It is economically rational for wind power producers to operate as long as the subsidy exceeds their operating costs plus the negative price they have to pay the market. Even if the market value of the power is zero or negative, the subsidies encourage wind power producers to keep churning the megawatts out.

Price-dependent volatility

It has just been stressed how extremely volatile is the price series in the electricity markets. But we can go a bit further observing how the volatility itself vary throughout the price series. In most financial markets, a decrease in the price of an asset leads to an increase in the volatility of the asset's price, which is referred to as the 'leverage effect' (Black 1976) . However the opposite occurs in the electricity market due to the convexity of the supply stack function. This curve is almost flat for low levels of load, but steeper as more expensive generating capacity is offered. When load is low, and the market clears at low prices, small fluctuations in demand level, are unlikely to change the price significantly, as the offer curve is virtually flat for low demand. On the contrary, as the demand increases, the marginal cost of an extra unit of electricity becomes more and more expensive to generate; mathematically the convexity at that point (the intersection of offer and demand) becomes more and more pronounced. Consequently a small shift in demand leads to a bigger variation in price, hence an increase in volatility, with respect to an equal load variation in the left part of the supply stack function.

This market structure leads to prices which are naturally more volatile for higher prices ('inverse leverage effect'), leading to clustering volatility effects for high demand levels.

Regardless of hypothetical market power, in a competitive market, the critical level where the convexity of the supply stack function starts to become pronounced is strictly related to the structural design of the different source of electricity generation.

Seasonality

Spot prices time series, are likely to exhibit strong seasonality, on account of both supply and demand displaying periodicity. Patterns can be distinguished over three different length of time: intra-day and intra-week, mainly lead by demand needs, and annual patterns driven both from demand and supply. Intra-day pattern has a clear morning peak, when people turning on heating, showering and cooking breakfast; a

higher general level is then reached during the day on account of commercial activity increasing needs, and an evening peak occurs when people dine and use appliances. On weekend the required load collapses dramatically, mainly because of the closure of most of the business activities. Load also varies according to the period of the year. This annual pattern is strictly correlated with climatic variations, which may both influence the demand behaviour and the capability generation of the producers that may be extremely sensible to the type of electricity produced (especially green energy is highly subjected to weather variations). In Europe the demand rises in winter, when electricity is required for heating; in the American countries instead, as well as in the north of Australia, the yearly peak is reached in summer due to the extraordinary high air conditioning usage. Especially in North American countries, as well as in some Asian countries, a second peak during severe winters is also displayed.

Mean reversion

Price mean-reversion, widely tested on a general commodity market base, is present in the electricity market too. Regardless the market specific seasonal patterns, we commonly observe price fluctuations throughout the years, which sooner or later revert back to such a seasonal structural pattern, a kind of hidden non liner trend. In competitive markets the underlying level, which represent an ideal long-term mean, is supposed to be determined by the marginal cost of generation. However, factors such as transmission and plant outages cause prices to fluctuate away from the mean level. Nevertheless, as the transmission constraints and generation outages are short term effects, once expired, the price level is expected to revert to its structural trend.

1.4 The Nord Pool market

The outline

In the present research we analyse the Nord Pool electricity market. Nord Pool ASA is the Nordic Power Exchange, recognized as the world's only multinational electric power exchange and one of the oldest European deregulated market. Designed to serve 24-million-customer system, the Nordic region comprises Norway, Sweden, Finland, Denmark and Iceland (although, as an island, Iceland must be treated as a separate part of the Nordic market-integration effort). Even if small in terms of population, the Nordic countries have a quite high per capita level of consumption, especially in Norway and Sweden. Thus in 2005 the total consumption of electricity was 402

TWh. This is less than the corresponding for Germany (545 TWh) and France (451 TWh), but greater to the consumption in UK (348 TWh) and considerably more than the consumption of electricity in Italy (307 TWh) and Spain (243 TWh). In other words the Nordic electricity market is both one of the major electricity markets in Europe in absolute terms as well as the biggest in terms of per capita consumption, which spans from the 28 MWh of Norway to the 7 MWh of Denmark, with an outstanding average of the entire region of 16 MWh per capita a year; these data may be compared with the about 7 MWh per capita of Germany and France, 6 MWh of United Kingdom and Spain and the 5.7 MWh of Italy. Further, Nord Pool is also one of the oldest and pioneering electricity market. A power exchange had been in operation in Norway since 1971, but the only exchange participants were power generators. It was Norway to pave the way to the liberalization and the integration of the electric power market with its adoption in 1991 of the Energy Act. This low introduced competition as the chosen mechanism to deliver a reliable, efficient electricity supply. The legislative intent was both to reduce electric power prices for consumers and businesses and to remove the price-setting from the hands of municipal councils. The initial beneficiaries were the heavy industry and other businesses, later a little residential-market was open to competition; finally a market fully opened to households, where customers could change power supplier without incurring any charges, was the target. In order to guarantee the access to the grid line, the Act imposed that authorities require network owners to make transmission capacity available to others under third-party agreements (TPAs) and to offer equal (non-discriminatory) tariffs to electricity suppliers and end users.

The Nord Pool ElSpot market was established in 1992. Sweden joined this market 1996, Finland in June 1998, Western Denmark in July 1999, and Eastern Denmark in October 2000. It is owned by the two national grid companies, Statnett SF in Norway (50%) and Affrsverket Svenska Kraftnt in Sweden (50%). Nord Pool influence spreads up to Germany, with its 35% ownership of Leipzig Power Exchange (LPX), which has merged with EEX in 2002, showing clear evidence of the Nord Pool plans for foreign expansion. Furthermore Powernext, the French electricity exchange, has also chosen Nord Pool knowhow and has signed a licence agreement for the Nordic system and technical services.

Strict regulation of the network service ensures that third-party access works. But the market is largely assumed to be able to take care of itself under the supervision

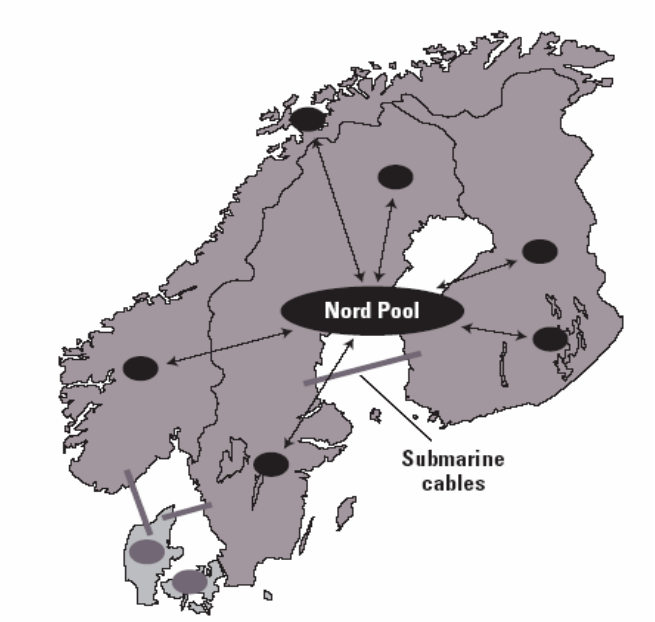

Figure 1.1: Finnish, Norwegian, and Swedish players trade on equal terms (Black bullets). From outside the free trade area Danish participants trade on special terms (gray bullets).

of national competition authorities. This approach differs from that adopted for instance, in England and Wales, another old electricity European market, where the pool is heavily regulated. Because the Nordic countries already had a large number of players, the reform was easier to implement. The spot market operated by Nord Pool is working well so far and it is one of the most stable. In contrast to the English and Welsh pool, where only the producers can participate in the bidding, the Nordic pool is a market for both sellers and buyers. Another difference is that the generators in the Nordic system are not obligated to offer their power to the pool. So, to keep business from going elsewhere, the pool must ensure that it is an attractive marketplace.

Nord Pool plays a complementary role to the grid owners and the transmission system operators (TSOs) of the four countries. The grid owners are monopolies responsible for building and maintaining the grid in their own local area, setting grid transmission tariffs, connecting customers, metering and topping up energy lost in the system. The TSOs are responsible for system balancing in real time and financial settlements, subject to overriding quality, reliability and safety criteria. The regulators, which have different powers in each country, ensure that an equitable, efficient and level playing field is achieved, with reduced costs to the consumer.

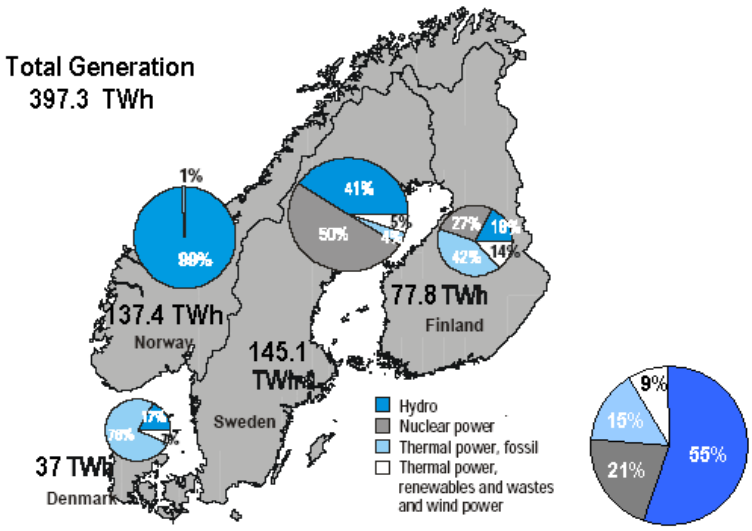

Figure 1.2: Electricity generation in Nordic countries 2007

Power generation is mixed: Denmark uses $85-90\%$ fossil fuel-based generation and $10-15\%$ wind power. Norway has nearly 100% hydropower production. Sweden and Finland rely on a mix of hydropower, nuclear power, and conventional thermal generation. The overall electricity generation in the region is 'green' in comparison with other developed economies, with Norwegian hydro-electric power providing almost a third of the region capacity.

Hence, the Nord Pool's role is to: market a price reference point, operate the spot and financial markets, provide counterpart security and a market mechanism to tackle with grid bottlenecks, record and report power deliveries for each TSO.

The traded contracts

Broadly speaking, the Nord Pool market may be divided into a physical market, which operates trough Elspot and Elbas platforms in order to determine the one-hour contracts spot price, and a separate financial market for derivatives trading. This market segmentation finds its counterpart in the Nord Pool group division. There is indeed the Nord Pool Spot AS, running the physical delivery spot markets; Nord Pool ASA, running the financial market; and Nord Pool Clearing ASA, running the power contract clearing services. Nord Pool Clearing, clears all contracts traded on the Nordic Power Exchange.

The physical-delivery spot market consists of two branches: the one day ahead spot

market, Elspot, and a continuous balancing spot market, Elbas. On Elspot, hourly power contracts are traded daily for physical delivery in the next day's 24-hour period. The price calculation is based on the balance between bids and offers from all market participants. Bids for the following day, split into hourly segments, are submitted by noon on the previous day. Bids and offers are aggregated into supply and demand curves and the intersection of the two, neglecting grid congestion, determines the market clearing price or the so called System Price. To be precise indeed, the total geographic market is divided into bidding areas; these may generate separate price areas if the contractual flow of power between bid areas exceeds the capacity allocated for Elspot contracts by the transmission system operators. When such grid congestion develops, two or more area prices are created. So, the Elspot market's system price, also denoted as 'the unconstrained market clearing price ', is the price that balances sale and purchase in the exchange area while not considering any transmission constraints. When there are actually no constraints between the bidding areas, the area prices are all equal to the system price.
The day-ahead Elspot market operates in competition with the over-the-counter (OTC) bilateral unregulated market, even if the System Price has become a reference point for the OTC trade as well. Nord Pool estimates that 25% of Nordic power generation is traded through Elspot, which uses an auction system.
Elbas instead, is the Nord Pool component that allows for real time trading. It works as an aftermarket to Elspot, giving backup in case actual demand differs from its expected value. The Elbas market provides continuous power trading 24 hours a day, 7 days a week covering individual hours, up to one hour prior to delivery. The traded products are one-hour long power contracts [2]. .

At present, the contract types traded at Nord Pool Financial Market comprise of power derivatives, European Union Allowance (EUA) and Certified Emission Reduction (CER) contracts. The derivatives are base- and peak-load futures and forwards, options, and Contracts for Difference. They are all cash-settled throughout the trading and/or the delivery period, starting at the due date of each contract (depending on whether the product is a future or a forward). Hence, there is no physical delivery of financial market power contracts with the exception of the EUAs and the CERs. Different lengths such as days, weeks, months, quarters and years are offered with

[2]Throughout the rest of this work, we will use however a daily time step since the finest time scale available for all the data is the daily one.

a maximum trading time horizon of currently five years. The reference price is the System Price of the total Nordic power market.

Let us briefly go trough the main specifications of the available power derivatives.

Futures are among the first derivatives to be introduced for trading in 1995 in the Nord Pool financial markets. They are currently listed as base-load day and week contracts. Their settlement procedure involves both a daily mark-to-market settlement and a final spot reference cash settlement, once the contract has reached its due date. Mark-to-market settlement covers gains and losses from day to day changes in the market price of each contract. The final settlement instead, which begins at maturity, covers the difference between the final closing price of the futures contract and the System Price in the delivery period.

For longer time horizon, Forward base load contracts are listed for each calendar Month, Quarter and Year. They are subject to a splitting procedure for trading: Year contracts are split into Quarter contracts, Quarters are split into month contracts and Month contracts are listed on a 6 month continuous rolling basis, and are not subject to any further splitting. The reference price for the Nordic Forward contract is the Nord Pool Spot System Price, as it is for the Futures. Apart from the different time horizon, the main difference, with respect to Futures contracts regards the settlement mechanism. In the trading period prior to the due date for forward products, there is no mark-to-market settlement. The mark-to-market amount is cumulated as daily loss or profit, but not realised, along the trading period. It is throughout the delivery period instead, starting at the due date, that cash is required in the Clearing Members pledged or non-pledged cash accounts, and that the settlement is carried out. The non-pledged cash account must be supported by a bank guarantee.

The option contracts at Nord Pool are European-style. The underlying contracts are quarters and year forwards. Nord Pool lists for trading the nearest 2 Quarters and 2 Years respectively available for trading up to 6 months and 2 years in advance. Asian-style options were issued in the past, but without success.

Another power derivative which is strictly peculiar to the electricity market, is the Contract for Difference (CfD). It is been pointed out how different area prices may arise because of physical constraints in the transmission grid. As actual physical-delivery purchase costs are determined by actual area prices, a specific price risk is present. A perfect hedge using forward or futures instruments is possible only in situations when there is no transmission grid congestion in the market area, that is,

area prices are equal to the System Price.

CfDs allow Exchange Members, Clearing Members or whoever is exposed to potential difference in area price, to hedge against this basis risk.

A CfD is a forward contract with reference to the difference between the Area Price and the Nord Pool Spot System Price. The market price of a CfD during the trading period reflects the markets prediction of the price difference during the delivery period. The market price of a CfD can be positive, negative or zero. CfDs trade at positive prices when the market expects a specific area price to be higher than the System Price, (that is, the selected market area is in a net import situation). CfDs will trade at negative prices if the market anticipates an area price below the System Price (the market area is in a net export situation). They were first introduced in 2000.

In recent times new products have been introduced: the 'green 'certificates. The EUAs and CERs are both forward contracts with physical delivery and Nord Pool was the first exchange to list such contracts. In February 2005, Nord Pool launched physical forward contracts for EUAs. The EU Emission Trading Scheme is the main policy being introduced across Europe to handle emissions of carbon dioxide and other greenhouse gases, in order to counter the threat of climate change. Nord Pool also has a EUA Spot product which started in October 2005. In June 2007 Nord Pool launched a standardised Certified Emission Reduction (CER) contract, which is an emission credit obtained through the clean development mechanism, implemented by the United Nations. The recipient has achieved a reduction corresponding to one tonne of carbon dioxide or carbon equivalent greenhouse gas in a developing country. The contract is designed in accordance with the requirements of the European Union Emission Trading Scheme (EU ETS) directives. Hence it enables European companies to comply with such requirements and governments to fulfil their obligations under the Kyoto protocol. To date Nord Pool offers both products up to year 2012, covering the entire Kyoto Period.

The traded volume at Nord Pools financial market has increased considerably since the first products were launched and at in the 2007 the record of 1060 TWh of total turnover was reached with a net increase of 38% with respect to the previous year.

Spot Price statistics

We conclude this overview of the of the Nord Pool market and of the electricity features with a roughly statistical description of the spot price time series in the Nord Pool. In figure (1.3) the daily System Price for the entire Nordic area is plotted

from 1992 to 2005. Spikes, mean reversion and seasonality may be immediately perceived. In the following chapters we will deal with the modelling conundrums of these features and in particular with the fitting of the price time series.

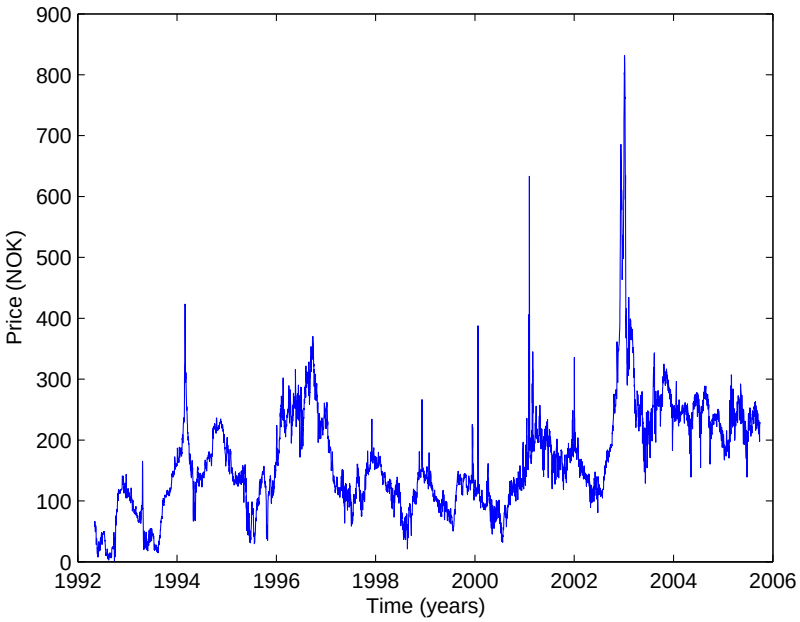

Figure 1.3: Arithmetic average of hourly System Price in the Nord Pool market from the 4_{th} of May 1992 to the 29_{th} of September 2005 at daily resolution.

In table (1.1) the main descriptive statistics are reported for the whole sample of observations and for individual subsamples of one year length. Our first result is the high value of the moments of the price distribution. High volatility is not a surprise, but the main characterization of the market and even looking at small subsamples, extraordinary high values are reported at several order of magnitude greater than any other financial asset or commodity. A special mention goes to the 2002-2003 period during which a big drought caused turbulent price variations with record levels of price and volatility. The skewness values witness a right asymmetry for the price distribution that is, the right tail is longer: the mass of the distribution is concentrated on the left of the figure with few relatively high values (namely the positive spikes), hence the mean is larger than the median. It is however worth mentioning that such an asymmetry does not seem to be so characteristic as among the several observed years, we shift from positive to negative skew. The interpretation is straightforward.

We are used to talk about electricity as characterized from large and more or less, rare positive spikes (which lead to a positive skewness in the price distribution), however negative spikes also occur and their predominance over a sample induces left-skew distribution. If we look closer figure (1.3) in correspondence of years 1995, 1998, 2004 and 2005 we can clearly observe the presence of negative spikes. Anyway the price distribution, whatever results to be more right- or left-skewed, is leptokurtic. The whole observed sample denotes a huge kurtosis, definitely higher than the normal distribution (which has a value of 3). This means that the distribution is fat-tailed and extreme values have higher chance with respect to the bell-shape distribution. However, even for the kurtosis we can observe wide variation through the subsamples. Similar results are obtained also for the relative price increments as reported in table (1.2).

Period	Obs	Min	Mean	Max	Std	Skewness	Kurtosis
1992-2006	4897	1,48	166,31	831,41	87,51	1,54	10
1992	242	1,48	58,09	143,60	44,01	0,512	1,698
1993	365	14,80	80,26	172,36	40,72	0,182	2,077
1994	365	66,64	182,65	423,38	48,87	1,037	6,627
1995	365	29,73	117,67	204,28	38,13	-0,564	2,742
1996	366	157,73	253,63	370,02	41,65	0,335	3,073
1997	365	58,21	134,99	261,79	38,19	0,870	4,065
1998	365	21,27	116,35	266,46	35,59	-0,275	3,219
1999	365	50,43	112,11	225,55	27,38	0,133	3,464
2000	366	31,85	103,33	387,78	32,10	1,819	18,828
2001	365	119,07	186,50	633,36	39,95	4,811	48,486
2002	365	80,65	201,02	685,63	122,20	2,189	7,367
2003	365	128,91	290,60	831,41	103,39	3,166	15,265
2004	366	139,25	242,05	296,11	22,63	-0,790	4,849
2005	272	139,20	228,11	306,96	28,01	-0,266	3,035

Table 1.1: Descriptive statistics for daily System Price in the Nord Pool market from 1992 to 2005

Period	Obs	Min	Mean	Max	Std	Skewness	Kurtosis
1992-2006	4896	-0,94	0,01	11,20	0,21	32,33	1633
(1992-2006)*	4896	-0,94	0,01	3,00	0,14	6,99	121,2489
1992	241	-0,94	0,09	11,20	0,81	11,255	151,350
1993	364	-0,49	0,01	0,90	0,14	1,821	13,541
1994	364	-0,29	0,00	0,77	0,07	4,300	49,044
1995	364	-0,45	0,01	1,02	0,13	2,314	18,092
1996	365	-0,19	0,00	0,35	0,06	1,146	8,283
1997	364	-0,24	0,00	0,69	0,10	2,050	13,836
1998	364	-0,51	0,01	0,74	0,13	1,962	12,958
1999	364	-0,31	0,00	0,73	0,08	2,534	23,320
2000	365	-0,51	0,01	2,17	0,18	5,803	66,127
2001	364	-0,54	0,01	2,29	0,18	6,672	81,257
2002	364	-0,29	0,01	0,82	0,09	3,202	26,659
2003	364	-0,22	0,00	0,69	0,09	2,351	17,285
2004	365	-0,29	0,00	0,58	0,07	3,249	33,387
2005	271	-0,24	0,00	0,38	0,08	1,263	7,602

Table 1.2: Descriptive statistics for daily relative increments of the System Price in the Nord Pool market from 1992 to 2005. * One extreme observation, corresponding to a variation of 1120%, has been removed.

Chapter 2

Spike detection

One of the main features of the electricity market is the presence of spikes: the sudden explosion and an as well sudden consequent burst in the price level (positive jump 'immediately' followed by a negative one).
Our purpose is to exactly define when a spike occurs. If we roughly look at a whatever price time series of a whatever electricity market, we may feel quite confident to localize simply by sight where a spike has taken place and in most of the cases this identification is quite obvious. Anyway, looking more carefully, we will encounter several non trivial and confusing situations and, moreover, this manual detection results to be too far from any scientific methodology and any kind of objectiveness, being extremely observer dependent.
We would like to derive a methodology, as much as possible objective, that can be automatically implemented, totally non parametric and model independent; we intend to avoid any kind of consideration about the generating process of the prices and of the spikes themselves.
Let us consider the price time series as a generic and unknown function $f(x)$, in other words a signal evolving through time of which we want to exactly identify the time location of spikes. It is a matter of fact that any spike may be thought as *a sequence of singularities*. This quite obvious observation suggests we have to deal with singularities detection. In achieving this task we borrow the well established techniques developed in the signal processing field. In particular we will make use of wavelet transforms. The use of this framework in financial time series analysis is not new. However its use has been so far focused on other issues such as price forecasting and time series denoising [see, e.g., Conejo et al.(2005)] and outlier detection [see,

e.g., Struzik and Siebes (2002)].
The idea of identifying spike like a sequence of singularities is of course, far from being complete; it is a necessary and not a sufficient condition, that simply enlightens a possible way to follow.
Now, before explaining the suggested algorithm for spike detection, we briefly outline the mathematical concept of singularity and we introduce the non familiar reader to wavelets as a tool for singularity detection. The reader, already acquainted with the *wavelet transform modula maxima* technique, may safely jump to the spike detection algorithm, described in section 2.4.

2.1 Singularities

Singularities, irregular structures and points of sharp variations often carry the most important information about a signal. A singularity can be defined as a point where the derivative of a given function of a complex variable does not exist, but every neighbourhood contains points for which the derivative exists. A function is singular when it contains a singular point and this results in a breakdown of the Taylor series: the function contains an edge, a point of rapid variation.
In mathematics, singularities are generally characterized by their Lipschitz / Hölder exponents. To be precise the Lipschitz attribute is used to defined the regularity of functions in terms of an integer, whereas the Hölder exponent refers to non-integer values, even though they are sometimes used as synonymous. The formal definition follows:

Definition 1 ***Regularity***. *A function f is pointwise Lipschitz (local Hölder) $\alpha \geq 0$ at ν if there exist $K > 0$ and a polynomial P_ν of degree $m = \lfloor \alpha \rfloor$, where $\lfloor \alpha \rfloor$ is defined as the largest integer less than or equal to α, such that*

$$\forall x \in \mathbb{R}, |f(x) - P_\nu(x)| \leq K|x - \nu|^\alpha.$$

A function f is uniformly Lipschitz (global Hölder) α over an interval $[a, b]$ if it satisfies the pointwise condition $\forall \nu \in [a, b]$, with a constant K that is independent of ν.

The Lipschitz (Hölder) regularity of f at ν or over the interval $[a, b]$, is the sup *of the α such that f is Lipschitz (Hölder) α.*

The above definition refers only to functions; the formal extension of Hölder regularity to tempered distributions[1] is not straightforward.
As a first step, we extend the concept of global Hölder regularity.

Definition 2 *Let $f(x)$ be a tempered distribution on an interval (a, b). The distribution $f(x)$ is said to have a global Hölder exponent α on (a, b) if and only if its primitive has a global Hölder exponent $\alpha + 1$ on (a, b).*

This apparently arbitrary definition is inherited from an equivalent rule which applies to functions. Indeed, in the function realm, it has been proven that the Hölder regularity is increased by one consequently to integration operation. With this definition of Hölder regularity, it is clear that a tempered distribution may have a negative α. The same definition can be used to characterize discontinuous and not-differentiable functions, which, thus, can also exhibit negative α. However, it is possible to show that values of α less than -1 are only found in distributions.
To get an equivalent extension for the local Hölder exponent is not trivial and, a sophisticated theory proposed by Bony (1983), Meyer (1989) and Jaffard (1991), called *2-microlocalization*, is needed for the purpose. Without going into details (we refer for the interested readers to the afore mentioned literature) we report the alternative definition for isolated singularities.

Definition 3 *A distribution $f(x)$ is said to have an isolated singularity with Hölder exponent α at x_0, if and only if $f(x)$ is global Hölder α over an interval (a, b), with $x_0 \in (a, b)$ and if $f(x)$ is global Hölder (uniformly Lipschitz) 1 over any subinterval (a, b) that does not include x_0.*

Briefly summarizing, $\alpha \geq 1$ denotes a continuous and differentiable function; $0 < \alpha < 1$ represents the continuous but non-differentiable case; $-1 < \alpha \leq 0$ is valid for discontinuous and non-differentiable functions and finally for $\alpha \leq -1$ we are dealing with tempered distribution, like the Dirac one.

A classical tool to measure the regularity of a function is to look at the asymptotic decay of its Fourier transform. A function f results to be bounded and globally Hölder α over $\mathbb{R}$ if

[1]Distributions are generalizations of functions. Intuitively whereas in a function one defines the punctual value, in a distribution only the local average has a well defined value. In a similar fashion, slow-growing locally-integrable functions can be generalized to tempered distributions. A remarkable property of tempered distributions is that they all admit a Fourier transform. For a more rigorous treatment refer to functional analysis and distribution theory.

$$\int_{-\infty}^{+\infty} |\hat{f}(x)|(1+|\omega|^{\alpha})d\omega < +\infty \tag{2.1}$$

where we define $\hat{f}$ to be the Fourier transform of a function f.
In so doing we can obtain a global regularity condition or to be precise, the minimum global regularity of functions, no more, as we can see from (2.1), the decay of $|\hat{f}(x)|$ depends on the worst singular behaviour of f; we cannot derive whether the function is locally more regular at a particular point. This is due to the fact that the Fourier transform unlocalises the information around the spatial variable, shifting the transformed information in a frequency-amplitude plane; so or there is not any localization purpose or, the signal is completely stationary, carrying the same frequency content along the entire observed signal. This is obviously not informative.
On the other hand, as we will show formally in the following section, wavelets seem to be the natural choice because of their ability to provide a localized information of the frequency content of the function $f(x)$.

2.2 Continuous Wavelet Transform

Continuous wavelets theory finds a huge space in the literature and they are the main choice of this thesis too. Obviously when we go down to the calculus, we work with finite number of convolutions, with discrete signals and sampling intervals; but it is a matter of fact that in discrete theory everything becomes more complicated, sometimes untractable and many nice properties and features are lost. Just to quote a few examples, in $\mathbf{L}^2(\mathbb{R})$ a wavelet basis, as we will see below, is constructed by dilating and translating a single function, whereas dilations are not even defined over a discrete sequence; several important theorems relate the amplitude of wavelet coefficients to the local regularity of the signal f. The regularity of a discrete sequence is not well defined either, which leads to interpretation problems for the amplitude coefficients themselves. The theory of continuous time functions gives asymptotic results for discrete sequences with sampling intervals decreasing to zero, precise enough to understand the behaviour of discrete algorithm. Of course, the transition between continuous and discrete signals must be done with great care; this discretization is obtained by means of a fast numerical algorithm over finite signals.

Let $\psi(x)$ be a complex valued function. The function $\psi(x)$ is said to be a wavelet if

and only if its Fourier transform $\hat{\psi}(\omega)$ satisfies

$$\int_{-\infty}^{+\infty} \frac{|\hat{\psi}(\omega)|^2}{\omega}\, d\omega < +\infty. \tag{2.2}$$

The condition (2.2) is called the *admissibility condition* and implies that we will work with functions spanning in $\mathbf{L}^2(\mathbb{R})$ space. A sufficient condition to guarantee that this integral is finite, is that $\hat{\psi}(\omega)$ has to be continuously differentiable and has to be ensured that $\hat{\psi}(0) = 0$; this last requirement straightforward implies another property: a wavelet is a function with zero mean

$$\int_{-\infty}^{+\infty} \psi(x)dx = 0. \tag{2.3}$$

It is normalized $\|\psi(x)\| = 1$, and centered in the neighbourhood of $x = 0$. A whole family of space-scale components is obtained by scaling the function $\psi(x)$ by s and translating by u, respectively the scale and the position parameter.

$$\psi_{s,u}(x) = \frac{1}{s}\psi\left(\frac{x-u}{s}\right). \tag{2.4}$$

All these components remain normalized as well: $\|\psi_{s,u}(x)\| = 1$. As all these functions, with different region of support, are obtained from one main function, $\psi(x)$ is called *the mother wavelet*, to stress its generating property.
The wavelet transform of a real value function f, is defined as the convolution product of the scaled and translated kernel ψ with f,

$$Wf(s,u) = \frac{1}{s}\int_{\Re} f(x)\psi\left(\frac{x-u}{s}\right) dx \tag{2.5}$$

or more compactly

$$Wf(s,u) = f \star \bar{\psi}_s(u) \qquad \text{where} \qquad \bar{\psi}_s(y) = \frac{1}{s}\psi(\frac{-y}{s}).$$

In (2.5) the scale parameter appears at the denominator and therefore the resulting multiplicative factor, has to be read in terms of frequency. Low frequencies (high scales) correspond to a global information of the signal, a non-detailed view that may span the entire signal; whereas high frequencies (low scales) correspond to a detailed information of an otherwise hidden pattern, that usually lasts a relatively short time

(like spikes).

The definition of wavelet transform in terms of a convolution, suggests that the wavelet analysis is a measure of similarity between the basis functions (wavelets) and the signal itself; here the similarity has to be intended in the sense of the frequency content. The calculated coefficients refer to the closeness of the signal to the wavelet at the resolution given by the scale parameter and in a neighbourhood of the position parameter.

The transformed signal in (2.5) is a function of scale and spatial position and this is the reason why we are used to refer to the scale-space (or equivalently frequency-time) plane generated by a wavelet transform. From now onwards we will refer to a wavelet transform indistinguishably as a scale-space or a frequency-time representation of a given signal, depending on which aspect we prefer to stress; as already underlined, if the frequency is the inverse of the scale parameter, the location parameter may be interchangeably interpreted as location in space or in time domain.

Any function $F(s,u)$ turns out to be the wavelet transform of some function $f(x)$ if and only if satisfies the *reproducing kernel equation*

$$F(s_0,u_0) = \int_0^{+\infty}\int_{-\infty}^{+\infty} F(s,u)K(s_0,s,u_0,x)duds \tag{2.6}$$

with

$$K(s_0,s,u_0,u) = \int_{-\infty}^{+\infty} \psi_s(x-u)\psi_{s_0}(u_0-x)dx. \tag{2.7}$$

Therefore a wavelet transform is intrinsically redundant, as it is directly expressed by the reproducing kernel itself (2.7), which measures the correlation of the two wavelets ψ_s and ψ_{s_0} or, loosely speaking, the degree of redundance between the value of the wavelet transform at (s,u) and at (s_0,u_0).

Henceforth, if we think that wavelet transform is a two dimensional representation of a one dimensional signal, it may result obvious the existence of some redundancy, reducible and even removable by sub-sampling the parameters of these transform; this would be equivalent to building a basis in signal space.

Hence, wavelets analysis acts as a mathematical microscope which allows to zoom in the fine structure of a signal; the usage of different time-frequency components of the chosen wavelet family, enables to analyse signal structures of very different sizes. To be more precise, we are referring to the resolution properties of the wavelet transform, and exactly to the contextual time and frequency resolution.

Since the Fourier transform is not suitable at all to localize different frequency contents, a very popular solution to overcome this limitation is to apply the Short Therm Fourier Transform (STFT)[2]. This methods enables to keep track of both the position and the frequency. The wavelet transform however, goes really further ahead, adding a lot of flexibility which we cannot obtain by mere STFT application. Let us try to give some intuition. The bottom line is essentially how differently the time-frequency domain is partitioned by the two methods under analysis. A visual representation of such domain may help to get a straightforward understanding. The usual box representation of the time-frequency plane will perfectly fit.

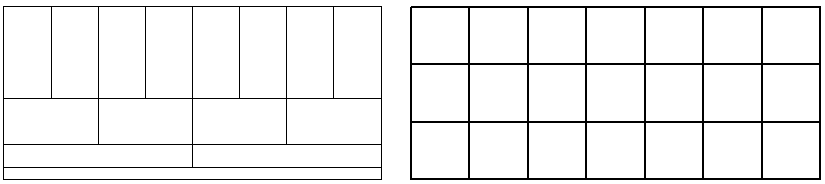

Figure 2.1: Time-frequency plane structure: a typical example for wavelet transform (left) and STFT (right). Horizontal axis represents time whereas vertical axis represents frequency.

Let us observe the left panel of figure (2.1) where each box corresponds to a value of the wavelet transform in the frequency-time space.

The fact that these boxes have a non zero area, means exactly that we cannot know the value at a particular point in the frequency-time plane, or better, with punctual precision of both variables, as all the points that fall in a certain box are represented by the same wavelet transform value. The main property is that, although the widths and heights of the boxes change, the area remains constant, representing an equal portion of the time-frequency plane, but with different proportion (read it: different precision) of the two indeed. If we get on one side shorter heights (better frequency resolution) we will have longer widths (poor time resolution) on the other side. This is the bottom line, this fixed area value is characteristic of each mother wavelet and trying and changing we could arrive to better and better resolution, but only up to

[2]STFT is a revised Fourier transform to overcome the need to analyse non-stationary signal. The key idea is to consider the non-stationary signal stationary over a short interval of time. A *window* function is defined, which determines the width of the segment inside which we assume valid the stationary hypothesis. The STFT results to be the Fourier transform of the signal multiplied by the window function. The choice of the window is crucial and carries the trade-off of Physics.

a certain point. All the possible areas we can construct are lower bounded by $1/4\pi$ (Heisenberg's inequality)[3] as the Heisenberg uncertainty principle cannot be violated. On the right panel, there is the corresponding representation for the Short Term Fourier Transform (STFT). Although a time frequency representation is provided there is a fixed resolution at all times.

A crucial role in measuring the local regularity of a signal is represented by the number of vanishing moments the wavelet we have chosen, has.

Definition 4 *A wavelet is said to have n vanishing moments, if and only if for all positive integer $m < n$, it satisfies*

$$\int_{-\infty}^{+\infty} x^m \psi(x) dx = 0.$$

The number of vanishing moments expresses the polynomial order to which the wavelets are orthogonal; a wavelet with n vanishing moments results to be orthogonal to polynomials up to degree $n-1$. So up to this degree, the wavelet is somewhat blind, enabling to filter out the "regular" noise and to concentrate on the eventually residual structure. To be clearer, let's think at a Taylor expansion; it expresses local polynomial approximations by means of the differentiability properties of functions. The differentiability order gives an upper bound on the approximation error, an integer one of course; the Hölder regularity refines this bound with a non integer exponent.

$$f(x)_\nu = c_0 + c_1(x-\nu) + ... + c_n(x-\nu)^n + K|x-\nu|^\alpha. \tag{2.8}$$

Now, in order to characterize the Hölder regularity of $f \in \mathcal{C}^n$, we will need a wavelet ψ so that $\int x^m \psi(x) dx = 0$, for $m = 0, 1, ..., n$ (i.e. $n+1$ vanishing moments). If f is a function which is a little bit more than n times differentiable at a point ν, than it

[3]In quantum physics, the Heisenberg uncertainty principle expresses a limitation on accuracy of simultaneous measurement of observables such as the position and the momentum of a particle. It furthermore precisely quantifies the imprecision by providing a lower bound for the product of the dispersion of the measurements. It could be measured as the product between the standard deviation Δx of the position measurements and the standard deviation Δp of the momentum measurements. Then we will find that $\Delta x \Delta p \geq \frac{h}{(4\pi)}$ where h is the Planck's constant; it denotes a physical constant used to describe the size of quanta. Note the time and the frequency of a wave in time are the analogous to the position and momentum of a wave in space, although their products is dimensionless; that's why the h constant disappear in our setting.

can be approximated by a polynomial of degree n plus an error. A uniform estimate of this error provides a tool for regularity analysis and, the wavelet transform is a strong candidate. The wavelet transform of this polynomial is zero, whereas around ν its order is that of the error between the polynomial and the function.

So, to be more specific, the number of vanishing moments constraints the maximum order of the detectable Hölder scaling exponent to $\alpha_{max} < n$. The wavelet's regularity on the other hand, restricts the accessible negative singularities to $\alpha_{min} > -N$ where N denotes the wavelet's regularity, $\psi \in \mathcal{C}^N$(Muzy et al. 1994); namely the smoother the wavelet is, the lesser are its localization capabilities, while the larger the number of vanishing moments are, the larger too are the number of extrema.

A key result so, is the explicit relation between the differentiability of f and the asymptotic decay of its wavelet transform (as s approaches zero), which indicates the order of the singularities. Assume that the wavelet $\psi(x)$ has n vanishing moments and n continuous derivatives $\psi^{(k)}(x) \in \mathcal{C}^n$ where $k = 1, 2, ..., n$, with a fast decay, this is that

$$\forall x \in \mathbb{R},\ |\psi^{(k)}(x)| \leq \frac{C_m}{1+|x|^m} \text{ where } m \in \mathbb{N} \tag{2.9}$$

We can derive a necessary and sufficient condition on the wavelet transform to estimate the Hölder regularity of the function f at a point ν.

Theorem 1 ***Pointwise condition.****If $f \in \mathbf{L^2}(\mathbb{R})$ has a local Hölder exponent $\alpha \leq n$ at ν, then there exists A such that*

$$\forall (u,s) \in \mathbb{R} \times \mathbb{R}^+ |Wf(u,s)| \leq As^{\alpha+1/2}\left(1+\left|\frac{u-\nu}{s}\right|^{\alpha}\right). \tag{2.10}$$

Conversely, if $\alpha < n$ is not an integer and there exist A and $\alpha' < \alpha$ such that

$$\forall (u,s) \in \mathbb{R} \times \mathbb{R}^+ |Wf(u,s)| \leq As^{\alpha+1/2}\left(1+\left|\frac{u-\nu}{s}\right|^{\alpha'}\right). \tag{2.11}$$

then f has a local Hölder exponent α at ν.

The whole theorem can be extended to an interval and to the entire real axis.

Theorem 2 ***Uniform condition.****If f is global Hölder $\alpha \leq n$ over $[a,b]$, then there exists $A > 0$ such that*

$$\forall (u,s) \in [a,b] \times \mathbb{R}^+,\ |Wf(s,u)| \leq As^{\alpha+1/2}. \tag{2.12}$$

Conversely, if f is bounded and $Wf(s,u)$ satisfies the above condition (2.12) for an $\alpha < n$, not integer, f is global Hölder α on $[a+\epsilon, b+\epsilon]$ for any $\epsilon > 0$.

In most of the cases the wavelet $\psi(x)$ is the n_{th} derivative of a smoothing kernel $\theta(x)$. A *smoothing function* is any function $\theta(x)$ whose integral is equal to 1 and that converges to 0 at infinity. When the scale s is large, the convolution with the dilated kernel $\theta(x)$ removes small signal fluctuations. Therefore it only detects the sharp variations of large structures. It can be proven that if the function ψ is the n_{th} derivative of a fast decaying function, such as θ, this is a necessary and sufficient condition to state that the wavelet ψ has n vanishing moments; moreover, if the integral of θ over the real (read also as its Fourier transform at zero, $\hat{\theta}(0)$) is different from zero, as it happens for smoothing functions, n turns out to be also the maximum number of vanishing moments affordable by the wavelet ψ.

2.3 The Wavelet Transform Modula Maxima (WTMM)

For an in-depth analysis of the Wavelet Transform Modula Maxima (WTMM), we refer the interested reader to Mallat and Hwang (1992) and for a comprehensive exposition to Mallat (1998). In the following we will expose the main related concepts and intuitions.
We have already emphasized the intrinsic redundancy provided by the wavelet transformed information. The Wavelet Transform Modula Maxima is essentially a procedure that enables to filter out the redundant information in the wavelet coefficients' matrix, in other words an efficient partition of the space-scale plane. By definition a modulus maximum of the continuous wavelet transform is a strict local maximum of the modulus at a fixed scale s and either on the left- and on the right-hand side of a given point u_0. As formally stated by Mallat and Hwang (1992):

Definition 5 *Let $Wf(s,u)$ be the wavelet transform of a function $f(x)$.*

- *Call a wavelet transform modulus maximum, a WTMM, any point (s_0, u_0) such that $|Wf(s_0,u)| < |Wf(s_0,u_0)|$ when u belongs either to the right or to the left neighbourhood of u_0, and $|Wf(s_0,u)| \leq |Wf(s_0,u_0)|$ when u belongs to the other side of the neighbourhood of u_0.*

- *Call a wavelet transform modula maxima line, a WTMML, any connected curve in the scale space (s, u) along which all points are modula maxima.*

To give full meaning to this definition, in order to measure the singularity strength, we need to introduce the concept of *cone of influence*. Let's assume to have a wavelet with a symmetric support on the closed interval $[-K, K]$, then the cone of influence with respect to x_0 in the scale-space plane, is the set of points (s, x) such that

$$|x - x_0| \leq Ks. \tag{2.13}$$

It is the set of point (s, x) for which $Wf(s, x)$ is influenced by the value of $f(x)$ in the neighbourhood of x_0.
The WTMML interconnects the maxima for the modula of the wavelet transform within the cone of influence and across the scale-space plane; they emanate from the abscissa where the singularities are located and proceed towards coarser scales, until they possibly arrive at a bifurcation. This bifurcation indicates the point where the cone of influence of two WTMML starts to overlap. This typically happens when the singularities are not isolated and at coarser resolution they may appear like a unique point of sharp variation, whereas as we approach to finer scales the ultimate structure has been revealed, for example two distinct singularities may appear evident.
When detecting local maxima, we can only record the values of the corresponding wavelet transform coefficients at the selected maxima locations; at this step we cannot differentiate between small amplitude fluctuations and important discontinuities.
It has been rigorously proven by Mallat and Hwang (1992) that the local maxima of a wavelet transform detect the locations of irregular structures. More precisely, it has been proven that there cannot be a singularity without a local maximum of the wavelet transform at finer scales; in the general case a sequence of modula maxima is detected which converges to the abscissa where the singularity occurs.

Theorem 3 *Suppose that ψ is $\mathbf{C}^n$ with a compact support, and $\psi = (-1)^n \theta^n$ with $\int_{-\infty}^{\infty} \theta(x)dx \neq 0$. Let $f \in \mathbf{L^1}$. If there exists $s_0 > 0$ such that $|Wf(s, u)|$ has no local maximum for $u \in [a, b]$ and $s < s_0$, then f has global Hölder exponent n on $[a + \epsilon, a - \epsilon]$, for any $\epsilon > 0$.*

This theorem implies that f can be singular at a point ν only if there is a sequence

of wavelet maxima points $(s_p, u_p)_{p\in\mathbb{N}}$ that converges towards ν at fine scales:

$$\lim_{p\to+\infty} u_p = \nu \text{ and } \lim_{p\to+\infty} s_p = 0.$$

A computational observation is due; to be precise when we perform the numerical estimation of these exponents, whatever method is chosen, we obviously have a discrete sequence, a finite resolution approximation of an unknown continuous function. Strictly speaking it is not meaningful to speak about singularities, discontinuities and Hölder exponents. We cannot compute the asymptotic decay of the wavelet transform amplitude since the wavelet transform is not available at arbitrarily small scales up to zero: it might happen that we detect a discontinuity at a given point, when instead the function might be continuous at that point and have a sharp transition at a point not visible given the available resolution. So, whatever singularity characterization we state by means of wavelet transform, it is precise at the adopted resolution. Our concern will be to check that the WTMM remain approximately constant over a large range of scale in the neighbourhood of the candidate discontinuity point.
From a practical point of view the theorem 3 dictates that all singularities may be detected by following the wavelet transform modulus maxima at fine scales. Now we should wonder how these maxima may propagate at finer and finer scale. Generally it is not guaranteed that a modulus maximum belongs to a line of maxima that propagates towards finer scale: as s approaches to zero there might not be no more maxima in the corresponding neighbourhood. We would require instead, that a signal feature, once present at some scale, should persist all the way through scale-space up to the zero-scale. Otherwise the feature in hand would be spurious, caused by the filter and not the original signal. This behaviour is termed the causality property (Koenderink 1984), in the sense that features at a higher level of smoothing are caused by features at finer level of resolution. The following proposition (Theorem 4) due to Babaud et al. (1986) and Yuille and Poggio (1989), states the remarkable result that derivatives of Gaussian filters are the unique convolution kernels which posses the causality property for one-dimensional signal and therefore they are the unique family of wavelets (that act as filters) which may assured for modula maxima lines never interrupting through finer and finer scales.

Theorem 4 *Let $\psi = (-1)^n\theta^n$ where θ is a Gaussian. For any $f \in \mathbf{L^2}(\mathbb{R})$, the modula maxima of $Wf(s,\tau)$ belong to connected curves that are never interrupted when the*

scale decreases.

The fact that maxima may not disappear when s decreases is, of course, a strong argument in favour of the choice of Gaussians' derivatives as mother wavelet. The procedure of chaining together maxima lines brings indeed, to the elimination of spurious modulus maximum created by numerical errors, which are more likely to happen in those regions where the wavelet transform is approaching to zero.

Following the maxima lines propagation up to the finest scale available, we end up with a set of singularity points. In order now, to estimate the corresponding strength, we need to have a closer look to condition (2.10); it can be equivalently written in logarithmic terms

$$\log |Wf(u,s)| \leq \log A + \left(\alpha + \frac{1}{2}\right) \log s. \tag{2.14}$$

This formulation in the log-log plane makes easier the interpretation and makes immediate the estimation procedure: in (2.14) the Hölder regularity at ν is thus the maximum slope of $\log |Wf(u,s)|$ as a function of $\log s$ along the maxima lines converging to ν.

For many purposes, the wavelet transform isn't required to keep a continuous scale parameter s. To allow a faster numerical implementation[4], we assume that the scale varies only along a dyadic sequence $(2^j)_{j \in Z}$.

Loosely speaking, in place of the generic scale value s we set the factor 2^j, introducing a discretization device that turns out to be very useful and efficient in practice. The resulting *Dyadic Wavelet Transform* maintains translation invariance by sampling only the scale parameter s of a continuous wavelet transform and not the translation parameter u. Moreover, if the frequency axis is completely covered by dilated dyadic wavelets, it may be proved they define a stable and complete representation.[5] We can thus characterize the regularity of a function from the behaviour of its dyadic wavelet transform local maxima and all the above theorems of this section are still valid if we restrict the scale parameter s to dyadic scales.

[4]Refer to Filter Banks literature.

[5]For more detailed explanation and proofs refer to *Frame Theory*.

2.4 The Algorithm

We propose a recursive wavelet transform procedure in order to identify the spike location. Let $f(t)$ be the finite one-dimensional signal that we observe at equally spaced time coordinates $t_1, t_2, ..., t_N$, in this case the spot price time series in the Nord Pool electricity market, daily measured. The basic steps are the following.

Variables set up. In order to simplify the exposition, let us follow a vectorial approach. Let us represent the discrete function $f(t)$, with the couple of vectors $(\mathbf{T}, \mathbf{P})$, where $\mathbf{T} = \{t_i\}_{i=1,...N}$ is the vector of dates to which is associated $\mathbf{P} = \{p_i\}_{i=1,...N}$ the corresponding vector of the observed prices; the dimension of the two is obviously the same, N.

Continuous Wavelet Transform. Let us perform the CWT on the discrete price series constituted indeed by the couple of points $\{(i, p_i)\}_{i=1,...N}$. Note that the x-coordinate is simply the index of the price entry in the vector $\mathbf{P}$ and it can be interpreted as a position indicator; this is a formal choice for coherence with the following step.
In figure (2.2) we show the image of the continuous wavelet transform applied to the spot price time series for different scale values.

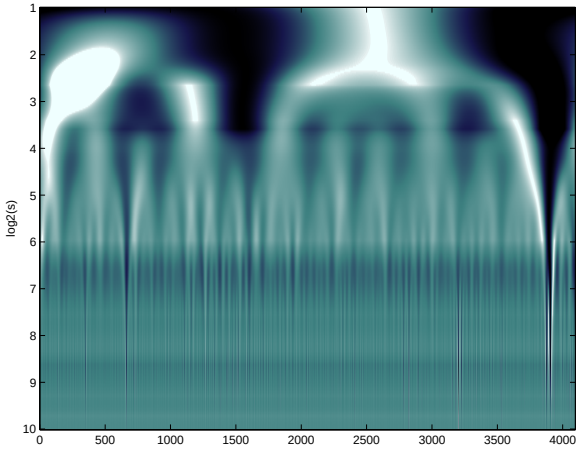

Figure 2.2: Continuous Wavelet Transform of Spot NordPool Electricity Prices. Horizontal axis is the position parameter; vertical axis is the base two logarithm of the scale parameter.

We adopt as mother wavelet the second derivative of the Gaussian kernel $\theta(x) = e^{-x^2/2}$, normalized in order to get the L^2 norm equal to 1. In so doing we obtain the

Mexican Hat[6] function

$$\psi(x) = \frac{2}{\sqrt{3}}\pi^{-1/4}(1-x^2)e^{-x^2/2}. \tag{2.15}$$

This function has an infinite support; nevertheless for this family of wavelets, it is common practice to define the so called 'effective support ', fixing an upper and a lower bound in order to force the wavelet to be compactly supported. The usual Mexican Hat effective support, is the interval $[-5, 5]$ as shown in figure (2.3). (It is an isotropic function in high-order dimension.) The choice of a gaussian's derivative brings a legacy of a lot of nice features, first of all the continuous and regular maxima propagation (i.e without any interruption at finer scales) when chaining the local modula maxima, as stated by theorem 4. The Mexican Hat function has two vanishing moments which indicate that correlations with constant or linear functions will be zero. In other words the wavelet function is orthogonal to polynomial up to order 1, i.e., $n = 2$. The number of vanishing moment adopted is supposed to be sufficient; basically we are advocating that computing the continuous wavelet transform the portion of the price series that is step by step convolved with the scaled and translated Mexican Hat wavelet, is well approximated by up to linear functions. This assumption sounds quite reasonable considering henceforth, the smaller and smaller portion of the signal under analysis as the scale decreases. One could advocate that, using a wavelet with an higher number of vanishing moments, could be better in order to be sure to be orthogonal to the polynomial of the order needed. The point is that in theory the observation may work, but we face a trade-off in order to perform computational tasks: the more vanishing moments the analysing wavelet has, the heavier the computation is. The number of maxima at a given scale increases linearly with the number of vanishing moments of the wavelet, consequently also the number of maxima lines results to be increased. This is not in the spirit of the WTMM procedure, that is designed to be

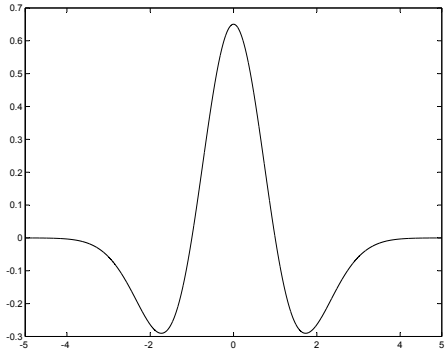

Figure 2.3: Mexican Hat mother wavelet

[6]The name is due to the fact that if we plot the function $\psi(x)$ as defined and we rotate it around its symmetry axis, we obtain a shape similar to a Mexican Hat.

indeed, an efficient representation of a redundant partitioning of the scale-space plane due to the wavelet transform; we thus want to have the minimum number of maxima necessary to detect the interesting irregular behaviour of the signal. So our ability will also be to select the right number of moments. Basically no exact criterion exists, apart from trying different configuration.

Wavelet Transform Modula Maxima. We proceed with the identification, at every available scale, of the modula maxima of the wavelet transforms depicted in figure (2.2). Loosely summarizing, we check, respectively for every points of the signal, for all the modula maxima belonging to the corresponding cone of influence determined by the chosen wavelet, as explained in section (2.3), and if any, we chaining them together on the base of an euclidian distance minimization criterion. In so doing we obtain the WTMML of Definition 5. In the following figure we plot the maxima lines we have identified for the continuous wavelet transform of the spot price time series of figure (2.2).

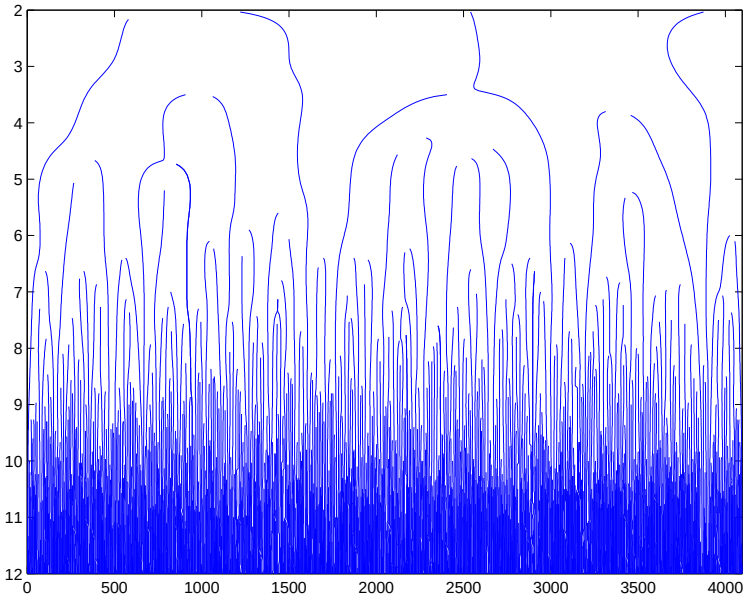

Figure 2.4: Maxima lines evolution across scales of the Nord Pool spot price time series. Horizontal axis is the position parameter; vertical axis is the base two logarithm of the scale.

The final output is a vector collecting the x-coordinates, in the transformed scale-space plane detected as point of sharp variation in the analysed discrete signal or, to be precise, the position indexes of the singular prices with respect to the vector $\mathbf{P}$.

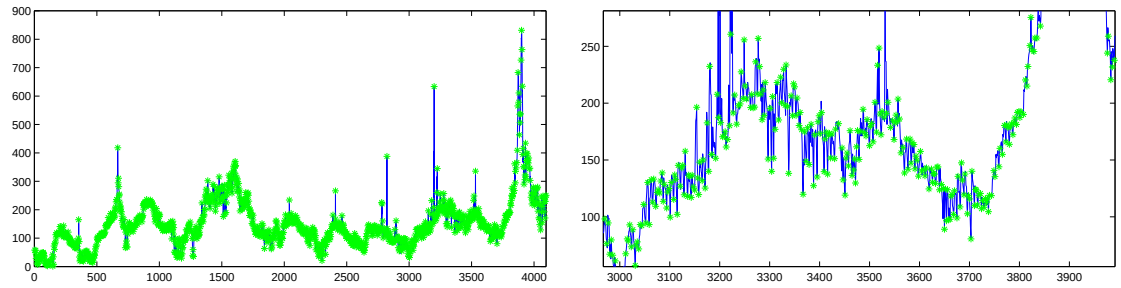

Figure 2.5: NordPool Spot Price Series with the detected singularities by the WTMM. The green star represent the elements of the vector $\mathbf{S}^1$.

Let us define by $\mathbf{S}^1 = \{s_i^1\}_{i=1,\dots n_1}$ this output vector, where n_1, indicates the number of detected singularities.

From the consideration that spikes can be seen as sequence of singularities we argue that inside $\mathbf{S}^1$ there should be the exact spikes' location too.

$\mathbf{S}^1$ *shrinkage.* The problem now is how to retrieve only the spike coordinates. A series of considerations applies. A first observation, as shown in figure (2.6), is that we expect to find inside $\mathbf{S}^1$, for every spike (i.e the location of the *on-peak value*) at least other two x-coordinates corresponding to the *base-values*. So, in the easiest and simplest case, we would have a triplet of coordinates, although a more complex situation with other singularities in the middle is likely to occur. Of course to identify the spike-triplet from a whatever triplet of x-coordinates of a sequence of singularities, one should look at the signal value (the corresponding price); it is indeed a sequence of singularities together with a huge gap in value, to denote properly a spike. When a spike occurs, there is a point of sharp variation, this causes a singularity and, being in the discrete realm , generates two x-coordinates: one indicating the starting point, let's say when the *normality* breaks down and the other one the proper spike location; finally another significant point marks the expiry of the spike-feature, representing the coming back

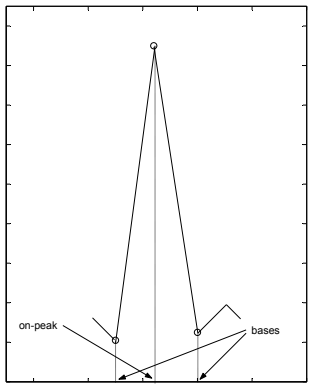

Figure 2.6: Schematization of the basic configuration of a spike in terms of singularities and the corresponding triplet of coordinates.

to normality. In between the two bases there is the anomalous behaviour carried by the spike occurrence and the term coming back to normality has to be intended in term of shape, behaviour, volatility and not simply in terms of price level, even if the price value for the two bases is very often essentially the same. This fact bears out the hypothesis that spikes are anomalies that as they come they go, without leaving any track of them. The need to reduce the set $\mathbf{S}^1$ derived also from the fact that it includes all the sharp transitions of the signal and, as the electricity price time series is for its nature a very jagged one, many singularities will be detected even if the value's transition is not significant with respect to the normal volatility of this particular market. Observe that in the complete series of the detected singularities, apart from the spiky transitions, we have disentangled, to some extent, the most highly volatility movements of the price series; in other words all the points of sharp transition. These consideration reveal the lack of effectiveness of the WTMM algorithm in detecting spikes. Spikes are not mere singularities, they are not simply outliers; the peculiar nature of this object requires a specific analysis. That's why we proposed an additional step to the regular WTMM algorithm.

Recursive Wavelet Transform. The idea is to perform a progressive filter on the vector of singularities $\mathbf{S}^1$ in order to extract step by step, the abrupt variations. This filtering is obtained once again by means of a wavelet transform but this time, no more on the original price time series, but on the signal defined by the set of points

$$\{(j, p_j^1)\} \tag{2.16}$$

where

$$j = 1, 2, ...dim(\mathbf{S}^1) \quad \text{and} \quad p_j^1 = \mathbf{P}(s_i^1)$$

with $\mathbf{P}^1 = \{p_j^1\}$ the vector of "singular" prices. Now the WTMM-tool will detect a new vector $\mathbf{S}^2$ of singularities (in terms of position-indexes w.r.t. $\mathbf{P}^1$), of strictly lower dimension than $\mathbf{S}^1$. We can thus define a new signal by the set of points $\{(j, p_j^2)\}$, but where $j = 1, 2, ...dim(\mathbf{S}^2)$ and $p_j^2 = \mathbf{P}^1(s_i^2)$. Repeat the procedure n times. At every step one remains with the most significant singularities in term of variations, going in such a way in the spike direction identification. This simple procedure from now on will be named *Recursive Wavelet Transform Modula Maxima* of order n, in short R_n-WTMM. After the n-th step is being computed, our new information set is constituted by the vector $\mathbf{S}^n$, assumed to be the vector of the spikes' coordinates,

and by the associated vector of *on-peak* prices $\mathbf{P}^n = \{\mathbf{P}^{n-1}(s_i^n)\}$. To be precise the spikes locations given by the final vector $\mathbf{S}^n$, are not expressed in a time measure immediately intelligible. So to retrieve exactly the dates of occurrence of the detected spikes, we have to follow backward the nested structure defined by the step by step constructed vectors $\mathbf{S}^i$, starting from the $\mathbf{S}^n$ one, up to the original time vector $\mathbf{T}$ defined by the available observations. Therefore the properly vector of dates of spike occurrences, detected by the proposed algorithm, will be

$$\mathbf{S}^t = \{\mathbf{T}(\mathbf{S}^1(\mathbf{S}^2(...(\mathbf{S}^{n-1}(s_i^n))...))\}. \tag{2.17}$$

The key point of the algorithm can be read in (2.16). As already pointed out, the basic idea is to recursively repeat the wavelet transforms, in order to select step by step the abrupt variations. But to make our procedure to work, we need somehow to emphasize the detected structure to make more "singular-relevant" certain points with respect to other. Remember that the tool we have is to detect singularities, whatsoever singularities, non matter the excursion value, which indeed represents the difference with a spike. We want, in someway to force this instrument to detect what we need and the solution we proposed is to construct the synthetic signals $\{(j, p_j^i)\}$. The peculiarity is that apart from picking only the "singular" prices, we totally ignore their time location considering the selected prices equally and unitary spaced by the unit of time: a day in our case. It can be seen as a kind of time change to flatten the time order at each step.

As spikes can be thought as the most abrupt variations identified by the WTMM, it is naturally therefore, to look for singularities by means of once again the WTMM, applied to a series of 'singular' prices.

Interrupt. In the just outlined algorithm the only thing left undefined is how to identify the previously called order n of the R_n-WTMM, in other words after how many steps the wavelet transform iteration has to be interrupted. Of course, if no criterion is specified the algorithm expires by itself, collapsing to a point, assumed to be the most abrupt variation. The aim is to halt the iterations earlier in order to end up with a non-trivial vector $\mathbf{S}^t$. The suggested solution is to give up the iterations as soon as the minimum of the variations between the step by step identified singular values and the nearest previous one, detected in the first step, is greater than a given threshold, say the five per-cent or two per-cent percentile of the empiric distribution

of the related variations. A detailed description of our procedure follows.

Once the first WTMM is been computed and the gained information is represented by the vector $\mathbf{S}^1$, we determine the empiric distribution F_m(where m is the sample size equal to the $dim(\mathbf{S}^1)$) of the absolute variations among the corresponding prices values

$$\{\mathbf{P}(s_i^1) - \mathbf{P}(s_{i-1}^1)\}_{i=2,...,m}. \tag{2.18}$$

This new variable gives us the increment or decrease between the hypothetical base and peak value of the spike; That's why we are not interested in the increments or decrements in the original prices series. Take as a reasonable threshold the 5% or better the 2%-percentile both on the right tail and on the left one. At every step of the recursive procedure, before going on, just perform a simple test. If we are at the iterated step j and we are wondering if we need to go on or we can stop, take the difference among the corresponding price values, $\{\mathbf{P}(s_i^j)\}$, and the price values that correspond to the previous singularity detected at the first step, i.e. the supposed spike base-value $\{\mathbf{P}(s_{p-1}^1|s_p^1 = s_i^j)\}$ where $i = 1, ..., dim(\mathbf{S}^j)$ and $p = 1, ..., dim(\mathbf{S}^1)$. If all these differences are in the tails of the empirical distribution afore defined, we stop, otherwise we keep going. Formally we stop at j-step if $\forall i = 1, ..., dim(\mathbf{S}^j)$

$$\begin{cases} min(\{\mathbf{P}(s_i^j) - \mathbf{P}(s_{p-1}^1|s_p^1 = s_i^j)\}|\, \mathbf{P}(s_i^j) - \mathbf{P}(s_{p-1}^1|s_p^1 = s_i^j > 0) > th^+ \\ max(\{\mathbf{P}(s_i^j) - \mathbf{P}(s_{p-1}^1|s_p^1 = s_i^j)\}|\, \mathbf{P}(s_i^j) - \mathbf{P}(s_{p-1}^1|s_p^1 = s_i^j < 0) < th^- \end{cases} \tag{2.19}$$

where respectively with th^+ and th^- we indicate the right- and left-tail threshold.

Graphical Results. The above procedure, applied to the Nord Pool data set, generates the result outlined in figure (1.7). It can be noticed as the procedure quickly converges to a meaningful output, displaying a strong decrease of the number of detected singularities. The algorithm has been iterated up to the sixth order, depending on the adopted threshold: with a selected percentile of 2% both on the left and on the right tail, the sixth step is required; otherwise with a choice of 5% the fifth is sufficient.

We've collected in table (2.1) the most relevant information concerning the detected spikes from the fifth step onward. We have reported the date of the spikes and the related base occurrences and price values. On average, the time elapsed from base to base is about a week ranging from a minimum of 4 days up to 9 days. This result supports the belief that the spike is a very short-lived feature. A particular mention

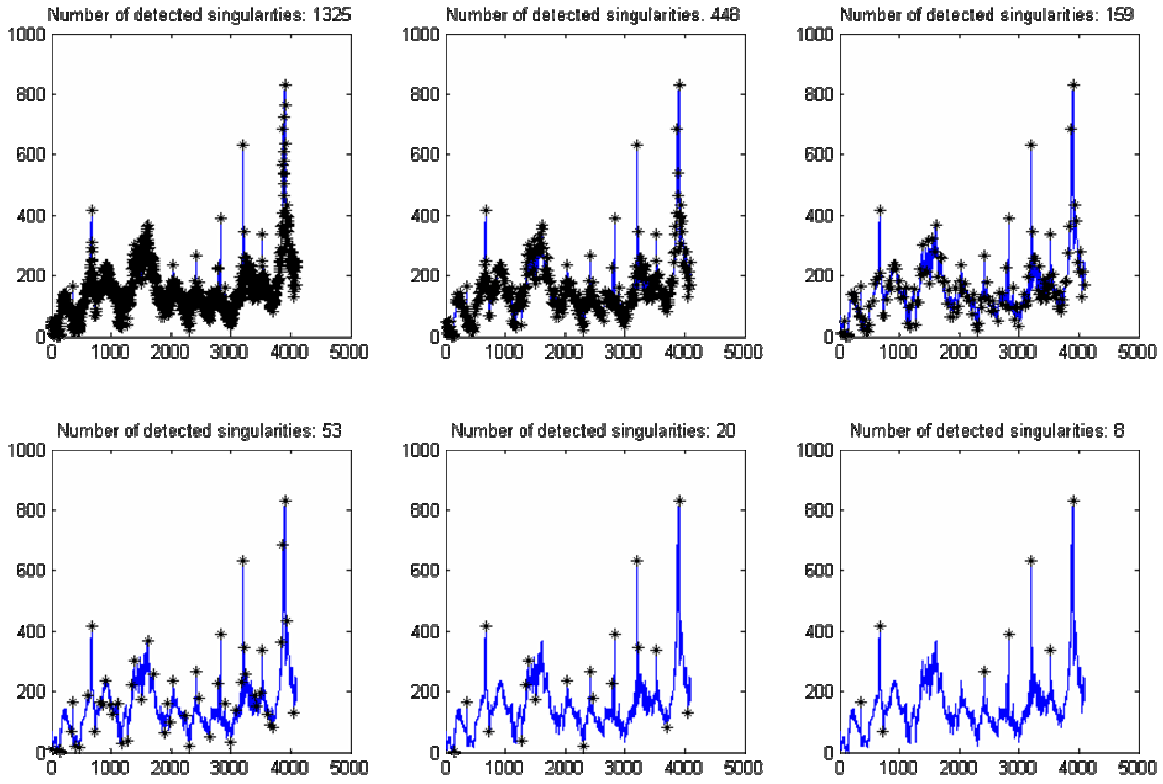

Figure 2.7: Graphical results of the R_6-WTMM. The star-symbol marks the detected singularities.

Positive	Spikes						Upward		Downward	
Peak	price	start	price	end	price	Days	Var. %	Index Var %	Var. %	Index Var %
22-apr-93	165.07	20-apr-93	100.23	26-apr-93	87.71	6	64.69	32.35	-46.86	-11.72
01-mar-94	417.98	23-feb-94	235.5	04-mar-94	294.84	9	77.49	12.91	-29.46	-9.82
04-Jan-96	224.12	31-dec-95	159.42	06-jan-96	173.0	6	40.58	10.15	-22.79	-11.40
20-feb-96	302.08	17-feb-96	232.77	24-feb-96	240.0	7	29.78	9.93	-20.57	-5.14
04-dec-97	234.25	30-nov-97	166.3	06-dec-97	174.2	6	40.86	10.21	-25.64	-12.82
08-dec-98	266.47	06-dec-98	148.21	10-dec-98	166.87	4	79.79	39.90	-37.38	-18.69
29-jan-99	179.05	23-jan-99	121.17	31-jan-99	125.62	8	47.77	7.96	-29.84	-14.92
13-dec-99	225.55	11-dec-99	128.85	18-dec-99	131.28	7	75.05	37.52	-41.80	-8.36
24-jan-00	387.78	22-jan-00	119.05	26-jan-00	134.22	4	225.73	112.86	-65.39	-32.69
05-feb-01	633.36	03-feb-01	187.31	07-feb-01	182.85	4	238.13	119.07	-71.13	-35.57
02-mar-01	344.91	25-feb-01	180.2	04-mar-01	191.47	7	91.40	18.28	-44.49	-22.24
02-jan-02	335.80	31-dec-01	187.69	05-jan-02	191.06	5	78.91	39.46	-43.10	-14.37
06-jan-03	831.41	02-jan-03	726.43	10-jan-03	763.5	8	14.45	3.61	-8.17	-2.04
Negative	Spikes						Upward		Downward	
Peak	price	start	price	end	price	Days	Var. %	Index Var %	Var. %	Index Var %
27-sep-92	1.48	25-sep-92	41.22	01-oct-92	34.37	6	-96.41	-48.20	2222.30	555.57
01-may-94	66.64	26-apr-94	145.3	03-may-94	121.18	7	-54.14	-10.83	81.84	40.92
22-oct-95	38.36	19-oct-95	99.29	25-oct-95	59.92	6	-61.37	-20.46	56.20	18.73
23-jun-96	175.99	18-jun-96	269.13	25-jun-96	239.91	7	-34.61	-6.92	36.32	18.16
22-aug-98	21.27	17-aug-98	79.1	25-aug-98	51.27	8	-73.11	-14.62	141.04	47.01
23-jun-02	80.65	20-jun-02	115.83	25-jun-02	140.07	5	-30.37	-10.12	73.68	36.84
08-jun-03	128.91	03-jun-03	219.89	11-jun-03	212.89	8	-41.38	-8.28	65.15	21.72

Table 2.1: Numerical information about the relevant spikes selected from the fifth steps onward.

is due to the 6-Jan-03 spike. It represents the very peak value of an anomalous spike: in that period the North of Europe was facing a big drought and consequently the aforementioned spike constitutes just the abrupt peak of a wider spike which lasted for more than a month. Finally in the last four columns we have reported the upward and downward price variations relative to the corresponding bases and the related daily price variation.

Chapter 3

The Electricity price modelling

3.1 Literature review of modelling approach

It is a matter of fact that electricity markets rank among the most challenging and complex of all markets operating at present. Electricity may be assumed as a commodity but its very nature makes it singular. The established financial literature in commodity pricing cannot be easily transposed. At the same time, the pressure for reliable tools of modelling and forecasting is constantly increasing, together with the establishment and widespread consolidation of deregulated and competitive electricity markets all around the world. In the last fifteen-twenty years indeed, a clear separation between services and infrastructures has taken place in the name of the liberalization process and now, with markets more or less mature, the power industry in several countries is no longer a centralized and vertically integrated structure. Hence, the need to understand the price formation mechanisms is stronger, as the requirement for a tractable approach to transform the available data together with the developed theory of the market mechanisms into simulated prices to be used as inputs for models for investment, production and risk management decisions. However, it is still a quite young market, at least in terms of the length of available for inference time series. It is indeed , in the last years that we have observed an increasing interest toward the electricity markets in the financial literature.

We can broadly summarize the several electricity pricing models, in two main approaches: a pure *financial* approach and a more *economic*-orientated one.
We refer as a pure financial approach, to the stream of literature which treats the

price of electricity as a stochastic variable without attempting to model the actual electricity system itself. A process is specified, which is totally independent of the underlying physical system state variables. These kinds of models focus only on past realizations of the prices and attempt to infer aspects such as price trends and volatility directly from those price series.
The other main stream of literature instead, the *economic* approach, concentrates itself more on the price formation mechanisms, on the fact that the short-term price for every period is set by some intersection of demand and supply. Hence it tries to analyse the decision making process of both the supply and the demand side, studying the interaction of factors such as generating capacities, marginal costs, loads, transmission constraints, with the market rules. It tries to mimicking the market, to calculate the prices in much the same way as do the actual market mechanisms: spot prices and their distributions are achieved endogenously. As a first consequence of course, a huge amount of physical system information is required.
Without any intent of completeness, we now briefly review the the main contributions to the two approaches. Let us first review the pure *financial* approach.

A price process has to be defined and the first natural candidate might be the geometric Brownian motion so widely and successfully used to model securities. The linear diffusion models of the type underlying Black and Scholes however, cannot capture the behaviour of the electricity trajectories such as spikes and mean reversion. Kaminski (1997) was the first to add jumps to geometric Brownian motion in order to consider the spiky behaviour of the observed trajectories, but still not mean reversion. Schwartz (1997) widely discuss why the mean reversion for commodities is reasonable on general economic grounds, but we have to wait Johnson and Barz (1999) for a mean reverting model. Comparing different models (Geometric Brownian motion and mean-reversion with/without jumps) across several deregulated markets, they suggest a mean-reverting model with an exponentially distributed (hence positive) jump component as a more adequate specification. Although crucial characteristics of price dynamics are captured, a deterministic price volatility is still assumed, which clearly contradicts empirical evidence.
Although to add a jump component looks like the natural solution to model spikes, it is not so straightforward how to perform this task. A pure jump model in the spirit of Merton (1976) is inadequate, as the effect of each jump is supposed to be permanent: the diffusion starts again from the new level of price once the jump has occurred and

no reversion to a normal (previous) level of prices is contemplated. It is quite simple to obtain large upward jumps, by making the positive tail of the jump measure fat enough, but because the times of the large positive and negative jumps have to be independent Poisson processes, it is not possible to ensure that a large upward jump will be followed by a large downward jump. Hence in order to reproduce a spike and not a simple jump in the trajectories, the main issue is how to quickly reverse back the level of price after a jump. The first possible solution is to use the mean reversion machinery as it happens in the Braz-Johnson (1999) or Clewlow-Strickland (1999) models. The fact is that, to efficiently damp out the big shocks in the level of price after a jump the small price movements result to be unreliable flattened by the high speed of mean reversion required to do a good job on the price jumps. Lucia-Schwartz (2002) even drop out the jump component and suggest that prices could be decomposed as the sum of two components: a deterministic component which represents the underlying mean level of prices and a stochastic component in the form of an autoregressive process, which accounts for decaying movement away from that level. This choice leads to simple pricing formulas. Villaplana (2004) specifies a price process that is the sum of two processes: one continuous and the other one with jumps with different speeds of mean reversion. Geman and Roncoroni (2006) introduced a threshold, estimated in order to preserve moment matching of the observed and the simulated trajectories, beyond which the simulated process is supposed to reverse down. In these settings however no successive up jumps are feasible once the threshold is reached and the intensity of the jump process does not depend on the fact that a jump has just occurred. Jump-type models, moreover, present some difficulties in the estimation procedure. An electricity model to be reasonable should include seasonalities which affect the intensity and the magnitude of a jump. Hence, estimating such a model on the limited time series available, is extremely challenging. Geman and Roncoroni (2006) perform the estimation but they have to specify the parameters of the non-homogeneous jump intensity function based on *a priori* considerations instead of estimating it from the data. Further, it has to be noted that jump risk is not hedgeable and hence the electricity market is incomplete. However, the non storability of the electricity, makes impossible to hold an hedging position in spot power, making the market incomplete even with continuous prices.

An alternative modelling framework to jump-diffusion is regime-switching. This can replicate the price discontinuities, observed in practice, by disentangling mean rever-

sion from spikes. The latter are truly time specific events and therefore independent from the mean reverting price process. Hence jumps occurrence may be considered as a change to another regime that follows a totally different stochastic process in terms of parameters values or even in terms of its nature. In these models a key point is the definition of the switching mechanism, which can be assumed to be governed by a random variable. Usually this is a Markov chain with two or more possible states. Ethier and Mount (1999) assume two latent market states and an AR(1) price process under both the normal and the abnormal regime; constant transition probabilities and constant mean prices, estimated for each season separately, and stationarity in the irregular spike process are imposed. Barone Adesi and Gigli (2001) proposed a discrete regime switching time model which define additively the changes in electricity prices; spikes are assumed to happen at random times with a distribution of sizes following a lognormal distribution. Their duration and frequency are independent, but they cannot cumulate.

The model suggested by Huisman and Mahieu (2003), allows an isolation of the two effects assuming three market regimes; a regular state with mean-reverting price, a jump regime that creates the spike and finally, a jump reversal regime that ensures with certainty reversion of prices to their previous normal level. This regime-transition structure is however restrictive, as it does not allow for consecutive irregular prices. This additional feature, not so infrequent, would required an extremely large number of switching probabilities. This constraint is relaxed in Huisman and de Jong (2003). The two-state model proposed assumes a stable mean-reverting regime and an independent spike regime of log-normal prices. Regime independence allows for multiple consecutive jumps.

It is worth to mention a further split in the literature between researchers who model the spot price and the ones who privilege the futures price. Most of the time the motivation of the choice between the two is the pricing purpose. It is a common practice to model the underlying of the contingent claim to be priced. This may be both the spot and the futures price, although based on modelling approach sometimes the reason behind a futures price seems to be the nicer shape of the futures term structure, with less volatile price and no such an extreme spiky behaviour as the spot price trajectories. We believe that the basic liquid market which is needed to be modelled is the spot price. The spot price is the principal underlying of many electricity derivatives and the availability of a well suited modelling process is of

primary importance for every risk management and hedging strategy in the electricity sector. Being aware, however, of the importance of the futures quotations, it will be our concern to propose a futures pricing model based on spot price evolution.

The alternative stream of literature, the *economic* approach, tries to make explicit the economic forces that, interacting with each other, lead to the formation of the observed price series, which is the given and exogenous starting point of the *financial* approach. This goal may be carried on at several degrees of detail. We have essentially supply/demand-oriented models, which try to simulate the operation of generating units aiming to satisfy demand at minimum cost. Hence, prices are derived from the intersection of the expected production costs of electricity and expected consumption. In other terms they aim to determine the theoretical equilibrium price of the whole market, see Fleten and Wallace (1998) for instance. This can be pursuited as an optimization problem for only one firm, or considering the market equilibrium for all the firms (Cournot equilibrium type or supply function equilibrium). Moreover this can be performed ignoring strategic bidding practices or accounting for them both in a static and a dynamic way. Such equilibrium models rely on the assumptions that prices are determined by industry participants rather than outside speculators, and that power companies are concerned with both the mean and the variance of their profits. Under this different shade of light the unique features of the electricity price trajectories, which has challenges us so far with the pure financial approach, find here an exquisite economic motivation which we want to model. Let us take spikes. Non-storability of electricity means that if a positive demand shock takes place in a given period of time (hourly, daily or monthly market), that is the demand surpasses production, there is no upper bound on price levels. Therefore in those situations where the demand level is near the maximum capacity of the system, the behaviour of electricity prices can be quite abrupt, since electricity must be generated trough inefficient plants with a higher marginal cost. This is a spike. It is a reflex of the convexity of the supply function. Another possible reason behind spikes is a reduction in supply. This reduction in generation capacity may be given by a decrease in the number of generators of a system or, in the case of interconnected systems, a reduction in the capacity to import from other electric markets, see for instance the analysis for the New England spikes June 1999, in Krapels (2000). Birnbaum et al. (2002) have empirically shown there exist an important relationship between price level and generation capacity.

To identify the relevant observable state variables mainly associated to supply and demand variables, is one of the main issue for the economic modeler. Pirrong and Jermakyan (1999 and 2000) propose to model the equilibrium price as a function of two state variables, electricity demand and the futures price of the marginal fuel. By introducing the futures price of the marginal fuel, the authors are trying to introduce an (observable) state variable related to the supply side. The authors postulate that electricity price should be an increasing and convex function of demand. Bessembinder and Lemmon (2002) derived an equilibrium model of electricity prices, in which the price volatility depends on the volatility of system demand and production cost. They explicitly model the economic determinants in the forward market. Producers face marginal production costs that may increase steeply with output. Aggregate demand is exogenous and stochastic, but generation capacity is not a random variable. They show, in case of increasing marginal costs, how price distribution exhibits positive skewness even in the case of symmetric electricity demand distribution.

The papers of Barlow (2002), Skantze et al. (2000) and Skantze and Ilic (2001) commonly impose a functional form for the relationship between price and the state variables. State variables are demand and a non-specified variable related to the supply side. Barlow (2002) proposed a non-linear Ornstein-Uhlenbeck process for the description of observed electricity prices. Basically the author consider the demand as the relevant state variable, and model it as a mean-reverting process incorporating a non-constant mean given by a deterministic seasonal function. From empirical observation he considers electricity price to be a convex function of electricity demand. In his empirical analysis shows how effectively the model is able to generate spikes, trough a non-linear filter that connects diffusive demand with electricity prices. The convexity between demand and prices is the element that generates jumps in electricity prices although demand is modelled as a diffusive process.

In Skantze et al. (2000) and Skantze and Ilic (2001), the authors impose an exponential functional form between electricity spot price and state variables. State variables are demand and a non-observable residual variable, related to supply conditions. Hence, electricity prices would be governed by a combination of demand and supply states. The parameters describing the load state dynamics can be estimated directly from the time history of the market demand. The non-observability of the supply variable (generation capacity), is overcome by the authors by an extracting procedure, in other words supply is considered a residual variable and this may be

seen as weakness of the approach. Any change in price that is not directly related to a demand shock will be captured by this residual variable. It also must be noted the relationship between price and demand is less clear at higher prices (or level of demand).

In order of better explaining the hidden market mechanism of price formation, many authors rely on an enlarged set of driving factors, not just a simple proxy for the demand and the supply, but many other collateral variable which may influence the decisions. These variables, called fundamentals, affect the spot prices. They are modelled as stochastic factors that follow statistical processes which result to be definitely more stable than the price process. Fundamentals factors may be climate data like hydro-inflow, temperature, snow levels and precipitations; alternatively fuels prices; penalties for production interruption introduced by law and many others.

However, the data set is usually hard to collect and maintain and it is often laborious to use such a models to create numerous spot price scenarios. Moreover these models are not particulary well suited for day to day market operations. Vahviläinen-Pyykkönen (2005) calibrated as many as 27 fundamental variables in their model of the Nordic market. These variables are typically collected only with low frequency, that is weekly, monthly and even quarterly.

The electricity sector, and the economy in general are characterized by difficult real-world aspects, such as asymmetric information, imperfect competition, strategic interaction, collective learning, and the possibility of multiple equilibria (Tesfatsion, 2006). Many of these factors cannot, or only with difficulties, can be accounted for with traditional economic modelling techniques. When the concept of complexity came up, the focus in economic analysis shifted from rational behaviour and equilibrium towards heterogeneity and adaptivity. Agent-based modelling is one appealing new methodology that has the potential to overcome some shortcomings of traditional methods. The actors are modelled as computational agents goal-oriented and adaptive, that is able to learn. A key word is heterogeneity. Agent-based models are not restricted to equally-sized or symmetric firms, or to other constraints that arise from the limits of analytical modelling. There are however extreme difficulties in the validation of the model outcomes against empirical data. For a detailed survey we refer to Weidlich-Veit (2008).

The choice between the two approach is not obvious. Researchers are always facing the trade-off of simplicity, computational tractability and realistic representation of the

complex market decision mechanisms. It is a matter of fact that even if the economic driving factors of the electricity price process may be on their own of greater simplicity to model, it is true as well that the simultaneous consideration of everyone of them may lead to an high degree of complexity. Consequently, reading between the lines of Green (2003) we choose the road of the pure *financial* models, where however, the preference for the stochastic approach does not mean we cannot understand the very origin of each period's price. Maybe explaining every price in turn is too cumbersome, and randomness should be taken as a shortcut for 'things that we could explain, but don't have time for in this application'

3.2 The price model

3.2.1 The setting

As we have emphasized in the previous chapter, one of our main objectives is to minimize the extent of the necessary parametric assumptions. To this end, some considerations are worthwhile. We notice that but for the 'singular' behaviour due mainly to spikes, the spot price can be sensibly approximated by a process with continuous trajectories. This is the classical assumption widely accepted for most of the financial markets, but now we are dealing with a very peculiar commodity, electricity supply, which breaks down the core of the no-arbitrage re-balancing price effect, due to its peculiar non-storable nature. This turns into impressive prices movements up to a sudden burst and explosion, namely the spike. The continuous sample paths hypothesis loses then any reliability. In the financial literature we have just reviewed, we find many different model proposals which try to mimic the electricity price behaviour.

We define P_t as the electricity price at time t and we take the stance of postulating a clear distinction between two different price regimes, the interbases regime and the spike regime. In so doing, we assume that the price process increments may be led by completely different equations both in shape and in the parameters values, depending on the regime in which we are. We decide to model directly the price level of the electricity P_t and we intentionally refrain from modelling the log-price, even if the log-transformation is common practice in financial literature and in electricity financial literature too. This is mainly done to ensure strict positiveness and to stabilize

statistical estimations. There are however, several supporting reasons for our choice. First of all, both Escribano et al. (2002) and Lucia and Schwartz (2002), widely test the better performance of price processes formulations rather than their logs in the Nord Pool market; further Villaplana (2003) remarks how log-transformation lowers the skewness of a series and so it may affect the estimation and the weight of the spike component too. Last but not least, it cannot be ignored the recent tendency of possible negative prices, which however may always be excluded in a second moment by different methods like barrier at zero, for instance.

The occurrence of interbases regimes and spike regimes is dictated by a Markovian model of time durations -which implies a sequence of stopping times as spike events- and jump amplitudes. This feature of the model will be fully clarified in the sequel.

For what concerns the interbases regimes - 'normal' evolution periods - we believe that a continuous sample path hypothesis still provides a reasonable description of the price dynamics. By 'normal' evolution periods we mean situations where the peculiarities of electricity prices do not arise. As of spike regimes, we refrain from postulating any parametric probabilistic assumptions about the price evolution and we propose a non parametric method to reproduce its main features: the occurrence of spikes, the price jumps implied by them and their lengths.

In order to identify those periods where the peculiarity of electricity impacts the most in the price evolution, we believe that the wavelet transform may give useful insights. The recursive application of the wavelet transform to the price series enables to disentangle, at different levels, the abrupt changes, the high volatility movements, that is the failure of continuity: the 'singular' prices.

Furthermore, the price increments due to distinct spikes may be considered to be i.i.d. observations. This is embedded in the concept of spike itself, as we have already notice there is no past influence and no future resemblance once the spike is ended: as it comes it goes, without leaving any track of it. If any kind of predictability were present we would have observed completely different shapes in the price evolution: no sudden burst, but a smoother growth of the prices that points towards the on-peak value. So, independence and spiky behaviour, at least at a first definition level, are two aspects of the same feature.

Therefore, a possibility is to bootstrap the spike price increments detected by the R_n-WTMM and assume a continuous sample path process in between. In other words, we propose a diffusion model, where the more extreme jumping part of the process

itself, is object of the bootstrapping procedure, which is extensively explained in the next section.

The first step is to select the set of spike/singular price occurrence. The output of the R_n-WTMM may vary depending on the order of iteration chosen. To select where the recursive algorithm should be optimally stopped we have to keep in mind the two main assumptions we have to preserve in order to justify the procedure, that is: independent prices increments of the selected observations and reliability of the continuous trajectories hypothesis for the branches in between. Looking carefully at the output figure (1.7) we realize that we are facing a trade-off. If we aim at the continuous sample path hypothesis, the more singular points we exclude the more sensible the assumption is. So, for the sake of diffusion hypothesis, the first scenario is indeed the best choice. On the other hand the assumption of independent observations would be seriously jeopardized if we stopped at the first iteration. As we have already pointed out, in the complete series of singularity points there are many different features; there are of course all the high volatile points, there are all the spikes and regarding the last ones not only the on-peak values but the corresponding bases too. This is just an example and represents by itself a first easy violation of the independence requirement: the two bases of the same spike result to be obviously correlated. Concerning the independence assumption indeed, the last scenario would be the best one: we retrieve just the abrupt on-peak values, namely the spikes, and there is no reason to believe in any correlation between the corresponding price jumps. In this case-study we suggest to halt the R_n-WTMM at the third iteration, with a total number of 159 detected singularities over more than four thousand observations. This middle step assures us a good degree of independence among the selected observations, that in the sequel we test, while allowing us to exclude a remarkable number of strong singularities to make the continuity assumption reliable.

3.2.2 The Bootstrap

The purpose of this section is to derive the spike regimes structure together with their occurrences.

The R_n-WTMM algorithm up to the selected order of iteration n, provides us with an output vector of singularities $\mathbf{S}^n$. In excess of the 'genuine' spikes, $\mathbf{S}^n$ is expected to include points of abrupt price variation , which are characterized by a very similar

behaviour, though not spikes according to a reasonable confidence level for the R_n-WTMM algorithm. The 'spiky' behaviour of these additional points of abrupt changes shows up in the strong correlation with the nearby prices. That is, we believe that we are able to find the same base-peak-base structure of a genuine spike. This highly volatile generalized behaviour is due to the very nature of the electricity market: its non storability feature makes the price very frenetically react to any kind of event, resulting in a price series not just jagged, but made up of spike-like reactions of any order. Some event occurs, a sharp transition follows and as soon as the adverse or favourable events are passed by, the price tends to revert back to the preceding level, losing somehow memory of the event. According to this reasoning, although a medium order R_n-WTMM does not detect pure spike alone, we feel confident to state that the independence of the price transitions corresponding to singular points in $\mathbf{S}^n$ is preserved.
To clarify the notation, let us define the following vectors:

$$\begin{aligned} &\mathbf{b}^n_{left} := \{s^1_{p-1} | s^1_p = s^n_i\} && i = 1, ..., dim(\mathbf{S}^n) \\ &\mathbf{b}^n_{right} := \{s^1_{p+1} | s^1_p = s^n_i\} \quad \text{where} && \\ &\mathbf{spk}^n := \mathbf{S}^n && p = 1, ..., dim(\mathbf{S}^1). \end{aligned} \tag{3.1}$$

This way, in the spirit of the recognized structure base-peak-base, we have disentangled the left and the right bases, $\mathbf{b}^n_{left}$ and $\mathbf{b}^n_{right}$, from the detected spike[1] locations $\mathbf{spk}^n$. Let us further define $\mathbf{J}^n_{left}$ and $\mathbf{J}^n_{right}$ to be respectively, the vectors of the price jumps from the left, (i.e. the difference in the corresponding prices between the $\mathbf{spk}^n$ and the $\mathbf{b}^n_{left}$ elements) and from the right (i.e. the same price difference between the $\mathbf{b}^n_{right}$ and the $\mathbf{spk}^n$ elements) corresponding to the n-th order. Let us denote by $\mathbf{D}^n_{left}$ and $\mathbf{D}^n_{right}$ the vectors of days elapsed from the left base to peak and from the peak to right base respectively. We say that the i-th quadruplet $(\mathbf{J}^n_{left}(i), \mathbf{J}^n_{right}(i), \mathbf{D}^n_{left}(i), \mathbf{D}^n_{right}(i))$ represents an independent observation. It is quite reliable to believe that, given a sudden jump-up of the price, the immediately jump-down is strictly correlated in terms of price excursion and in terms of days elapsed. So, to be precise all the jump-up and the jump-down defined by the singular

[1]Remember that in this section, the word spike has to be intended in a wide sense. It refers not only to the proper spikes, but more generally to a spike-like behaviour, in short to the base-peak-base structure.

points detected by the R_n-WTMM are not independent between each other as such, but the aggregation of the relative jumps, up and down together with the related distances occurred, define an independent object. It is exactly the ensemble of all these quantities that we bootstrap in order to obtain all the needed trajectories, in the spirit of an historical filtration by means of a very general re-sampling procedure.

We decide to adopt a non parametric bootstrap. We do not hypothesize any model for the evolution of this price jumps considering them pure i.i.d. observations. Let $\mathbf{Q}_i$ represent the i-th quadruplet $(\mathbf{J}^n_{left}(i), \mathbf{J}^n_{right}(i), \mathbf{D}^n_{left}(i), \mathbf{D}^n_{right}(i))$ just defined and, let $\chi^n := \{\mathbf{Q}_1, \mathbf{Q}_2, ...\mathbf{Q}_m\}$ be the corresponding random sample of size m.

The bootstrap method enables us to generate a generic number, say M, of sequences of quadruplets.

In order to retrieve the trajectories of the electricity price process, we need to locate temporally the information of the quadruplets (i.e. a given price jump in a given interval of time). To accomplish this task we define the vector $\mathbf{I}^n$ to be the vector of the distances between each left base and the right one of the preceding *spike*. We assume these interbase distances to be a sequence of i.i.d observations; there is no reason indeed, to assume that these distances may affect each others. The *spike* turbulence, as we have previously emphasized, expires in between the period bounded by the two corresponding bases. In light of this consideration, the independence of the interbase time sounds reasonable. Given this, a possibility is to bootstrap this sample of observations in order to obtain G bootstrap samples of interbase distances. This information by it self does not provide the dates of occurrence of the *spikes*; to retrieve the complete time grid, the two independent bootstrap outcomes have to be combined. From the price jumps bootstrap we get also the distance from the left and the right base of the spike location and this completes the temporal grid. The only requirement is that we need to retrieve all the new time axis from the beginning of the data we have available. Only afterward we are able to select the time interval we need for the pricing and to simulate only the trajectory portion that we need.

The Monte Carlo trajectories have to be indeed constructed dynamically. Now the bootstrap of the interbase distances gives us additional information regarding the temporal allocation of the bases, but it says nothing about *spikes* allocation. It is only performing the trajectory simulation itself (i.e. performing the jump price bootstrap too), that the complete temporal grid becomes known. So, to be precise, each trajectory of this Monte Carlo will have a different sequence of spikes and bases.

This does not mean we are simulating something different each time, that otherwise would violate the basic Monte Carlo convergence principle. Ours is a non parametric way of simulating an undefined price generating model, where the spike-base sequences are endogenously determined. This exactly what we want to accomplish.
It is worthwhile stressing that this double bootstrap procedure gives an extraordinary flexibility in the possible combination of spike and interbase regime without increasing modelling complexity. Just to quote same of the main restrictions usually encountered in the regime-switching specifications, the proposed model may easily generate multiple spikes (i.e more than one spike in a row) of different lengths, both positive and negative.
Our double bootstrap procedure, by the way, provides us only with disconnected portions of the desired trajectories of the spot electricity price we need, or better with disconnected points: three for each bootstrapped quadruplet, that is the left base, the peak value and the right base. To connect all these points in order to obtain a full path we make a distinction between the kind of path's portion we are implementing. We distinguish between an *interbase regime* and a *spike regime* as it is exemplified in the following scheme:

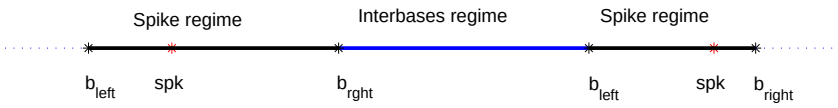

Figure 3.1: Schematization of the price series in terms of the base-spike-base structure.

Let us denote by *spike regime* the price evolution between the two bases of a detected *spike* (i.e. between the couples $\{\mathbf{b}^n_{left}(i), \mathbf{b}^n_{right}(i)\}$) and on the other hand, with *interbase regime* the price evolution from, for instance, the second base of the i-th spike, $\mathbf{b}^n_{right}(i)$ to the first base of the following *spike* detected, $\mathbf{b}^n_{left}(i+1)$.
In the next subsection we illustrate the interbase process. For what concern the spike regime process instead, in the spirit of the bootstrap choice we have made, we intentionally refrain to specify any parametric dynamic. We stress once again that the adoption of the bootstrap technique is exactly to avoid any parametric specification. We believe that the information the double bootstrap procedure gives us is more than satisfactory in most cases: we know the extreme values taken by the price and we know

when these happen. So, from our point of view the price process is essentially fully defined. By the way for more demanding pricing purposes, such as path dependent options for instance, where we have to be able to simulate the price process for every future time, we propose a modelling solution in the next chapter where we deal with the American option pricing. That solution will be just a simulation tool to overcame the problem of getting continuous trajectories, neglecting the hidden and unknown dynamic of the spike process regime.

3.2.3 The interbase regime process

Let us now focus on the evolution of the electricity price P_t followed during the interbase period, the so called period of normality. In this case we will specify a parametric model. This process has to take into account as much as possible the peculiarities of the electricity market regardless its spiky feature, which our bootstrapping procedure accounts for. First of all we focus on the **price-proportional volatility** feature. This behaviour is directly induced by the supply stack function, in other terms the graph of the marginal cost of the electricity supply. The exact shape of the curve will vary from market to market depending on the characteristic of the different plants, on the local industry structure and consequently on the related cost for an additional unit of electricity, however the *leit-motiv* of all markets is the convex shape of the supply stack. The relationship between demand and price is non-linear, it is expensive to bring supplementary power stations into operation for a short time of high demand. When the usual base load power stations are working up to their capacity, prices start to increase quickly; on the other hand when the demand is unusually low, electricity prices fall suddenly. In order to further reduce supply, power stations would have to be turned off: that is expensive. Thus, it is preferable to stimulate demand by lowering the prices. This non-linear relationship between demand and supply explains the price-dependent volatility property: when demand rises, prices reach the steeper part of the supply stack, where even small demand fluctuations cause large price changes and, thus, a high volatility. (This result holds for seasonal fluctuations and price spikes too.)

Another important aspect to be reproduced is the **price mean-reversion**. The tendency for fluctuating prices to return to some mean price over time is observable in all the electricity market. Such behaviour is consistent with the fact that the

overall supply must match the overall demand that is, prices should be related to the long run marginal production cost. Spot electricity prices are perhaps the best example of anti-persistent data. This statement may be easily verified by calculating the corresponding Hurst exponent H of the spot price series. The Hurst exponent is indeed, a measure of self-affinity: if the timescale is zoomed by a factor n, then the process looks statistically identical by scaling the series by a factor n^H where H is the Hurst exponent[2]. It is a powerful tool in detecting long range dependence. The Hurst exponent is equal to 1/2 for Brownian motion (classical example of self-affine time series) indicating uncorrelated Gaussian increments with finite variance (just recall that random walk diffuses as $\sigma \sim t^{1/2}$), while $H < 1/2$ or $H > 1/2$ indicate anti-persistent and persistent series, respectively. Anyway, we refer the interested readers to Malamud and Turcotte (1999) for a plain and detailed presentation of the main concept behind the Hurst exponent and the principle methods for its estimation.

To our purpose, in order to estimate H, we apply the *Average Wavelet Coefficient* (AWC) method of Simonsen et al. (1998). The idea is to use the wavelet transform in order to measure the temporal self-affine correlations, the Hurst exponent indeed. Once the price series is been shifted to the wavelet domain (the scale-space plane) we look, for every location, for the representative amplitude (wavelet coefficient) simply taking the arithmetic average across all the scale values available. The application to the Nord Pool data gives an estimate of $H = 0.4 \pm 0.02$ for time interval ranging from a day up to five years, indicating mean reversion, whereas for time intervals of less than 24 hours, H results above 0.5. Our results are perfectly in line also with the extensive Hurst estimation research performed by Erzgräber et al. (2008) on the Nord pool price series.

In light of these considerations, during the interbases periods, we proposed the following diffusion for the electricity price P_t.

$$dP_t = K(\theta - P_t)\, dt + P_t \sigma dW_t \tag{3.2}$$

[2]The Hurst exponent was first introduced by Hurst (1951) analysing the record of floods and droughts of the Nile River. He introduced empirically the concept of rescaled-range (R/S) analysis. Given a discrete time series of length N, let us consider its cumulative sum relative to its mean. The range R is defined as the difference between the maximum and the minimum value of the cumulative sum series and S denotes the standard deviation of the same series. There is a power low dependence between the different n R/S ratios that may be calculated for all the n subintervals of the total length N and their frequency n. The exponent which identifies this power low is exactly the Hurst exponent.

where the parameters θ and K represent respectively the long-term mean and the reversion speed. The proposed model results to be a mixture of an arithmetic Ornstein-Uhlenbeck process, from which inherits its drift and of a geometric brownian motion, for the diffusion term. In so doing we are able to match both the requirements of mean reversion and price-proportional volatility.

Another well established and recognized feature is the presence of strong **seasonal fluctuations**. Regarding the demand side, they mostly arise due to changing climate conditions, such as temperature and the number of daylight hours and business-industrial activity. The supply side too may display seasonal variations in its output, this is mainly evident in markets where the hydroelectric production is predominant, like the Nord Pool indeed. Hydro units are heavily dependent on precipitations, drought and snow melting, which vary from season to season. All these fluctuations both in the demand and in the supply side obviously translate in the well known seasonal behaviour of the spot electricity prices. Typically we recognized in the Nord Pool spot price series an annual cycle, with low prices in summer, and a weekly one, with low prices during the weekend. A daily cycle is also evident if we consider hourly data; price is low at night with two peaks during the day: before noon and in the late afternoon. The obvious solution is to embed these predictable features in the parameter of mean reversion θ, the long term mean, letting it become time varying instead of keeping it constant. The seasonal fluctuations are then modelled by letting the level of the mean reversion to follow a deterministic sinusoidal function plus a linear trend to better fit the long run trend in total production cost, typically increasing. In other words we can define

$$\theta := \theta_t = \bar{\theta} + \beta t + \sum_{\nu \in \mathcal{F}} \theta_\nu sin(\omega_\nu t + \phi_\nu) \tag{3.3}$$

where the set $\mathcal{F}$ is constituted by the ν values corresponding to the frequency cycles one wants to embed, say yearly, weekly and even daily; the parameters θ_ν represent the amplitude of the corresponding fluctuations, ω_ν is chosen such that the relative ν frequency is achieved. If for example the time is expressed in years and ν is set to yearly cycle, ω_ν should consequently be 2π. Moreover the phase ϕ_ν has to be chosen such that the maximum occurs when the prices are actually peaking. Consequently, in order to account for seasonality too, the process in (3.2) simply becomes

$$dP_t = K(\theta_t - P_t)\, dt + P_t \sigma dW_t \tag{3.4}$$

Given the initial condition P_s with $s < t$, the strong solution to the SDE (3.4), is

$$P_t = e^{\sigma(W_t - W_s) - \left(\frac{\sigma^2}{2} + K\right)(t-s)} \left(P_s + K \int_s^t \theta_u \, e^{-\sigma(W_u - W_s) + \left(\frac{\sigma^2}{2} + K\right)(u-s)} du \right) \tag{3.5}$$

The above solution may be easily retrieved by means of a suitable integrating factor. Let us define a new variable $Z_t := e^{-\sigma W_t + \frac{\sigma^2}{2} t} P_t$ and rewrite (3.2) in terms of the new variable. Applying Ito's lemma we obtain the following SDE

$$\begin{aligned} d(e^{-\sigma W_t + \frac{\sigma^2}{2} t} P_t) = \; & e^{-\sigma W_t + \frac{\sigma^2}{2} t} \, dP_t \\ & + P_t \left\{ e^{-\sigma W_t + \frac{\sigma^2}{2} t} \sigma^2 dt - e^{-\sigma W_t + \frac{\sigma^2}{2} t} \sigma \, dW_t \right\} \\ & - e^{-\sigma W_t + \frac{\sigma^2}{2} t} \, \sigma^2 \, P_t \, dt. \end{aligned} \tag{3.6}$$

Substituting the dynamic for P_t, after simplification we obtain

$$d\left(e^{-\sigma W_t + \frac{\sigma^2}{2} t} \, P_t \right) = \left(e^{-\sigma W_t + \frac{\sigma^2}{2} t} \, K \, \theta_t - e^{-\sigma W_t + \frac{\sigma^2}{2} t} \, P_t \, K \right) \, dt \tag{3.7}$$

In terms of Z_t, (3.7) results to be a linear ODE

$$Z' + K \, Z = K \theta_t \, e^{-\sigma W_t + \frac{\sigma^2}{2} t} \tag{3.8}$$

with solution

$$Z_t = e^{-K\,(t-s)} \, \left(Z_s + K \, \int_s^t \theta_u \, e^{K(u-s) - \sigma W_u + \frac{\sigma^2}{2} u} \, du \right) \tag{3.9}$$

which exactly matches equation (3.5).

Concerning the distributional behaviour of (3.5), little can be said because of the time-varying term θ_t. The long term mean indeed, being inside the integral, affects the limit distribution of the process P_t in a non trivial way. However, if we restrict ourselves to the simpler case of a constant mean reversion term, we can retrieve the limit distribution of the process, that in this case is the one given in equation (3.2). Its solution, has the form of equation (3.5), but with the now constant term θ, out of the integral. Dufresne (1990) shows that the limit distribution of the integral of the

exponential of the brownian motion is the Inverse Gamma. In particular he proves that

$$\int_0^\infty e^{aW_s+bs}ds \rightsquigarrow \frac{2}{a^2 Z_{2b/a^2}} \tag{3.10}$$

where Z_ν is a gamma variable with shape parameter ν, $a \neq 0$ and $b > 0$ in order to insure stationarity. Hence, as the limit distribution of the process P_t , with constant θ, depends only on the behaviour of

$$K\theta \int_0^\infty e^{-\sigma W_u + \left(\frac{\sigma^2}{2}+K\right)u}du, \tag{3.11}$$

we can easily conclude that, given $K > -\sigma^2/2$, the stationary distribution of (3.5) is an Inverse Gamma distribution with parameter $1 + 2K/\sigma^2$, up to a multiplicative constant. In other words:

$$P_t \rightsquigarrow \frac{2K\theta}{\sigma^2}\frac{1}{Z_{1+2K/\sigma^2}}. \tag{3.12}$$

Moreover Dufresne (2001) derives a general formula for all the moments of a larger class of mean-revering processes, from which can be easily derived the corresponding moments for the process (6.1). Let us define $m_q(t) = \mathbb{E}P_t^q$ to be the q-moments of the process P_t, with $q = 0, 1, ...$ and let $\bar{p} \geq 0$ be the initial value of the process. It is shown that the moments satisfy the following system of ODEs:

$$\begin{cases} m_q'(t) &= a_q m_q(t) + b_q m_{q-1}(t) & q \geq 1\ t > 0 \\ m_q(0) &= \bar{p}^q & q \geq 0 \end{cases} \tag{3.13}$$

where

$$\begin{aligned} a_q &= q(-K) + \frac{q(q-1)\sigma^2}{2} \\ b_q &= qK\theta \end{aligned} \tag{3.14}$$

If the $\{a_q\}$ are all distinct, the solution of (3.13) is

$$
\begin{aligned}
m_q(t) &= \sum_{j=0}^{q} d_{qj} e^{a_j t} \quad q = 0, 1, ...Q \\
&\text{with} \\
d_{qj} &= q! \sum_{i=0}^{j} \frac{\bar{p}^i (K\theta)^{q-1}}{i!} \prod_{l=i\,, l\neq j}^{q} \frac{b_l}{a_j - a_l} \quad j = 0, ...q
\end{aligned}
\tag{3.15}
$$

In particular we report the expressions for the mean, M_t and the variance V_t, conditional to P_s.

$$
M_t = \quad \theta + (P_s - \theta) e^{-k(t-s)}
$$

$$
V_t = \quad e^{(\sigma^2 - 2K)(t-s)} \left(P_s^2 - \frac{2\theta(P_s-\theta)}{1-\frac{\sigma^2}{K}} - \frac{\theta^2}{1-\frac{\sigma^2}{2K}} \right) - e^{-2k(t-s)} (P_s - \theta)^2 + e^{-k(t-s)} \frac{2\theta(P_s-\theta)}{\frac{K}{\sigma^2}-1} + \frac{\theta^2}{\frac{2K}{\sigma^2}-1}
$$

Summing up, we have proposed a regime-switching spot price model which is able to reproduce the main features of the observed electricity-price time series, such as price dependent volatility, mean-reversion, seasonality and spikes occurrences. The latter, in particular, has not been achieved by mean reversion neither by adding a jump component, but with a non parametric approach: a double bootstrap procedure based on the outcome of the R_n-WTMM applied on the spot price time series. This proposed solution provide us with a lot of flexibility in terms of possible trajectories shapes: both positive and negative spikes are allowed, with different duration; multiple spikes are contemplated as well, contrary to many of the models proposed so far in the literature (see the review in Section 3.1). Moreover, a small number of parameters are needed, and Markovianity is preserved (for a detailed discussion on the Markovianity issue, refer to Section 4.3).

Chapter 4

American Option Pricing

American option pricing is one of the most challenging problems in modern derivative finance and its goal is even more valuable in an electricity market setting. As we have shown so far, the peculiarity of the electricity prices are the high volatility movements in conjunction with a spiky behaviour. This intuitively implies that the early exercise feature of an American-style derivative to be extremely valuable; even a deep out-of-the-money option may lead to high gains if a spikes occurs.

Let us consider an American option contract on spot electricity supplies $f(t)$ and consider as illustration the put case.[1] Given an underlying complete probability space $(\Omega, \mathcal{F}, P)$ and finite time horizon $[t, T]$, the theoretical price is

$$P_A(t, T, K) = \sup_{\tau \in S_{t,T}} \mathbb{E}^* \left[e^{-\int_t^\tau r(s)ds} (K - f(\tau))^+ | \mathcal{F}_t \right] \tag{4.1}$$

where K is the strike, $S_{t,T}$ the set of $\mathcal{F}_t$-stopping times no grater than T and the adapted filtration $\mathcal{F}_t$, represents the current information. The mathematical problem then is an optimal stopping problem. From the theory it is well known that the value process of the optimal stopping problem can be characterized as the smallest supermartingale majorant to the discounted reward (Snell envelope).

So far an analytical closed-form solution is not available and several different approaches may be followed. For a recent and detailed review, we refer to Barone-Adesi (2005).

We decide to adopt numerical methods based on Monte-Carlo techniques in the light

[1] For positive spikes American calls are more interesting. However, we illustrate here the put case to give relevance to the unusual presence of negative spikes in the analysed time series.

of Longstaff and Schwartz (2001) pricing algorithm. The starting point is to replace the time interval of exercise dates by a finite subset, approximating in so doing the American option by a so called Bermudan option; the finer is the time discretization, the better the original American option is approximated. A control of the error due to the restriction of the stopping time is generally easily obtainable. [See Clement et al. (2003) for instance]. The solution of the discrete optimal stopping problem reduces to an effective implementation of the dynamic programming principle. The key quantity to determine is the conditional expectation involved in the iteration of dynamic programming, that is we need to determine at each exercisable date the expectation under the risk neutral measure of the discounted future cash-flows, conditional to the adapted filtration at the time of valuation; in short the *continuation value* of the option. The Longstaff-Schwartz solution is to approximate this value by projecting future cash-flows on a set of orthonormal basis functions and by cross-sectionally regressing the projections on the state variables. The formal justification of this procedure relies on Hilbert space theory; assuming that the conditional expectation we are looking for, is an element of the $\mathcal{L}^2$ space of square-integrable functions relative to some measure, it has a countable orthonormal basis, henceforth the conditional expectation can be represented as a linear function of the elements of the basis. As of the basis choice, several alternatives can be distinguished, ranging from the simple power polynomial to Laguerre, Hermite, Legendre, Chebyshev, Jacobi and even Fourier series. The robustness of the Longstaff-Schwartz algorithm, relatively to the choice of the basis function and the order of approximation, has been widely confirmed.

To summarize, once we have simulated a given number, say M, of trajectories of the underlying price process under the risk-neutral measure, the core of the pricing algorithm starts: the backward induction procedure. Starting from the maturity date and at each exercisable time up to the date of valuation, we compute the cash-flow from immediate exercise and the continuation value as just explained. Now, for each path, the comparison between the intrinsic value and the continuation one triggers the exercise decision. At the end of the backward procedure, our information consists of all the optimal exercise dates and their corresponding cash-flows. The sample average of these suitably discounted cash-flows is the option value.

In order to apply the Longstaff-Schwartz procedure, the first problem we have is how to simulate the needed trajectories of the underlying (i.e. spot electricity price). To

this purpose we still have to specify how the electricity price process evolves inside the spike regimes. This is the content of the next section.

4.1 The spike regime process

So far we have specified a spike regime in terms of occurrence times and peaks amplitudes. Those being the fundamental characteristics of a spike, we decide to describe the detailed price evolution in this regime only for simulation trajectories rather than price modelling purposes. To this end, we need a process that, if on one side respects the general features of the electricity market, on the other is bounded with respect to the final value. Once it will be the spike on-peak value and the other it will be the coming-back-to-normality price, both indeed obtained by the bootstrap procedure previously illustrated. In light of these considerations we propose to use an Ornstein-Uhlenbeck Brownian Bridge. Widely used in finance in several context, the standard Brownian Bridge is constructed in order to converge to zero at the endpoint T. Given an arithmetic O-U process we can define the corresponding bridge towards zero simply introducing a time varying drift parameter $K(t) = \alpha/(T-t)$, with α strictly positive. Now in order to get the convergence to a given value different from zero, we introduce another parameter, $\theta(t)$, in the drift. Given the dynamics

$$dP_t = (\theta_t - \frac{\alpha}{T-t})P_t dt + \sigma dW_t \tag{4.2}$$

the solution conditional to an initial value P_s is

$$P_t = P_s \left(\frac{T-t}{T-s}\right)^{\alpha} + \int_s^t e^{-\int_u^t \frac{\alpha}{T-q}\,dq}\,\theta_u du + \sigma \int_s^t \left(\frac{T-t}{T-u}\right)^{\alpha} dW_u \tag{4.3}$$

with $s < u < t$. In order to force the convergence of P_t to a constant value, say Q, as $t \to T$, we need to solve the following integral equation

$$\int_s^t \left(\frac{T-t}{T-u}\right)^{\alpha} \theta_u \, du = Q. \tag{4.4}$$

Simply differentiating with respect to the upper integration bound t we obtain

$$-\alpha \int_s^t \frac{(T-t)^{\alpha-1}}{(T-u)^{\alpha}}\,\theta_u \, du + \theta_t = 0 \quad \Rightarrow \quad \theta_t = \frac{\alpha}{T-t}\,Q \tag{4.5}$$

which immediately leads to the solution

$$P_t = \left(\frac{T-t}{T-s}\right)^{\alpha} (P_s - Q) + Q + \sigma \int_s^t \left(\frac{T-t}{T-u}\right)^{\alpha} dW_u \tag{4.6}$$

As it can be easily verified for $t \to s$ $P_t = P_s$ and for $t \to T$, the diffusion vanishes and the drift converge to Q, giving exactly $P_t = Q$ as we want. P_t is normally distributed, with mean and variance conditional to the initial value P_s respectively equal to A_t and B_t

$$A_t = \left(\tfrac{T-t}{T-s}\right)^{\alpha} (P_s - Q) + Q$$

$$B_t = \tfrac{\sigma^2 (T-s)}{2\alpha - 1} \left[\tfrac{T-t}{T-s} - \left(\tfrac{T-t}{T-s}\right)^{2\alpha}\right]$$

4.2 The simulated electricity price process

From all the consideration done so far let us resume all the assumptions and let us outline the overall structure of the simulated electricity process.

The state variable to simulate is the spot price evolution P_t. It is assumed to follow a two-regimes process. The transition from a regime to another is identified by a sequence of stopping times, represented by the left and right basis of the spike events detected by the R_n-WTMM algorithm. In the spirit of the definition given in (3.1), we are referring to the set of couples $\{b^n_{left}(j), b^n_{right}(j)\}_{j=1,\dots,N/2}$, a couple for each detected spike. For simplicity, we indistinguishably call the generic stopping time τ_i, where

$$\{\tau_i\}_{i=0,\dots,N} \quad \text{with the convention that} \quad \tau_0 = 0\,, \tau_N = T.$$

Let us note moreover that at this stage, for simulation purpose, we are not focusing anymore on the iteration order n of the spike detection algorithm, that is why we have drop it in the stopping times definition as well as in all the following quantities. So, for a fixed order of iteration n fo the spike detection algorithm, the double bootstrap procedure illustrated in the previous chapter, creates dynamically two sets of information

$$\{I_p\}_{p=1,\dots,N/2}$$

$$\{D^j_{left}, D^j_{right}, J^j_{left}, J^j_{right}\}_{j=1,\dots,N/2}$$

respectively the interbases times lengths and the quadruplets of the spikes configurations. The size of the stopping times set, is obviously double with respect to the length of the bootstrapped samples: one bootstrap indeed provides us with $N/2$ interbases times, that is determines the interbases regimes, while the other bootstrap output is needed to determine other $N/2$ spike regimes, for a total amount of N regimes plus the initial time instant τ_0, set for convention equal to zero. Finally, in order to flag each regime, we define a two-value function r_t such that

$$r_t = \begin{cases} 0, & \text{if} \quad \tau_{2j-2} < t \leq \tau_{2j-1} \qquad \text{(interbases regime)} \\ 1, & \text{if} \quad \tau_{2j-1} < t \leq \tau_{2j} \qquad \text{(spike regime)} \end{cases} \tag{4.7}$$

Now, we have all the information to simulate the price P_t, which is obtained as

$$dP_t = \begin{cases} K(\theta - P_t)dt + \sigma P_t dW_t & \text{, if} \quad r_t = 0 \\ \frac{\alpha}{\gamma_t - t}(w_t - P_t)dt + \widetilde{\sigma} dW_t & \text{, if} \quad r_t = 1 \end{cases} \tag{4.8}$$

Under the interbases regime however, we need two further pieces of information, which are derived by the bootstrapped quadruplet values. The Brownian bridge dynamic to be fully defined required also the end value w_t and the end time γ_t towards it is directed. It has to be stressed that these values are not constant throughout the spike regime, but depending on whether we are to the left or to the right of the spike location, they assumed a different value. In details we have that

$$\gamma_t = \begin{cases} \tau_{2j-1} + D^j_{left} & t \leq \tau_{2j-1} + D^j_{left} \\ \tau_{2j-1} + D^j_{left} + D^j_{right} = \tau_{2j} & t > \tau_{2j-1} + D^j_{left} \end{cases} \tag{4.9}$$

$$w_t = \begin{cases} P_{\tau_{2j-1}} + J^j_{left} & t \leq \tau_{2j-1} + D^j_{left} \\ p_{\tau_{2j-1}} + J^j_{left} + J^j_{right} = \tau_{2j} & t > \tau_{2j-1} + D^j_{left} \end{cases} \tag{4.10}$$

In the aforementioned setting, we assume that we always start with an interbase

regime (i.e a period of normality). This is only apparently restrictive for at least two main reasons: it is sufficient to have in the interbase times sample, just one length equal to zero (as it happens in our sample) to give full generality to the possible starting regimes; further, in the simulation procedure, we can assume to start the creation of the temporal grid in an indefinite far away time in the past and then choose as starting point a time instant in the middle. This gives full generality, in consideration also of the fact that in so doing, it is highly probable that the starting point may fall in the middle of an already started regime, which is indeed, the most reliable assumption. Never the less, if with a new regime we have to start, the interbases regime, given its average length, definitely larger than the average spike regime length, is the obvious choice. In figure (4.1) a schematization of the typical time grid follows.

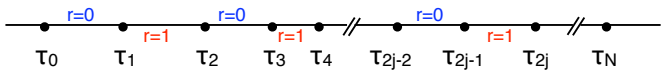

Figure 4.1: Regimes structure and stopping times.

4.3 Markovianity issue

Now, we know how to simulate a continuous trajectory of the P_t process but, in order to apply the Longstaff and Schawartz algorithm, we still have to clearly identify, which is the set of information required to our knowledge, to consider the P_t price evolution a Markov process. The variables which carry such information will define the basis onto which we will project the discounted future payoffs to estimate the continuation value of the American contingent claim. The continuation value, as we have already remarked, is the decision triggering quantity to select the optimal exercise strategy, which in turn solve the free-boundary problem.

Let us defined a variable β_t to be the countdown of the length of the generic regime in hand at time t. Under the spike regime this variable is already defined as the denominator of the Brownian bridge drift. Under the interbases regime instead, as soon as the interbases length, the generic extraction I_p, is bootstrapped, the countdown variable decrease linearly as the process evolves. Hence in symbols

$$\beta_t = \begin{cases} I_p - t & , r_t = 0 \\ \gamma_t - t & , r_t = 1 \end{cases} \tag{4.11}$$

In between each regime, the β_t variable is a continuous and monotonically decreasing linear positive function with a discontinuity in correspondence of each change of regime. The width of the jump is the total length of the new regime that is going to start. From an operational point of view, if we observe a β_t grater than zero, we know that in the following time instant its value will be decreased by one; if we observe instead, a β_t equal to zero we know we are at the end of a regime and we have to perform a new bootstrap extraction.

$$\Delta\beta_t := \beta_{t+1} - \beta_t = \begin{cases} -1 & , \beta_t > 0 \quad \forall r_t \\ I_p - 1 & , \beta_t = 0 \quad , r_t = 1 \\ D^j_{left} + D^j_{right} - 1 & , \beta_t = 0 \quad , r_t = 0 \end{cases} \tag{4.12}$$

The P_t process, as described in equation (4.8), given the knowledge of the regime status, the r_t value, and the countdown variable β_t just defined, is a Markov process. In first approximation this is true, however if we are under the spike regime, $r_t = 1$, further information are required to distinguish between the different Brownian bridges, namely the end value variable w_t defined in equation (4.10) is required. Hence in a rigorous way, the set of variables $\{P_t, r_t, \beta_t, w_t\}$ define univocally the evolution of the process P_t. This, in terms of the Longstaff and Schwartz algorithm, means that at every step of the backward induction procedure, we can estimate the continuation value of the option as a linear combination of the elements of the chosen basis functions up to a certain order, evaluated for all the observed realizations of the state variables, in our case P_t conditional to r_t, β_t and eventually w_t. Just as an example, we may choose as possible functional form of the basis functions, the power polynomials, say up to the second degree. In this case we have to fit a constant, and the coefficients for the terms in P, P^2, β, β^2 and for the cross term $P\beta$ for all the sample paths that in the given instant are in the interbases regime, for which $r_t = 0$; for all the other sample paths which have a value of $r_t = 1$ we have to estimate another set of coefficients, but this time for an extra variable too, that is we have a constant and terms in P, P^2, β, β^2, w, w^2 and for the cross terms Pw, $P\beta$, $w\beta$. A total of six basis functions for the interbases regime paths and ten basis functions for the spike regime paths. This is relatively cumbersome and still nicely tractable.

Obviously we can add more terms to improve the estimation, even if it is been widely tested by Longstaff and Schwartz (2001) that additional basis add little or no effect on the result.

4.4 The Simulation Method

The Monte Carlo simulation of the Longstaff-Schwartz pricing technique, as any backward induction procedure, is a very memory intensive procedure, requiring to store the entire matrix of all the simulated values of all the trajectories; in order to have a good accuracy the dimension grows very fast, obliging us to work with very 'heavy' objects. A nice trick to overcome this problem is been suggested by Chan et al. (2004). The key idea is to simulate the random process that moves your underlying, not in the traditional way, in the time-increasing direction, but instead backward moving: in the same direction of the pricing procedure. This results in a very efficient allocation of the memory storage: moving as the pricing induction moves, there is no need to save all the price values and at every valuation time instant, we can simply overwrite the new values. So, we do not work any more with matrices, but just with vectors of dimension given by the number of desired trajectories for the Monte Carlo, say M, and the storage requirement shrinks from $O(MN)$ to $O(M)$ given N to be the order of the discretization time grid. In short the properties of a whatsoever random number generating algorithm used, are been exploited . As we know, to generate a proper random number by means of an algorithm, is in itself a contradiction with the inner essence of randomness. By the way we are not questioning at all on the goodness of the random number generating algorithms, commonly accepted as such, but we simply want to exploit them. The key is the so called *seed*, a sort of starting point; giving as input the same seed, we will obtain the same random number as output on any computer. This means we can pilot the generating algorithm to give us what we want. The idea is simple and logical, but the question is if it is possible and how we simulate backward the random process that leads our underlining. Chan et al. (2004), in their paper, address the case of a geometric brownian motion, which results to be the perfect candidate to be backward simulated as it has a closed form solution and the random shocks enter the solution in an order-invariant way, as a simple summation. These two features simplify the procedure, even if we can generalize the backward simulation technique to any random process.

Let us now, shortly review the methodology for the geometric brownian motion as an easy benchmark. The strategy to follow is: to simulate one shot, the entire trajectories in the usual way in order to obtain (i) the final value, the starting point in the backward simulation; (ii) the seed that has generated the trajectory in hand; (iii) the cumulative sum of all the random shock needed to get the final value. Now the backward simulation could start, simply imposing the current seed equal the one corresponding to a given paths and at each step subtracting a random number to the cumulative sum. In formula what happens can be schematize as follow. Let us analyse the generic j-th trajectory and assume to discretize the time horizon into N time steps of equal length; in the traditional time marching situation the simulated price, after the i-th time step is:

$$\textit{Forward Path:} \quad \mathbf{P}_i = \mathbf{P}_0 e^{i(\mu - \frac{\sigma^2}{2})\nu + \sigma\sqrt{\nu}(\epsilon_1 + \epsilon_2 + \ldots + \epsilon_i)} \tag{4.13}$$

where the ϵ_i are independent and identically distributed standard normal random numbers. Now starting from the final value up to the first one our backward path will evolve like this:

$$\begin{aligned} \textit{Backward Path:} \quad & \mathbf{P}_N = \mathbf{P}_0 e^{N(\mu - \frac{\sigma^2}{2})\nu + \sigma\sqrt{\nu}(\epsilon_N + \epsilon_{N-1} + \ldots + \epsilon_1)} \\ & \ldots \\ & \mathbf{P}_i = \mathbf{P}_0 e^{i(\mu - \frac{\sigma^2}{2})\nu + \sigma\sqrt{\nu}(\epsilon_N + \epsilon_{N-1} + \ldots + \epsilon_{N-i+1})} \\ & \ldots \\ & \mathbf{P}_1 = \mathbf{P}_0 e^{(\mu - \frac{\sigma^2}{2})\nu + \sigma\sqrt{\nu}\epsilon_N}. \end{aligned} \tag{4.14}$$

Let us observe that the random shocks subtracted step by step are exactly in reverse order with respect to the traditional forward path generation. Nevertheless, this upsidedown order, does not compromise the nature of the random process in hand: we still obtain a brownian motion, a different one of course, but with the same behaviour and with a 'final' value coinciding with the true initial one. This is what we call the time order-invariance property of the random process solution, relatively to the random shocks themselves. This property makes our simulation easier, as we, having stored the initial seed, can generate only one random number at each step, disregarding indeed, the original order. Unfortunately it is not always the case, and processes with much more complicated solution form than the brownian motion one require to preserve the order of the shocks, to not modify their intrinsic nature. This

is the case of the process (4.8) we are interested in. To preserve the order of the shocks, has obviously a time-computational cost, as we are forced at each step to draw the entire sequence of random number up to that date in order to use only the last one. To give an idea of the slowing effect, for the process (4.8), we obtain in average a 0.06 seconds extra time for each year of simulated trajectory.

For completeness, we mention that, even if the process we could be interested to simulate backwards, does not possess a closed form solution, we can still get rid of the problem. Given indeed, any discretization scheme, the Euler or the Milstein ones for instance, of the corresponding dynamic, we simply have to express the preceding, in order of time, state variable as a function of the following one.

Summing up, to apply correctly the backward simulation technique, we have to distinguish first between processes with closed form solution or not and, with functional form which possesses the time order-invariance property or not. By the way , the memory reduction, obtained in all the cases, will be achieved at a different computational cost. It can be objected that there is no interest in slowing down the procedure, but the gain in terms of memory storage requirement is considerable, and to our opinion worthwhile adopting, considering moreover that the gain may be even more valuable also in terms of time; the more you increase the M and N parameters indeed, the higher is the chance to have to turn to the out-of-core memory[2] in storing the intermediate prices in the traditional forward simulation procedure.

4.5 Tests and numerical results

4.5.1 Independence tests

In the preceding sections we have performed a non parametric bootstrap , simply justifying the crucial independence assumption by intuition, independence which however sounds reasonable. Let us check the reliability of this hypothesis first for the selected sample of interbases time and then for the quadruples of the prices jumps. For the following numerical tests we are refereing to the output of the third order of iteration of the recursive wavelets transform modula maxima which leads to 159 detected singularities and consequently to the same number of interbase regimes; let us denote

[2]It is well known that the usage of this memory strongly slow down the computational time. It intervenes only to make up CPU's deficiencies.

the vector $\mathbf{I}^3$ to be the corresponding vector of the interbase time distances as already defined in the previous section. In the sequel, some statistics and the corresponding histogram, of $\mathbf{I}^3$ follow. Let us note that also interbase regime of length zero are likely to occur, meaning that it is reliable to observe more than a spike regime in a row, feature that is generally not captured by traditional regime-switching solution. On average the length of the interbase regime is two weeks, stressing the very turbulent nature of this market given moreover that the longest, period of normality detected is less than two months. In figure (4.3) are shown the lengths of the interbase regimes as they come in a row. Our impression is that there is no time correlation between such lengths; in other words after a short interbase regime it is not obvious that another short one follows, which would have meant that after a spike the chance of having another spike would have been greater. So even a very first look of the data seems to clearly suggest intrinsic independence. From the Box-Jenkins representation of the autocorrelation function in figure (4.4) indeed, we can conclude that there are no significant autocorrelations and we can assume a randomness in the data. Almost all of the autocorrelations fall within the 95% confidence bounds. In addition, there is no apparent pattern, exactly as we expect to see for random data. A few lags slightly outside the 95% and 99% confidence bounds, do not necessarily indicate non-randomness. For a 95% confidence interval, we might expect about one out of twenty lags to be statistically significant due to random fluctuations. Absence of correlation is a first step, but it is not sufficient to assure the independence of the observations. Furthermore, we cannot say that our sample is drawn from a Normal distribution, and neither that it looks like normally distributed. A rough look at its histogram in figure (4.2) shows an evident positive skewness.

$\min(\mathbf{I}^3)$	=	0
$\max(\mathbf{I}^3)$	=	56
$\mathrm{mean}(\mathbf{I}^3)$	=	19
$\mathrm{median}(\mathbf{I}^3)$	=	16

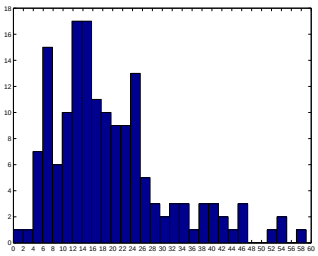

Figure 4.2: Histogram of the length of the interbases regimes expressed in days.

To test the *i.i.d.* hypothesis we perform a BDS[3] test. The test is based on the es-

[3]W.Brock, D. Dechert, J. Scheinkman originally developed the test in 1987.

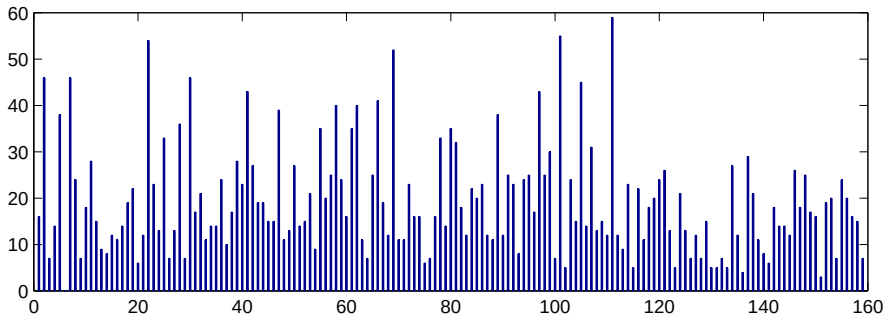

Figure 4.3: Sequence of the interbases time lengths.

timation of the correlation integral[4] at various dimensions. The correlation integral of dimension m measures the spatial correlation of a sample of N scattered points in m-dimensional space and picks up the fraction of m-dimensional pairs of points in that sample whose distance from each other is less than a fixed radius ϵ. Where the observations are truly *i.i.d.*, there is a power relationship between the correlation integral for dimension 1 and the m-dimensional correlation integral. Brock et al. (1988) showed that the standardized difference between the correlation integral for dimension m and the 1-dimensional correlation integral to the power m is asymptotically normally distributed regardless of the ϵ and the dimension m chosen.

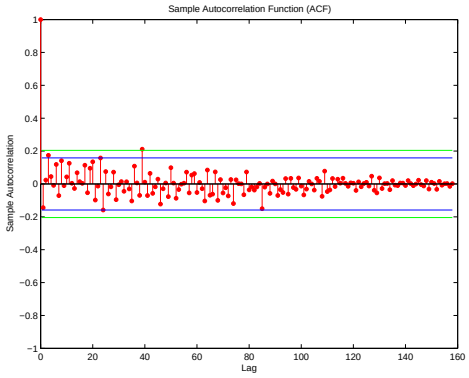

Figure 4.4: Sample ACF. Confidence bounds at 95%, blue lines and at 99% green lines.

The question is that we are dealing with a small sample (159 observations) and the standardized normal probabilities may lead to reject the independence hypothesis. To this purpose we adopt the small sample quantiles tabulated by Kanzler (1999). Even though Brock et al. (1992) point out that 'even with 50 to 200 observations, BDS test performs fairly well compared to the other tests'. Kanzler clearly showed that the finite sample distribution is fat-tailed, always displaying excessive kurtosis increasing so the error with which one would reject the null hypothesis of independence when the data was,

[4]The concept of correlation integral was used for the first time in Grassberger and Procaccia (1983) in tests for chaos and non-linearity

in fact, independent. Furthermore, the size of this error varies considerably not only with the sample size, obviously, but also with the embedding dimension and the dimensional distance. So an appropriate choice of these two parameters becomes crucial. It's been shown that better results are obtained with the radius ϵ of the order of 1.5-2 times the standard deviation of the tested data, with a correlation integral for the 1 dimension ranging from 0.7 to 0.84. We report below the obtained results for up to the sixth dimension.

Panel 1: c1=~ 0.7 ε = 1.5 σ

Dimension	w	c	c1	p-value
2	-0.8375	0.5117	0.7193	0.4023
3	-1.6472	0.3655	0.7265	0.0995
4	-0.8994	0.2669	0.7267	0.3684
5	-0.1774	0.1979	0.7251	0.8592
6	-0.5864	0.1434	0.7302	0.5576

Panel 2: c1=~ 0.84 ε = 2 σ

Dimension	w	c	c1	p-value
2	-0.5521	0.7102	0.8443	0.5809
3	-1.9243	0.5982	0.8510	0.0543
4	-1.5217	0.5041	0.8510	0.1281
5	-0.7609	0.4318	0.8503	0.4467
6	-1.1183	0.3658	0.8537	0.2634

Figure 4.5: Output of the BDS test. w is the BDS statistic, c is the correlation integral at different dimensions, c1 represents the first-order correlation integral estimate computed over the last $N - m + 1$ observations (where N = sample length, m = dimension). Finally the p-value indicates the two side probability of the failure to reject the null hypothesis for the standard Normal distribution.

In both the performed cases reported in Panel 1 and Panel 2, we do not reject the null hypothesis at considerable high probabilities, on a two-side test. Only the 3-dimension case, in Panel 1, appears slightly under the 5% probabilities (one side), and the 3- and 4-dimension cases in Panel 2 denote a low significance level. But, if we take account of the non exact convergence to the Normal distribution, because of the small sample under analysis, we can conclude that the BDS statistic estimated leads to a failure to reject the independence assumption, at all the dimension considered, at a level definitely grater than the 5% (one side hypothesis test). We are not able to invert exactly the percentiles represented by the w values, but the tabulated quantiles up to the 5% show clearly this tendency.
In the sequel, given the BDS test results, we feel confident to consider the set of the interbases distances retrieved from R_3-WTMM, independent observations.

Apart from the interbases distances, we claim the independence also of the quadruples $\{\mathbf{Q}_i\}_{i=1,\dots n}$ defined as the set of variables $(\mathbf{J}^n_{left}, \mathbf{J}^n_{right}, \mathbf{D}^n_{left}, \mathbf{D}^n_{right})$, for a given sample size n, that we retrieve from stopping the recursive wavelet transform modula maxima,

Dimension	left 5%	right 5%
2	-1.9799	1.9413
3	-1.992	1.9413
4	-2.0199	1.9292
5	-2.0099	1.9553
6	-2.0202	1.9531

Dimension	left 5%	right 5%
2	-2.1345	2.1105
3	-2.1687	2.0784
4	-2.1969	2.0481
5	-2.203	2.0481
6	-2.1969	2.0441

Figure 4.6: The left table refers to the case of $\epsilon \simeq 1.5\sigma \simeq 16$, whereas the right table concerns the $\epsilon \simeq 2\sigma \simeq 23$ case.

	$\mathbf{J}^{159}_{left}$	$\mathbf{J}^{159}_{right}$	$\mathbf{D}^{159}_{left}$	$\mathbf{D}^{159}_{right}$
min	-93	-83	2	2
mean	43*	38*	3	3
max	431	450	14	11

Table 4.1: * The jump average is been calculated for the absolute value, as both positive and negative jumps are present.

at the third step. The main statistics of the selected quadruples are listed in table (4.5.1).

To test the independence we can perform the BDS test indifferently on the $\mathbf{J}^n_{right}$, or the $\mathbf{J}^n_{left}$. What we claim indeed, is that the variables in the quadruples are highly correlated between each other, but that they represent *i.i.d.* observation on its own. In the following table (figure 4.7) the BDS test is performed for the $\mathbf{J}^n_{left}$; for the other variables the results are very similar and so we have not reported them.

As in the previous output table the p-value is referred to the standardized Normal distribution, hence to check for the appropriate small sample quantiles, we can refer to the left table in figure (4.6) being the sample length the same. By the way in this case also the row approximation given by the standard Normal quantiles shows a very strong level of significance, safely leading us to conclude the independence of the variable in hand, $\mathbf{J}^n_{left}$.

Dimension	w	c	c1	p-value
2	-0.7841	0.4807	0.6980	0.4330
3	-0.3177	0.3341	0.6968	0.7507
4	0.0012	0.2342	0.6956	0.9990
5	0.1139	0.1702	0.7002	0.9093
6	0.2643	0.1204	0.6987	0.7915

Figure 4.7: BDS statistic output for $\mathbf{J}^{159}_{left}$ ($\epsilon \simeq 1.5\sigma$).

4.5.2 Option prices

Let us investigate now some numerical results obtained applying the bootstrapped version of the Longstaff and Schwartz pricing method and an electricity spot price evolving as described in the previous chapter with trajectories simulated according to equation (4.8). The table below, figure (4.8), shows the price of a Bermudan option with different times to maturity and spanning from deep-out of the money to deep-in the money cases. The allowed exercise frequency is a daily, and the clock of the brownian motions used is set to 5 minutes, that is every five minutes the brownian motion is calculated to better approximate continuity, even if the price is registered only once a day. The R_n-WTMM has been halted at the third order ($n = 3$) leading to a set of 159 singular points detected, which implies 159 relevant price jumps and 159 interbase times for the double bootstrap procedure. The volatility of the interbase regime is been set to $\sigma = 0.2$, whereas the volatility of the spike regimes is been set to $\widetilde{\sigma} = 0.3$; the long-term mean θ and the speed of mean reversion K are respectively been set to 80 and 0.1. The numerical results shown, are been obtained combining each of the $G = 100$ bootstrap samples of $\mathbf{I}^n$, with $N = 500$ every time different bootstrap samples of χ^n, for a total number of 50′000 trajectories simulated under the risk neutral measure.

American Put Prices

tau / K	70	90	105.09	119	140
1 m	6.0142	9.765	15.27	24.198	41.926
3 m	11.295	16.709	23.022	31.019	46.774
6 m	17.831	24.006	30.464	37.726	51.977
9 m	22.641	29.759	36.106	43.223	56.043

European Put Prices

tau / K	70	90	105.09	119	140
1 m	4.0603	7.008	11.827	20.48	38.079
3 m	9.0478	13.243	18.756	26.05	40.68
6 m	15.127	20.127	25.642	32.218	44.761
9 m	20.172	26.129	31.452	37.557	48.947

Figure 4.8: American and European prices at different strike K and different time to maturity **tau**. The moneyness is enlighten in blue: $K = 105.09$.

The prices trends are perfectly coherent with what we are used to find; the option prices both in the European and in the American case are increasing functions of the time to maturity and of the strike price as well (being Put options), furthermore the American option prices strictly dominate the European ones. What is interesting is the huge degree of dominance. This is obviously due to the electricity prices evolution for which the right to choose when to exercise, has an incredible value, as in the length of few days, the market conditions may turn to be unfavourable.

Looking carefully the American percentage premia, we can do further considerations relative to the different impact of the strike and the time to maturity.

tau / K	70	90	105.09	119	140
1 m	0.324881	0.282335	0.225475	0.153649	0.091757
3 m	0.198955	0.207433	0.185301	0.160192	0.130286
6 m	0.151646	0.161585	0.158285	0.146	0.138831
9 m	0.10905	0.12198	0.128898	0.131088	0.126617

Figure 4.9: Percentage Premia. $(A - E)/E$

A first observation concern a certain degree of convergence of the premia as the maturity becomes longer and longer and the strike indeed, seams to be totally irrelevant, even if we have allowed for a wide variability of the strike itself. The conclusion that the strike matters really little, is perfectly in accordance with the spirit of electricity market. For prices with so high volatility, even a huge gap in the strike price is a tiny difference with respect to tremendous variation that could very likely happen in a short time; consequently having more time to our disposal has a really high value, which tends to be a characteristic of the price process itself and to converge to a given value. Only at very short maturity the different strikes play a stronger role: the more you are out of the money the higher is the advantage in holding an American option, as , given the particular nature of the electricity market, it is very likely to witness in the middle to a sharp price transition to profit from, whereas exactly at the maturity day we expect to be more or less at the same price level. For the same reasoning, the more we are in the money, the more our advantage in holding an American option becomes evident in the middle maturities, as the longer horizon allows to encounter such a favourable situation to overcome the intrinsic value of the option already positive.

Chapter 5

Electricity Futures market analysis

5.1 Nord Pool Futures Market

In the following analysis we refer to a database of daily futures quotations in the Nord Pool market, spanning from September 1995 to October 2005. During this decade many changes took place in the issuing and trading rules of the futures contracts in response to changing market requirements and consequently to increase liquidity and promote trade.

Mainly, we have witnessed to a progressive shortening of the available time horizon for trading. At the beginning futures contracts were issued up to three years in advance, they were classified in *Season* (four months), *Block* (four weeks), *week* and *day* contracts, deriving one from the other in a cascading structure: as the corresponding maturity approaches, the season contract were split in block ones, the block in week, the week in day contracts and so on up to maturity.

Since the end of 1999 the Season futures were no longer issued and the maximum time horizon was reduced to $8 - 12$ months. As of Fall 2003 the Block futures were suspended in favour of forward month contracts and now only Week and Day futures contracts are listed with 8 consecutive contracts in a continuous rolling cycle, without any cascading mechanism. This results in a further shortening of the futures horizon, now up to 8 weeks.

The market thus, seems to prefer short-term futures close to maturity and long term forwards at the far end of the time horizon. The main reason lays in the different settlement mechanism: financial settlement of futures includes daily mark-to-market

settlement which requires a large amount of cash for the margin account updating, whereas the financial settlement of forwards involves no daily cash movements but requires posting cash collateral only during the delivery period starting at the contract's due date.

In order to overcome the substantial lack of homogeneity of the data, we decide to consider only the quotations in line with the present rules of issuing and trading; hence we take into account only week futures contracts from 1995 to 2005, consequently with a maximum time horizon of 8 weeks.

The futures prices evolution shows a clear convergence towards the spot price at delivery as the time to maturity approaches to zero, a behaviour perfectly in line with the futures theory, but exactly at the maturity date the coincidence dictated by the theory for the two prices, fails. In figure (5.1) we show this divergence. The average spread is around 0.9 unit of currency (NOK), but it spans from a minimum, in absolute value of 0.016 up to interesting peaks of 322 or -161 as well. Not surprisingly we have the wildest behaviour when the maturity of a futures contract falls within a spike regime: the futures market is a bad forecaster of the spot market. The explanation for this anomalous behaviour has to be searched, partially in the market clearing mechanisms.

Financial electricity contracts are cash-settled, they do not involve any physical delivery of traded volumes at the maturity. The settlement of financial contracts is based on changes between the underlining product price and the member's exposure in the market. In particular the Futures contract settlement has two components: (i) the daily mark to market settlement (obviously financially settled) and (ii) the final spot reference cash settlement. The last settlement on the delivery *period* means the financial settlement of the difference between the contract's last closing price before its maturity and the spot reference price for the corresponding hours in the delivery period, typically one week. This daily settlement occurs throughout the *delivery period*.

The futures clearing procedure implies that the futures and the spot prices refer to different objects; on one side the spot contract refers to a load in MWhours during a given hour, whereas on the other side the futures refers to an electricity supply for an entire week. Let us define $F(t,T)$ as the futures price at time t for maturity T and $P(t)$ the electricity price at time t. So, in the electricity market there is a structural misalignment regarding the underlying object when we check if $F(T,T) = P(T)$.

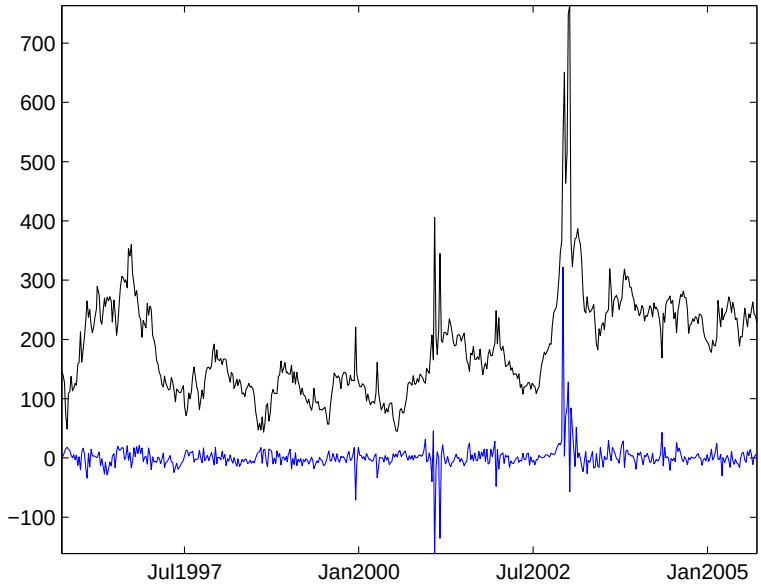

Figure 5.1: Future-Spot divergence at maturity (blue line) compared with the System Prices time series (black line)

In general we have that

$$F(t,T) = \mathbb{E}^{\mathcal{Q}}[P(T)|\mathcal{F}_t]$$

$$F(t,T) = \mathbb{E}^{\mathcal{Q}}[F(T,T)|\mathcal{F}_t] \tag{5.1}$$

where $\mathcal{Q}$ is the risk-neutral pricing measure. Now as we know that $F(T,T) = P(T)$ does not hold anymore, we want to determine $F(T,T)$ such that

$$\mathbb{E}^{\mathcal{Q}}\left\{\sum_{i=1}^{7}[F(T,T) - P(T+i)]|\mathcal{F}_T\right\} = 0 \tag{5.2}$$

This straightforward implies that

$$F(T,T) = \frac{1}{7}\mathbb{E}^{\mathcal{Q}}\left[\sum_{i=1}^{7} P(T+i)|\mathcal{F}_T\right] \tag{5.3}$$

Substituting $F(T,T)$ in (5.1), the general price of a futures contracts results to be:

$$F(t,T) = \frac{1}{7}\mathbb{E}^{\mathcal{Q}}\left[\sum_{i=1}^{7} P(T+i)|\mathcal{F}_t\right] \tag{5.4}$$

Note that this contract may be considered a forward start, in T, Asian option with strike zero.

The considerations conducted so far, lead to the theoretical price of a futures contract traded in the Nord Pool and moreover, give new insights regarding the advocated convergence futures-spot at maturity: it is no more $F(T,T) = P(T)$ to be verified, but rather equation (5.3). In order to estimate the expected value over the future spot realizations in the week following the maturity, we should introduce a model for the required simulations. At a simple data analysis stage, we just can take as a proxy the ex-post spot prices realizations. The financial implications are not trivial and shed new light on the futures-spot relation. The futures at maturity has to embed the expected evolution of the spot prices system over the next week, and we know that in an extremely volatile market as electricity, the risk of a spike has to be taken seriously into consideration.

The observed divergence futures-spot at maturity moreover, casts doubts over the forecasting ability of the futures prices states by the classical theory. Let us define the basis $F_t(T) - P_t$ as the contemporaneous futures-spot spread for a given time to maturity $T - t$ of the futures contract; if the futures prices were unbiased forecasts of the subsequent spot prices, we would expect the basis to perfectly anticipate the future variation in the spot price between t and T. In order to test this hypothesis we perform a conventional OLS-test which enlightens indeed, the poor forecasting capabilities of the futures quotations. We just have to regress the absolute change in the spot price over a given time period, as a function of the absolute basis measured at the beginning of the reference period or, even better, we can use relative measures for both variables. Below, the exact regression we have performed follows

$$\log\left(\frac{\bar{P}_T}{P_t}\right) = \alpha + \beta\,\frac{F_t(T) - P_t}{P_t} + \varepsilon_T \tag{5.5}$$

Note that, for coherence with the aforementioned peculiarity of the electricity futures settlement, the spot price change realized from t to T has to be calculated not with respect to the spot price P_T at maturity, but with respect to the average spot price that will prevail during the delivery period, which we denote by $\bar{P}_T$. According to the

Nord Pool settlement rules, as the delivery period starts three days after the futures end of trading, for the week-futures contracts we have that

$$\bar{P}_T = \frac{1}{7}\sum_{i=1}^{7} P_{(T+3)+i} \tag{5.6}$$

We test equation (5.5) both for the one week to maturity basis that for the four weeks. From the available data set of week-futures we collect respectively 521 and 464 observations for the one week to maturity and the four weeks to maturity variables weekly spaced indeed, but for the regression analysis we pick only one observation a month in order to avoid overlapping trading and consequently serial correlation in the variables themselves. We end up with sample sizes of 131 and 116 respectively. By the way, before performing the regressions, a careful look to the variables plot provide us with useful insights.

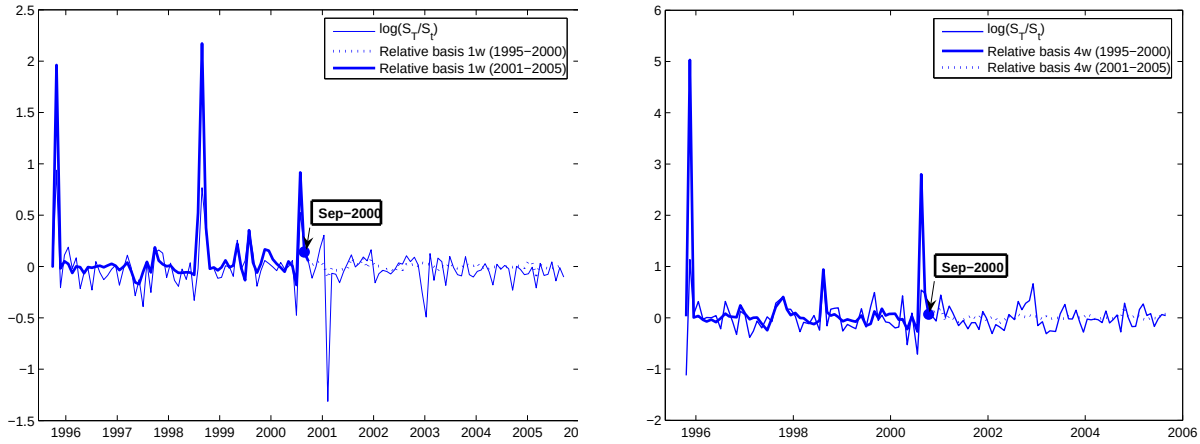

Figure 5.2: Graph of the relative basis (per cent) and of the relative spot price change in logarithm terms. One week to maturity (left) and four weeks to maturity (right).

In figure (5.2) respectively the one and four weeks basis have been plotted along with the relative change in the spot price. As stressed by the different mark-style, we witness an evident change during the last five years regarding the explanatory power of the basis over the spot price changes; whereas up to the end of 2000 the basis actually anticipates the spot price movements to a good extent, afterwards the things change drastically and the basis, which exhibits even a lower volatility, explains very little of the spot price changes. In light of these considerations we split in two our

sample to estimate separately the equation (5.5). A table of the regression outcome follows.

Time horizon: 1 week to maturity

	Sep-95/Sep-00	**Oct-00/Sep-05**	**Full sample**
Obs	65	66	131
α	-0.0413 (-2.4777)	-0.0515 (-2.4595)	-0.0444 (-3.09)
β	0.4749 (11.4035)	3.022 (4.7781)	0.4965 (9.7327)
R^2_{adj}	0.68	0.26	0.42
$DW^{\dagger}$	2.05	2.21	2.18
Lilliefors‡	0	0	0

Time horizon: 4 weeks to maturity

	Sep-95/Sep-00	**Oct-00/Sep-05**	**Full sample**
Obs	58	58	116
α	-0.032 (-0.8373)	-0.0219 (-0.8744)	-0.0177 (-0.7981)
β	0.2661 (5.5102)	1.3403 (2.9871)	0.2679 (6.6337)
R^2_{adj}	0.36	0.1	0.27
$DW^{\dagger}$	1.7	1.5	1.6
Lilliefors‡	0	0	0

† For a sample size of about 65 the interval to not reject the null hypothesis is [1.45,2.55], while for a sample size around 100 is [1.6,2.3]

‡ We set 0 in case of not rejection of the null hypothesis of normal distribution and 1 otherwise

Table 5.1: Spot price change versus relative Futures basis regression outcome. 1 week and 4 weeks to maturity time horizon.

It is worth mentioning that in the Nord Pool market, more than 55% of the generated electricity is based on hydropower, therefore reservoir technology plays a substantial role. If electricity as a commodity cannot be stored in general, hydroelectricity may be stored to some extent keeping water in the reservoirs. This is a clear advantage, which creates an asymmetry between producers' and consumers' spot/futures arbitrage possibilities via storage. The available reservoir data consists of weekly registration of the percentage of filling of the global reservoir capacity. Let us define $\mathbf{R}_t$ the reservoir time series. In figure (5.3) we show the relative basis between futures and spot prices, compared with the corresponding reservoir level $\mathbf{R}_t$.

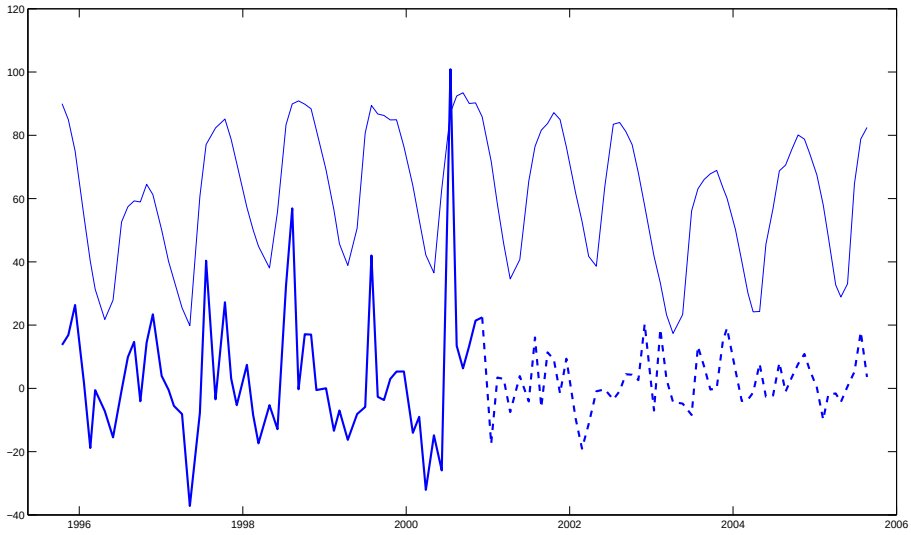

Figure 5.3: Relative percentage basis futures-spot with 4 weeks to maturity from September 1995 to December 2000 (solid blue line) and from January 2001 to September 2005 (dotted blue line), compared with the reservoirs level (thin blue line). Monthly observations

It can be noticed that the higher values of the basis are observed in accordance with extreme levels of the reservoirs. When the futures price is much lower than the spot we always observe reservoirs are almost at their minimum, whereas when the futures price widely exceeds the spot the reservoirs level lays mostly over the half reservoirs capacity. By the way the converse is not verified all the times; there are many situation where even if the reservoirs level is extremely low or almost at its maximum, we do not witness to a similar strong divergence between futures and spot prices. As an example figure (5.3) shows the basis for the futures with 4 weeks to maturity, but basically the same behaviour may be observed for all the available time to maturity.

Similar considerations indeed, have leaded Gjolberg and Johnsen (2001) to advocate the presence, even in the electricity market, of a convenience yield induced by the water reservoir levels. In short, when the water level is low, the cost of additional 'water storing' (i.e. to not increase the spot supply) is zero. The construction of reservoirs requires very large investments, but once the reservoir is built, the marginal cost of water storage is zero as long as the reservoir capacity is not fully utilized. Conse-

quently the convenience yield is high: to maintain a good level of reservoir filling assure several benefits to the producers like potential profits from temporary shortages, ability to keep the production process running, avoiding penalty for production interruptions. As soon as the reservoir is full, additional inflow is lost trough overflow, making the marginal opportunity cost jumping from zero to the value lost for not having produced electricity with the overflowing water. The convenience yield results obviously to be zero or even negative in the case of concern of excess supply. The reasoning is perfectly in line with the interpretation that the convenience yield reflects the market expectations concerning the future availability of the commodity, in this case of the water to produce it.

A closer look to figure (5.3) suggests once again that a deep change in the relation between the reservoirs level and the futures-spot basis has taken place: if across the first part of the available sample (1995-2000) the positive relation is evident, supported even by a mild seasonality of the relative basis, from 2001 onward, the correlation between the two variables is drastically reduced. The regression analysis clearly shows the measure of this different attitude across time.

	Sep-95/Dec-00	**Jan-01/Sep-05**	**Full sample**
Obs	59	57	116
α	-21 (-4.83)	-5.85 (-1.51)	-34.5 (-4.67)
β	0.6 (5.52)	0.12 (1.94)	0.39 (5.77)
R^2_{adj}	0.35	0.003	0.22
$DW^{\dagger}$	2.2	1.92	2.08
Lilliefors‡	0	1	1

† ‡ Same confidence levels and considerations as in table (5.1).

Table 5.2: Relative Futures basis versus reservoirs level regression outcome. 4 weeks to maturity time horizon.

In order to avoid serial correlation we take only one observation each month and then we estimate a linear relationship of the relative basis versus the reservoirs level.

$$\frac{F_t(T) - P_t}{P_t} = \alpha + \beta R_t + \varepsilon_t \qquad \text{where} \quad T - t = 4\text{weeks}$$

This results to be positive and statistically significant throughout the sample, even if from 2001 the reservoirs level were able to explain just a 2% (R-square) of the observed

variation of the basis, resulting, de facto, uncorrelated. The big gap between the two subsample cannot be a chance and clearly denote a structural change. It seems that from a certain moment onward the market has started to embed the information about reservoir capacity in the price formation and price expectation mechanism, denoting an upgrading in terms of efficiency.

5.2 The future risk premium

Futures contracts are growing in importance as both financial risk management tools for hedgers as well as liquid investment vehicles for electricity trading firms. In order to efficiently use these instruments, it is important for the power industry to gain knowledge about the hidden information in the futures term structure.
We know from the theory that under the risk-neutral pricing measure $\mathcal{Q}$, the expected rate of change in the futures price is zero, as the futures price is a $\mathcal{Q}$-martingale process. Under the objective measure $\mathcal{P}$, however, this expected return may be different from zero and may provide us with preliminary insights regarding the existence and the nature of the futures risk premium. Let us define the observed expected return δ like

$$\delta(\tau) = \mathbb{E}^{\mathcal{P}}\left[\frac{F(t,T) - F(t-1,T)}{F(t-1,T)} \quad |\mathcal{F}_{t-1}\right] \quad \text{where} \quad \tau = T - t \tag{5.7}$$

As a proxy of $\mathbb{E}^{\mathcal{P}}[F(t,T)|\mathcal{F}_{t-1}]$, we can take its ex-post realization. In figure (5.4) we plot the estimated $\hat{\delta}(\tau) = (F(t,T) - F(t-1,T))/(F(t-1,T))$ and we find strong evidence (the p-value is equal to 0.0015) against the null hypothesis that $\hat{\delta} = 0$.

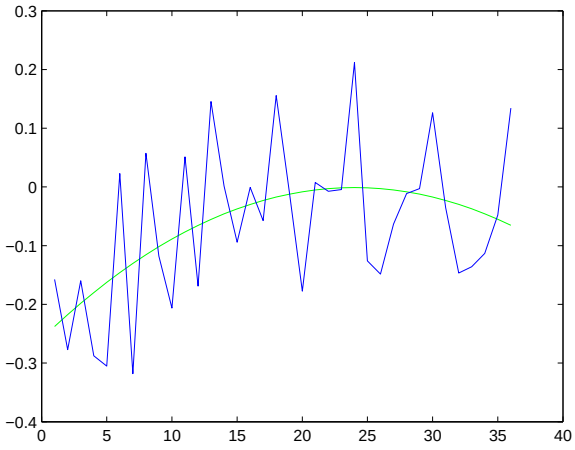

Figure 5.4: The blue line represents the estimated futures daily return $\hat{\delta}$ as a function of the time to maturity expressed in days; the green smooth line is the corresponding second order polynomial fit.

The first observation is that we find an expected return that is negative in mean across all the available time to maturity (see figure 5.4). This preliminary empirical

result suggests the classical contango market equilibrium, characterized by futures prices which exceed the expected future spot prices. To verify this we estimate the spread between the futures prices and the expected spot prices during the settlement week and in figure (5.5) we plot a cross-sectional mean of this spread as a function of the time to maturity.

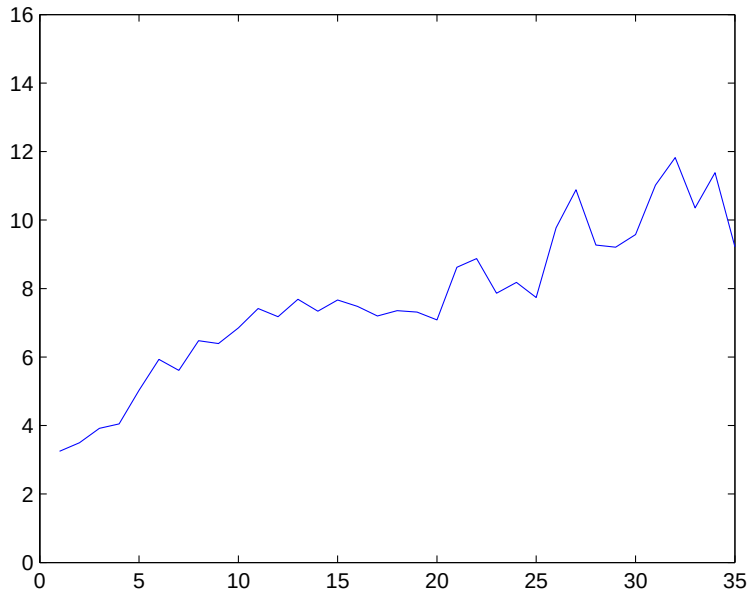

Figure 5.5: Estimate of the spread between futures and expected spot at delivery versus time to maturity.

The observed negative futures returns suggest the existence of a negative risk premium. An easy way to verify the supposed negativeness of the risk premium is to estimate the risk premium as the needed adjustment to the expectation, under the physical measure, of the spot price at maturity in order to match the futures prices , which are supposed to be simply the expectation of the future spot prices at maturity, but under the $\mathcal{Q}$ measure. Assuming that

$$F(t,T) = \mathbb{E}^{\mathcal{P}}[P_T|\mathcal{F}_t]e^{-p(\tau)} \quad \text{where} \quad \tau = T - t \tag{5.8}$$

the premium p may be estimated using again the spot ex-post realization at the maturity.

$$p(\tau) = log\frac{\mathbb{E}^{\mathcal{P}}[P_T|\mathcal{F}_t]}{F(t,T)} \quad \text{and} \quad \hat{p}(\tau) = log\frac{P_T}{F(t,T)} \tag{5.9}$$

Given the $\hat{\delta}$ values estimated in figure (5.4) we expect to find at least a decreasing $\hat{p}$ as a function of the time to maturity. The figure below confirms the intuition.

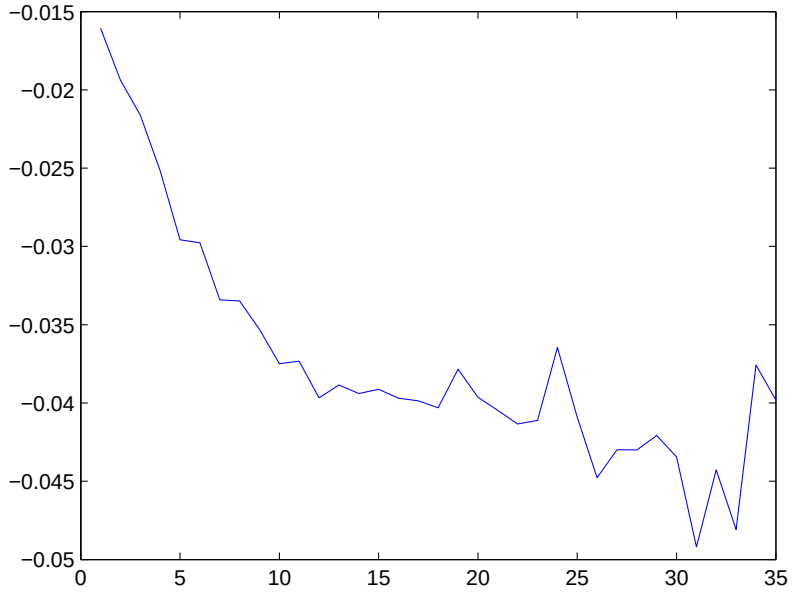

Figure 5.6: $\hat{p}$ plot as a function of the time to maturity expressed in days.

Once again a negative estimate of $\hat{p}$ indicates futures quotations that exceed the expectation, under the physical measure $\mathcal{P}$, of the future spot prices at maturity. A reason for this evidence may be found in the conditions within the specific commodity market. A risk premium could arise if either the hedging demand on the supply side differs substantially from the demand side, or if the degree of risk aversion varies substantially between the two sides. For example an overweight of a risk averse demand with respect to the producers side, may lead to a negative risk premium $\hat{p}$, or let us better say a discount for risk. The key explanation may be the consistent asymmetry in the flexibility of adjusting the quantity between the two sides. If generators may adjust the production on a very short notice, the demand side may vary its load needs very little and consequently hardly profit from the price fluctuations. So it is reasonable for the buyers to lock as much as possible of the expected futures demand

(given that buyers are risk averse)using the futures market. This is a peculiarity of the electricity market, that may lead to an excess hedging demand in the futures market. In order to further analyse the behaviour of the premia across the year, in figure (5.7) we disentangle the effects month by month.

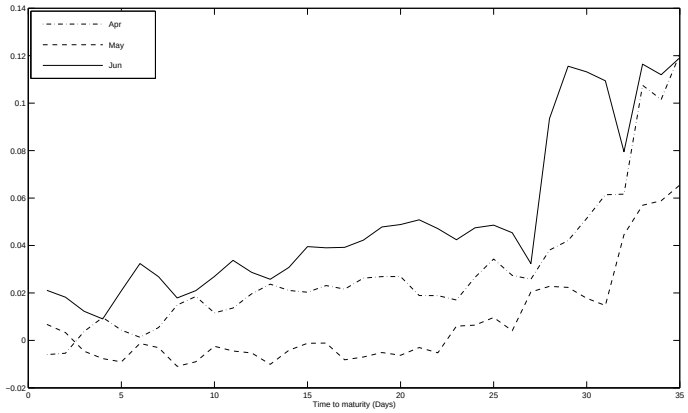

(a)

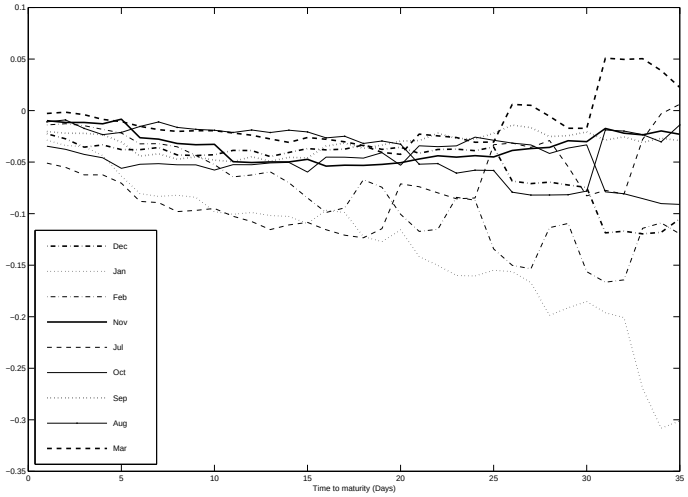

(b)

Figure 5.7: Estimated futures risk premium per month. Panel (a) refers to months with positive premia prevailing and panel (b) to the negative.

A seasonal pattern is indeed evident. Even if the majority of the year is characterized by a negative premium , more or less pronounced, during spring months we detect significant positive premia. The classical backwardation equilibrium is verified, where

hedgers go short and speculators, who require a premium, go long. The very low consumption and low demand risk characterize this period of the year; furthermore the snow melting reduces the producers' flexibility who, in order to hedge their production, accept to fix a future selling price under the expectations. Let us suppose the premium to be a linear function of the time to maturity, $p(\tau) := q\tau$, an estimate of the daily premium q is plotted in figure (5.8).

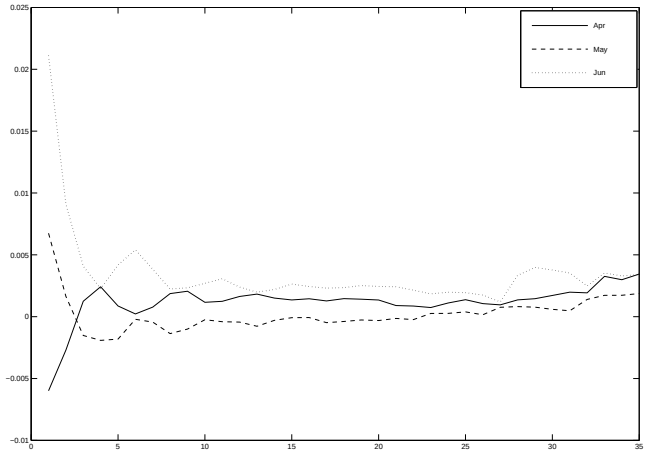

(a)

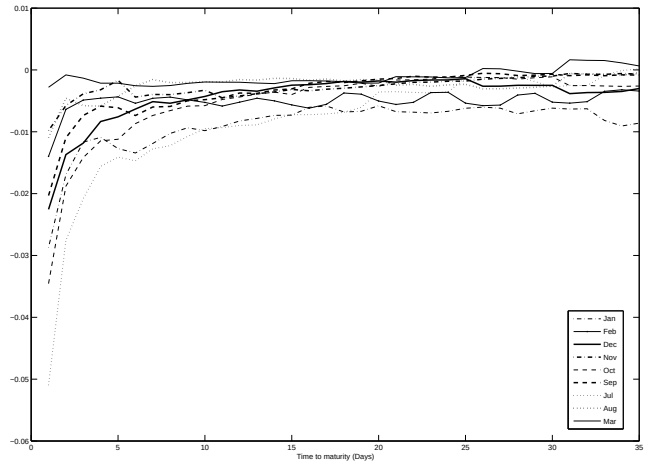

(b)

Figure 5.8: Daily contribution to the estimated futures risk premium. Panel (a) refers to months with positive premia prevailing and panel (b) to the negative.

This daily premium seams indeed to be almost a constant across time to maturity supporting the linearity hypothesis. An estimate of the daily percentage premium follows.

Jan	Feb	Mar	Apr	May	Jun	Jul	Aug	Sep	Oct	Nov	Dec
-0,888	-0,508	-0,117	0,119	0,020	0,349	-0,834	-0,249	-0,345	-0,526	-0,276	-0,441

For each month of the year, a typical value is so detected, but the premium results still time varying across the year. If we observe the evolution of the reservoir levels across the year compared with the premium q above defined, a negative correlation ($\rho = -0.5$) between the two variables is quite evident, figure (5.9).

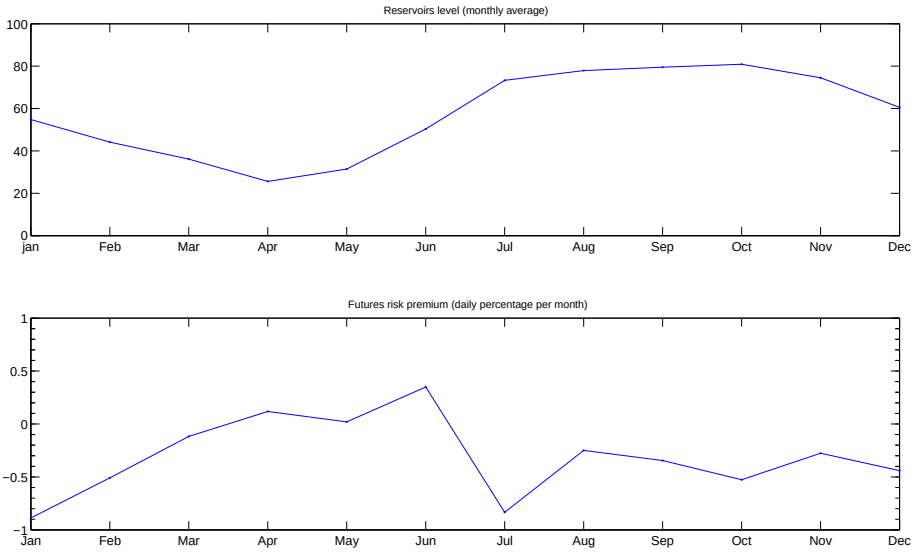

Figure 5.9: Average reservoirs level across all the data sample (above); average daily premia for all the available contracts (below).

To further investigate the correlation, and hence the explicatory power of the reservoirs level with respect to the futures risk premia, it would be interesting to regress for each futures contract the time series of the related premia versus the time series of the reservoirs level as the maturity approaches. Unfortunately, because of the contracts specifications, we are not supplied with time series of statistically relevant length. On one side, we remember that each futures contract is available for trading for no more than 8 weeks, that is a maximum of 40 daily observations, on the other side we are provided with only one observation a week for the the reservoirs

levels, generating time series of eight observations each. Nevertheless, just to have an idea, even if perfectly conscious of the statistical poorness of the exercise, we perform the aforementioned independent regressions. We select, out of the full sample of available futures contracts, 120 contracts with a recorded trading period of eight weeks. We disregard the regressions which produce autocorrelated and non normally distributed residuals according respectively to the Durbin-Watson and the Lilliefors[1] tests; finally we end up with 86 significant regressions. The slope of the estimated premia-reservoirs relation in the 60% of the cases is positive with an average value of 0.0188, in the remaining cases the average slope is -0.0186. The average R-square detected is of 65% , but with a 47% largely over 70%.

By the analysis conducted so far, we have been able to observe the evolution of the futures risk premium up to a maximum of 35 days to maturity. In order to investigate a longer term behaviour we need to look at the forward market. Once we assume no significant correlation between the electricity prices and the interest rates evolution, we can consider equivalently the two markets. As for the futures contracts, the forwards market is in a transition phase. The old Season contracts Winter 1 (January-April), Summer (May-September) and Winter 2 (October-December), with a delivery period respectively of four, five and three months, are substituted by the new Quarters contracts: four contracts each year, with equal delivery period of three months each and a trading period spanning from two year for the first quarter up to 33 months for the last one. Moreover a completely new forward contract is introduced in 2003, the Month one, this contract issued one for each month of the year, in which the delivery takes place, is traded up to six months in advance. Finally Year contracts are issued up to three years in advance.

Unfortunately, due to the relatively recent market (the forward financial market starts in October 1997) in conjunction with the longer trading period with respect to the futures contracts, we are provided with thin samples, which prevent us from reaching strong conclusions. We have 24 Month and 23 Season forward contracts with ended delivery and only 4 year contracts. Obviously disregarding the Year contracts we try to retrieve at least a tendency behaviour from the Month and the Season contracts price series.

Keeping in mind the average reservoir cycle of figure (5.9), what emerges from figure (5.10), is that the clear negative premium tendency observed in the forward market

[1]The significance level is been set to $\alpha = 5\%$

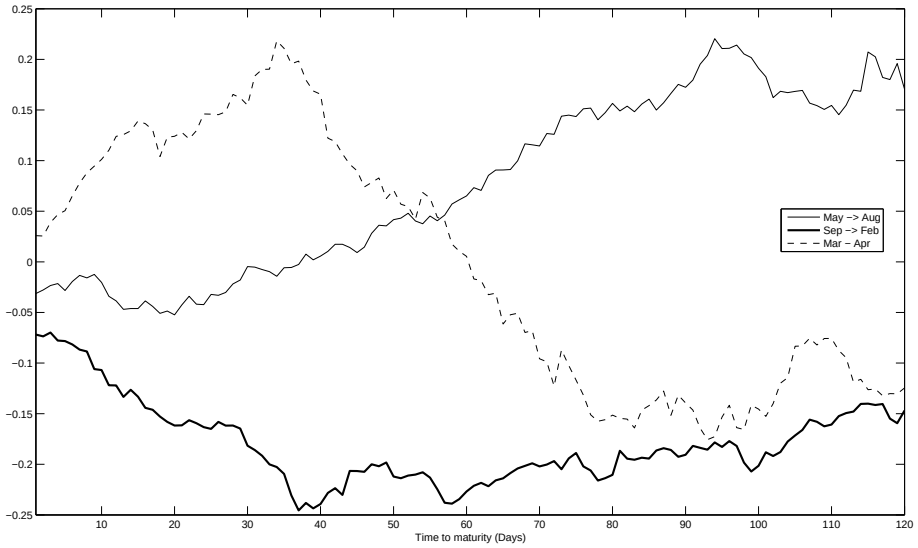

Figure 5.10: Forward risk premium for the Forward Month contracts.

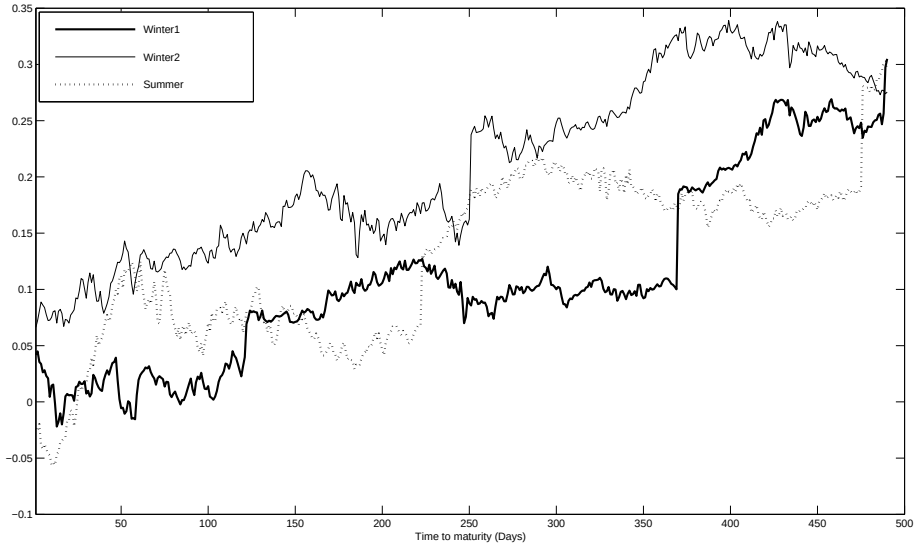

Figure 5.11: Forward risk premium for the Forward Season contracts.

from September to February has to be explained with the usual seasonal decrease of the reservoirs level in conjunction with the high winter consumption demand. From May to August instead, even if we observed a negative premium for short time

to maturity, the trend is of an increasing and positive premium. The water level even if quite low at the beginning is expected to increase together with the natural consumption decrease experienced during the summer in the northern Europe. Hence the producers are inclined to accept a forward price even below the expected future spot quotation (positive premium). The March and April behaviour instead, looks quite weird at first glance: a clear inversion of the premium sign is observed as long as the time to maturity increase. What we can observe is that these are probably crucial and difficult months, in the sense that the usual reservoirs level is very low, the minimum of the year, and the consumption is hardly predictable and may vary a lot depending on weather variations. A mild spring for instance, may influence a lot the electricity demand, making it decreasing and may increase instead the water inflows anticipating the seasonal snow melting or the rain season. On the other way round, a severe and prolonged cold winter may boost up the demand, which has to be faced with the lowest availability of water of the year. Finally in figure (5.11) the three season contracts are plotted. Stressing once again the sample thinness, they show a clear positive premium with relative few exceptions for the Winter and the Summer contracts close to the maturity.

5.3 A reservoirs based model for the Futures prices

The market data analysis conducted so far puts clearly in evidence that the peculiarity of the hydroelectric production strongly influences the price formation mechanism to such an extent that a specific model for electricity futures price has to be taken into consideration. Availability of water is the only way to produce electricity as no other storage is feasible, hence reservoirs level is a key variable to understand this market and the behaviour of the producers. Water is a scarce resource, that has to be optimally allocated. To sell a futures contract, the needed water to produce the underlining supply of electricity, has to be already available in the reservoirs. If it is not so, it means that it's betting on a future water inflow. There is no way to go on the market and buy the water as we would have done for any other financial asset, storable commodities or electricity produced with resources easier to transport and/or easier to recruit.

Water inflows obviously are a variable with a very strong seasonality as figure (5.12) puts in evidence. Even if each year it denotes huge variations in absolute value, the

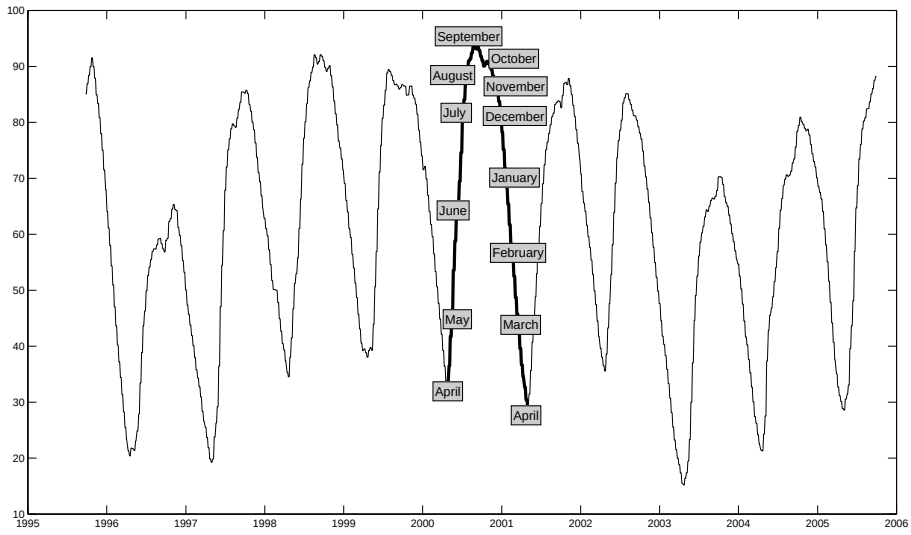

Figure 5.12: Percentage level of the overall reservoirs belonging to the Nord Pool area spanning from 1995 to 2006

tendency is always predictable: a minimum in April, after the high winter consumption, then the spring rain and the following snow melting, as the temperature becomes milder and milder, refill the almost empty reservoirs, bringing the water level at its utmost after the summer season. This means that afterwards, no significantly water inflows are expected and that, the amount of available water is fixed up to the new spring; this water hence, has to be optimally distributed between the spot and the futures market as the intrinsic time dilation of the futures market doesn't bring the usual advantage from a supply point of view.

Reasoning in this direction, the electricity producers result to be natural owners of an American call option on each unit of water, that is to be precise, on the electricity amount producible with such unit of water. The strike price of the option is zero, as they already own the water. The time horizon of the option is given by the aforementioned water cycle: each April let us say, a cycle ends and hence an option comes to maturity and a new one starts. So, the option's maturity is fixed and it is only one every year. Therefore, the time horizon of the American option changes time by time according to the period of the year in which the futures is issued. So, according to the suggested pricing equation, the time horizon of the American option involved, may span from one year to few weeks.

The reason why this optimal water allocation is so important in the hydroelectric market is essentially because of the spike possibility. The future occurrence of a positive spike in the spot market, would represent a unique opportunity for the producers to make an extra profit: the same electricity that in the previous week was economically profitable to supply at a given price, now the spot market is willing to pay, let us say, a double price. This represent for the producers a unique chance that they have to be able to exploit, without running the risk to have their hands tied because they are too much exposed on the futures market and do not have enough available water to profit from the spot market. The issuing of a futures contract will be convenient for the producers only at a price which maximize the expected return of the needed unit of water from the issuing date up to the beginning of a new water cycle. Let us note that, this time horizon has nothing to do with the contractual maturity of the futures itself and it is totally independent on this. It is an economic consequence due to the nature of the commodities and to its production system.

On the other hand, from equation (5.4) we have inferred that the futures contract in the Nord Pool, because of its contractual specifications, is a one week forward start Asian option with strike zero on the spot electricity price.

Now, let us define $F_T(t,S)$ the futures price observed in t with maturity S belonging to the water cycle that ends in T. Hence we have $t \leq S \leq T$. We state that the futures price is given by a linear combination of two options written on the spot electricity price: a one week Asian option and an American option. In formulas

$$F_T(t,S) := \alpha\, \mathbb{E}_t^Q \left\{ \frac{1}{7} \sum_{i=S+3}^{S+10} P_i \right\} + (1-\alpha) \sup_{\tau \in (t,T]} \mathbb{E}_t^Q \left\{ e^{-r(\tau)} P_\tau \right\} \tag{5.10}$$

So, the futures price observed in the market is the result of two different components, the contribution of which is normalized to one. The predominance of one of the two is led by the scarcity of water and by its optimal allocation. If, on one side, the futures contract is simply an Asian option and its price formation should be influenced by the expectation on the future spot price only during the settlement week, on the other side, depending on the level of the reservoirs, the water optimal allocation becomes more urgent, leading to the prevalence of the American components.

So, we expect to find abrupt changes from one component to another and not a mild transition. Obviously, there will be present mixed situations in which both the components contribute to the price formation, but they would be short period with a

very fast adjustment. This, in terms of α, means that we expect ideally, to estimate values alternatively very close to one and to zero.

Let us now estimate the proposed pricing equation (5.10) on the available futures market data. In order to simulate the underlining spot price P_t we refer to the dynamics in equation (4.8). Historical calibration is used to estimate the parameters required for the interbases regime dynamic. In order to get a parameter estimate more meaningful and coherent with the proposed pricing model, we need to estimate the interbases regime parameters, not from the entire available time series, but only from the portion of it that we recognized as generated from the supposed interbases regime price process. In order to do so, we exploit once again the R_n-WTMM algorithm. We chose as order of iteration a value of $n = 3$; this provide us with the location of the spikes for the n level chosen; we then remove from the entire spot price time series the portions in between the left- and the right- bases associated with the detected spikes. The so 'cleaned' time series has been used to calibrate the interbases regime parameters. Let us note that the empty spaces left by the removed spikes regimes, have been substituted with a simple linear interpolation, as we believe that adding more sophistication is pointless. In the following figure (5.13 and 5.14), we plot both the spot price time series, with the spike regimes removed, and the estimated long term mean θ_t as describe in equation (3.3). We decide to calibrate an annual component together with a week component, resulting in a long term mean of the form:

$$\theta_t = \bar{\theta} + \beta t + \theta_1 sin(\omega_1 t + \phi_1) + \theta_2 sin(\omega_2 t + \phi_2) \tag{5.11}$$

As the time is expressed in days counted from the beginning of the available time series, we have an angular frequency $\omega_1 = 2\pi/365$ to take account for the annual component and $\omega_2 = 2\pi/7$ for the week component. For the other parameters we have $\bar{\theta} = 60$ for the intercept, $\beta = 0.02$ for the linear trend, $\theta_1 = 55$ for the annual wave amplitude, $\phi_1 = 3.6$ for the annual phase, whereas we have $\theta_2 = -8.2$ for the week amplitude and $\phi_2 = 8.4$ for the week phase.

We then obtain a volatility of $\sigma = 0.1147$ and a speed of mean reversion of $K = 0.01$. Now we can simulate the spot price process P_t. For each futures market price available we estimate the corresponding Asian option simply by simulation. In order to determine the American component we estimate three different prices. As reference price we adopt the Monte Carlo least square method proposed by Longstaff and

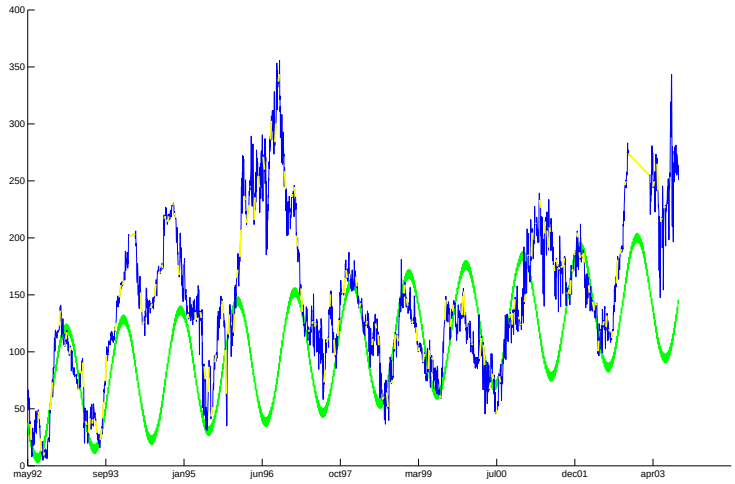

Figure 5.13: Deterministic component calibration. Long term mean θ_t, given by a linear trend plus an annual and a week seasonal component (in green) together with the spot price time series (in blue) with the spike regimes removed. The linear interpolation among the several interbases regime has been plotted in yellow.

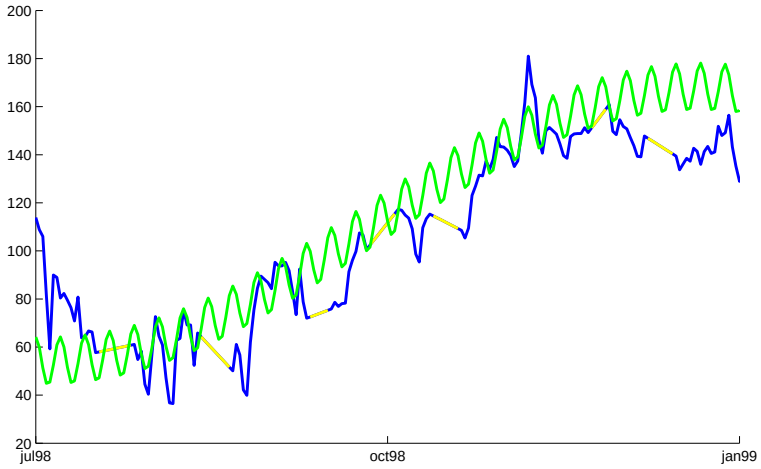

Figure 5.14: Same of figure(5.13), zoomed as indicated, so as to better appreciate the contribution of the week component.

Schwartz combined with the double independent bootstrap as illustrated in the previous chapter. With little computational effort, we then calculate as well an upper and a lower bound to the American price. To determine the lower bound we follow

this strategy: in order to price an American option the key point is to determine the optimal stopping time, to this end as soon as we encounter a spike we exercise the option otherwise we wait up to the maturity as it was an European option. The rationale is that being the American option a call one, we want to exercise at the maximum price; if we encounter a spike is sensible to bet that in the remaining life of the option we cannot expect to find a more favourable situation. If no spike , that is no extreme high values[2], is encountered it is always more convenient to wait up to the final maturity. This is a simple and very sensible strategy which however risks to underestimate all those situations where there are not evident spikes occurrences; the decision so, to wait until the final maturity, might imply the loss of intermediate good occasions. Furthermore, the lower bound strategy is not expected to perform very well during period of market turbulence, as the first spike may not be the largest. As upper bound we choose the maximum ex post, that is we simulate all the trajectories up to the maturity of the option and then, knowing the history, we simply exercise when the highest spot value is reached.

Let us analyse now, in more details, the performance of the proposed futures pricing model. In the sequel we plot several graphs of the futures term structure together with the two components and other involved variables in order to focus on the economic implications of the pricing model. But, before going ahead, a mention has to be done regarding the way the futures term structure has been drawn. Because of the Nord Pool futures market specifications, we never have more than 8 and less than 4 different futures contracts contemporarily quoted; henceforth with a time horizon spanning over ten years, the representation of the term structure as a surface, would be ineffective, as it would result too squeezed, looking like a line and not like a surface. So, as in this section we are focusing on the performance of the pricing model and not on the eventual interpretation of the shape of term structure, we decide to plot it in an unconventional way, that is with all the quotations in a row, ending up with a simple line. This is the reason why, in the following figures, the term structure appears to be a one-dimensional object.

In figure (5.15) we show the simulation results of the entire futures term structure only for the American component, that is we plot the lower and the upper bound together with the Monte Carlo least square pricing. As expected, the bootstrapped

[2]The definition of what is an high value is crucial of course

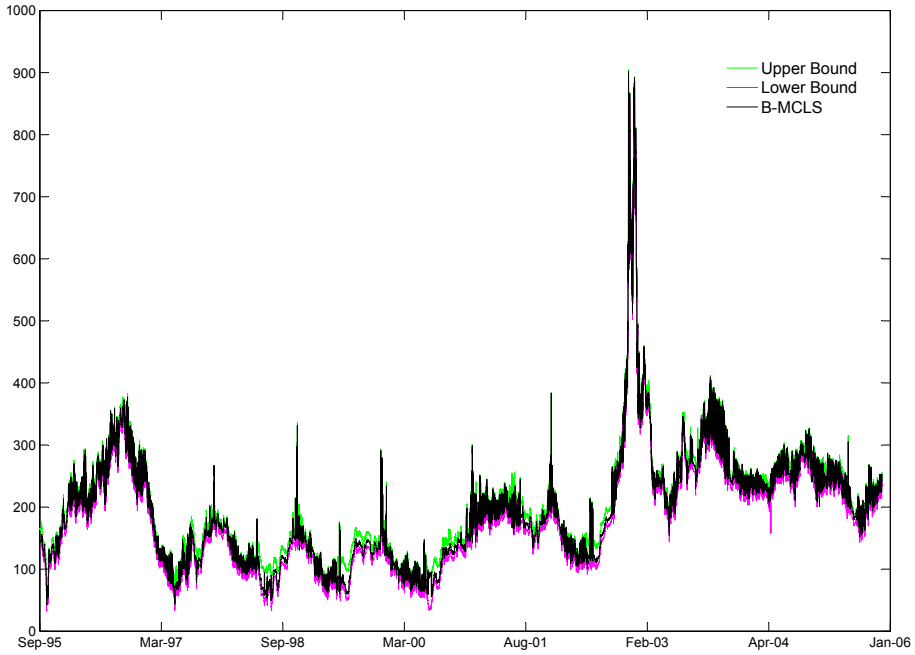

Figure 5.15: American component pricing. B-MCLS estimate together with the lower and the upper bound.

Longstaff and Schwartz price always lays in between the two mentioned bounds, generally much closer to the upper bound that to the lower, even if sometimes the reverse is also true. We cannot expect, of course, a perfect performance from these two easy bounds. On average, the width of the band, traced by the two bounds with respect to the corresponding Longstaff and Schwartz price level, is around the 15% even if in almost the 40% of the cases, the band width is under the 8%. The corresponding histogram follows in figure (5.16).

Let us now analyse the performance of the two bounds separately. Let us take the Longstaff and Schwartz price (from now on the B-MCLS price) as the reference price, and let us calculate the distance in relative price terms of the two bounds with respect to such a price. In figure (5.17) we plot indeed, the histogram of this distance for the two bounds. At a first sight, we observe a huge dispersion of the lower bound with respect to the upper bound. The latter indeed, denotes a values' range which spans from 1% to 22% in contrast to a maximum value of almost 81% of deviation of the lower bound. This huge dispersion anyway, is not so relevant in frequency terms and is more than compensated by the high concentration of very small values: more than 50% of the occurrences is indeed, under the 4% deviation from the B-MCLS

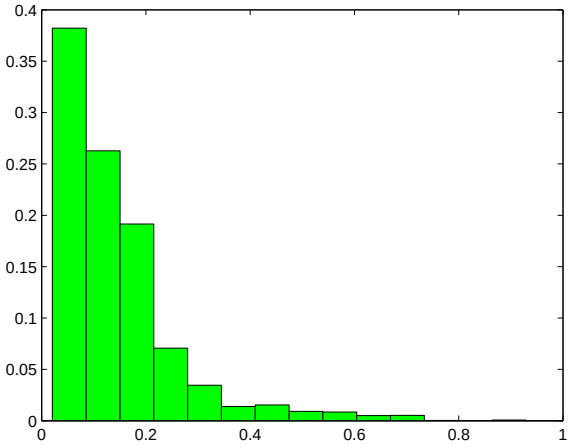

Figure 5.16: Histogram of the relative width of the upper-lower bound band with respect to the corresponding B-MCLS price. The y-axis indicates the relative quote for each bin

price and more than 70% is under the 8% deviation. What we wonder is, if it exists some relation between the reservoirs level and the major or minor closeness of the upper bound estimates to the B-MCLS, and what we find out is that for deviations grater than 16% the reservoirs are mainly (89% of the cases) over the 70% level. This seams to suggest that the lower bound may work worse with reservoirs almost full. On the other hand the upper bound shows the bigger deviation from the B-MCLS with reservoirs mostly empty: in 90% of the cases, deviations larger than 15% happen with reservoirs below 30% of level of fulfillment. Because of its definition, the upper bound efficiency has to be interpreted on the other way round, that is, as it represents the ex-post optimal stopping strategy, its deviation from the B-MCLS price gives us insight about the performance of the B-MCLS price itself. So the bottom line is that the modified Longstaff and Schwartz procedure risks to underestimate the future revenues, with very low reservoirs levels.

With this consideration in minds, from now onwards, let us adopt the B-MCLS price as the reference price for the American option component.

In figure (5.18), we plot the same simulated term structure of figure (5.15), focusing on the two price components: the Asian and the American one. Plotting together the two components, it is evident that the Asian is always smaller than the American one. This is not surprising as we are comparing an option on the average (the Asian)

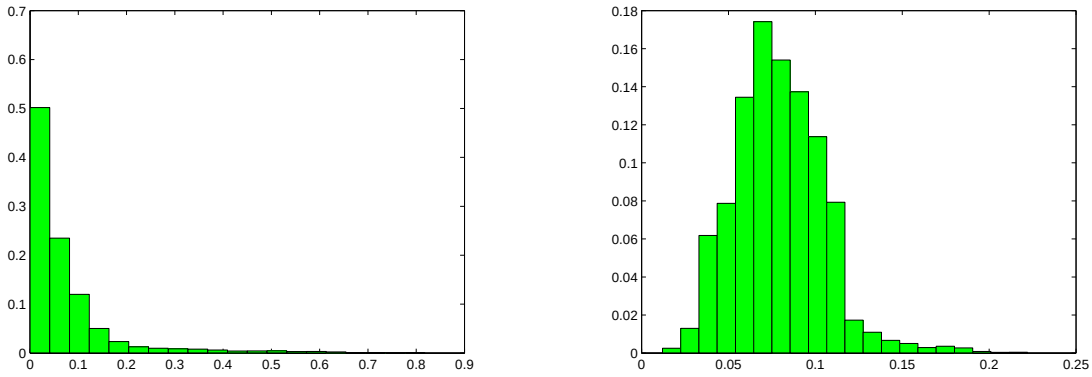

(a) Lower Bound

(b) Upper Bound

Figure 5.17: Histogram of the discrepancy of the two bounds with respect to the B-MCLS price. The y-axis indicates the relative quote for each bin

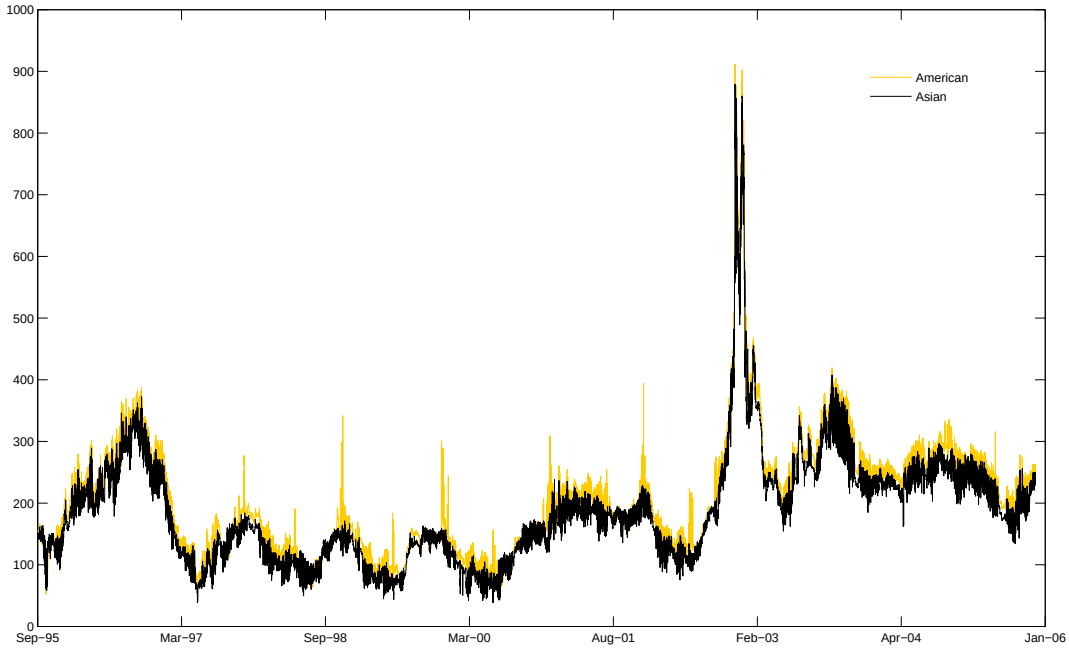

Figure 5.18: Two components

with an option on the supremum (the American), even if not strictly obvious, as the American and the Asian options in hand are not written on the same underlying, at least from a time point of view. On one side we have a one week Asian option and on the other side we have an American option with a life spanning from one year to few weeks.

Hence in figure (5.19), we finally compare the simulated model pricing components

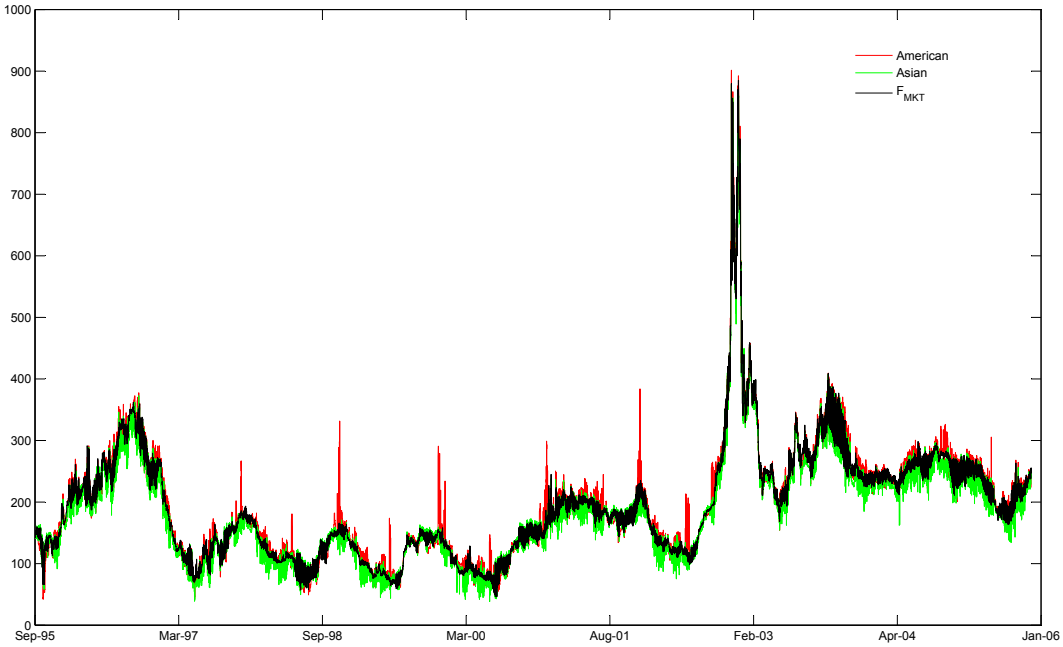

Figure 5.19: Two components and Futures market

with the observed market futures prices. In figure (5.20) the reservoirs level series is added in the background. The reservoir percentage level is multiplied by a factor 10 in order to make the time series comparable and the graph readable.

It is interesting to note that it is during decreasing reservoir level periods, or in any case for low reservoir levels, that the American component futures price estimation, reaches the highest values. This suggests that when the water is perceived as scarce, at a low level, the American option held by the electricity producers becomes more and more valuable.

The plots observed so far, give us just the flavour of the role played by the two components in the overall pricing model. We can clearly deduce that both the components follow the trend and the ups and downs of the observed market price, but that none of the two alone is sufficiently close to the market price.

As implied by the pricing equation (5.10), to understand in more details the role of the two components, the parameter α is crucial. For each available futures price an α is estimated as function of the specific time to maturity of the futures contract in hand, and of the observed reservoir level at those date. In figure (5.21) the entire surface of the α values is shown.

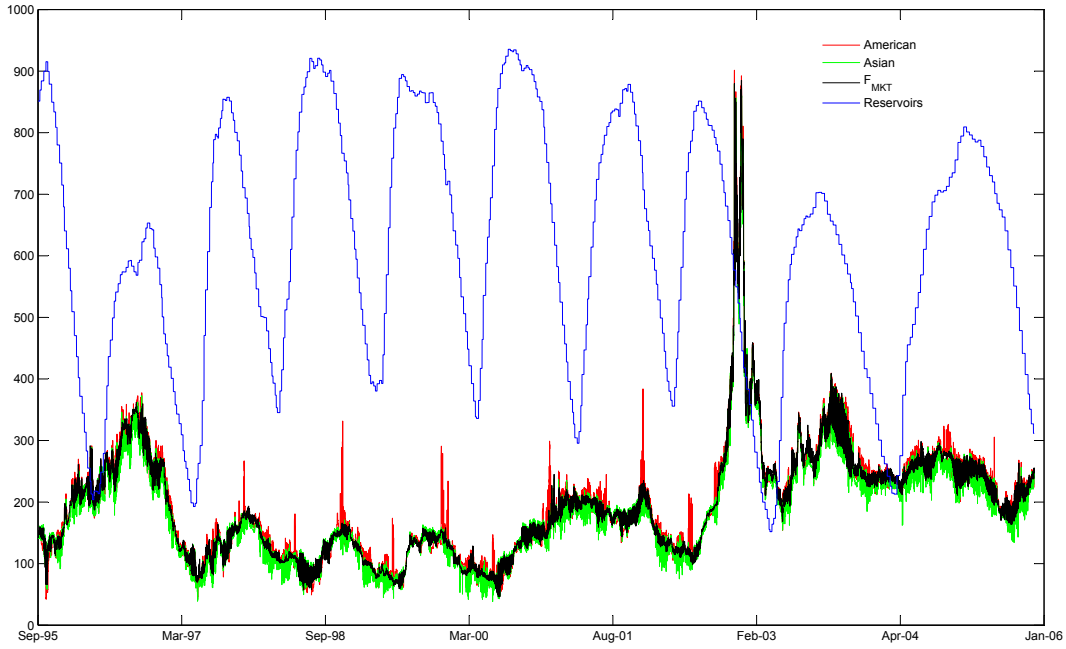

Figure 5.20: The two components, Futures market price and Reservoirs level.

At a first glance the behaviour of α appears quite smooth and clear at least in function of the reservoir level: very high α values for full reservoir and very low α for reservoir almost empty. Reminding the meaning of α assigned in equation (5.10), it means we have a strong predominance of the American component over the Asian one when the reservoir are low, whereas the American component becomes almost negligible when the water is plentiful. This behaviour moreover, seems to be preserved and not significantly modified, through the life of the futures contracts, that is across the several values of the time to maturity. Hence, averaging across the time to maturity we plot the estimated α just as a function of the reservoir level. The result is shown in figure (5.22) where the reservoirs level is expressed by an integer $n \in [0, 10]$, where for $n = i$ it means that the observed percentage of fulfillment may span from $(i \cdot 10)\%$ included, to $(i + 1) \cdot 10\%$ excluded. The resulting logistic type shape is perfectly in line with what we have predicted, that is a predominance of extreme values, ranging from zero to one, with a sharp transition in between.

Ideally, taking to the extreme the implication of the proposed futures pricing model, we might have desired to observe a step-like function taking just the value 0 and 1 with a discontinuity for a precise value of reservoir level which would have represented a kind of break-even point of the hydroelectric futures market. The fact that we

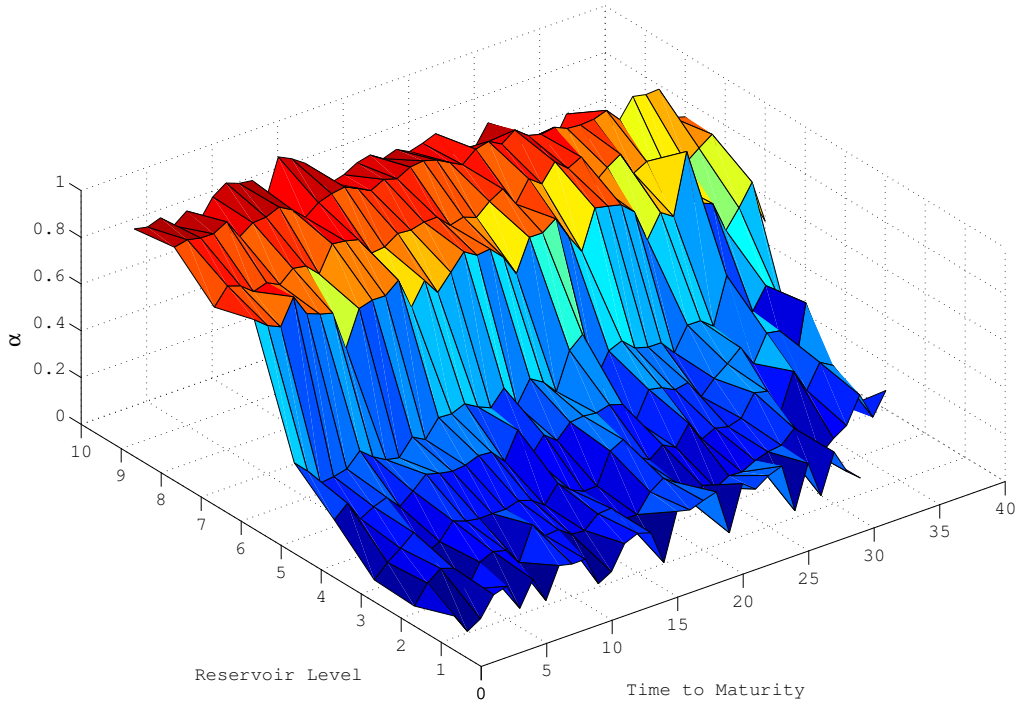

Figure 5.21: α surface as function of the futures time to maturity expressed in days and of the reservoir level.

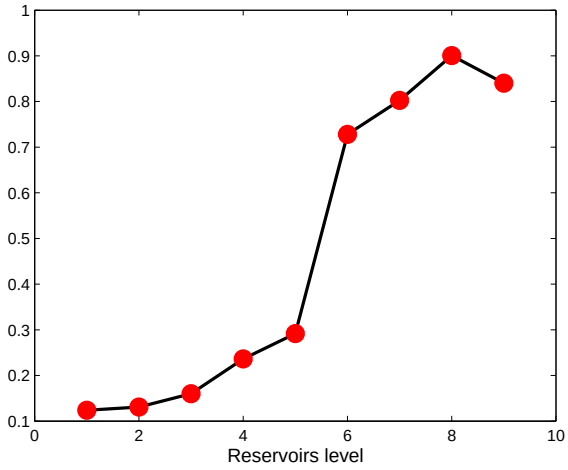

Figure 5.22: Average α across the futures time to maturity in function of the reservoir level.

have estimated a milder transition from one component to the other is anyway quite reasonable; we can think of a critical reservoir level that may slightly change time by time depending on several external condition implying a smoother transition when we try to estimate this value. For reservoirs level up to 40% excluded we observe an α value almost negligible ,just above 0.1, but from 40% to 60% excluded, we observe a slight increase even if the real jump is observed after the 60% where the α estimation suddenly jumps from 0.3 to 0.74; for higher reservoirs level a consolidation of the Asian component is reached with an increasing value of the estimated α up to 0.92.

Coming back to the α surface of figure (5.21), the time to maturity influence is less strong and evident with respect to the reservoirs level. Nevertheless some considerations may be outlined. To better disentangle the effects of the time to maturity we plot, separately, the α as a function of the time to maturity for each given level of reservoirs. Looking through the panels of figure (5.23) we observe at glance, an inversion of the sign of the estimated relationship: up to a 60% of the reservoirs level the data seems to exhibit a positive correlation of the estimated α with the time to maturity length, in terms that, *ceteris paribus*, the longer the time horizon of the futures contracts, the stronger the Asian component is, in the futures price formation. From a strategic point of view, this is quite reasonable: the further is the futures maturity, the less strong is the pressure for the producer regarding the water's unit allocation, hence it is sensible to estimate a weaker concern regarding the optimization over the entire water cycle; maybe some moderate water inflows may still happen. This situation seems to persist up to a certain point: when the reservoirs level is high, the data support exactly the opposite situation and the α value becomes a decreasing function of the time to maturity. This structural change appears less straightforward to interpret. Anyway, it is relevant to underline that there seems to be a connection between the predominance of the Asian component to the futures price formation, and the negative correlation of α and time to maturity. The turning point in both of the cases is represented by the level 6 of the reservoirs. So, summarizing, when futures are close to maturity if there is plenty of water the Asian component is the leading contribution to price formation whereas, if there is little water in the reservoirs the need to optimally allocate the available water overwhelms other considerations. When the maturity date of the contract in hand is further, this shift ahead of the due date, seems to have the effect to mitigate the situation, giving more weight to the non-leading component. In other words, a grater importance is

given to the hypothetical events that may happen during this time horizon. Relevant events may be spikes, chance of overflow and the risk to face a decreasing demand, for instance. This attitude of the data confirms even more the idea the futures price formation in this market is two-folds, fully supporting equation (5.10).

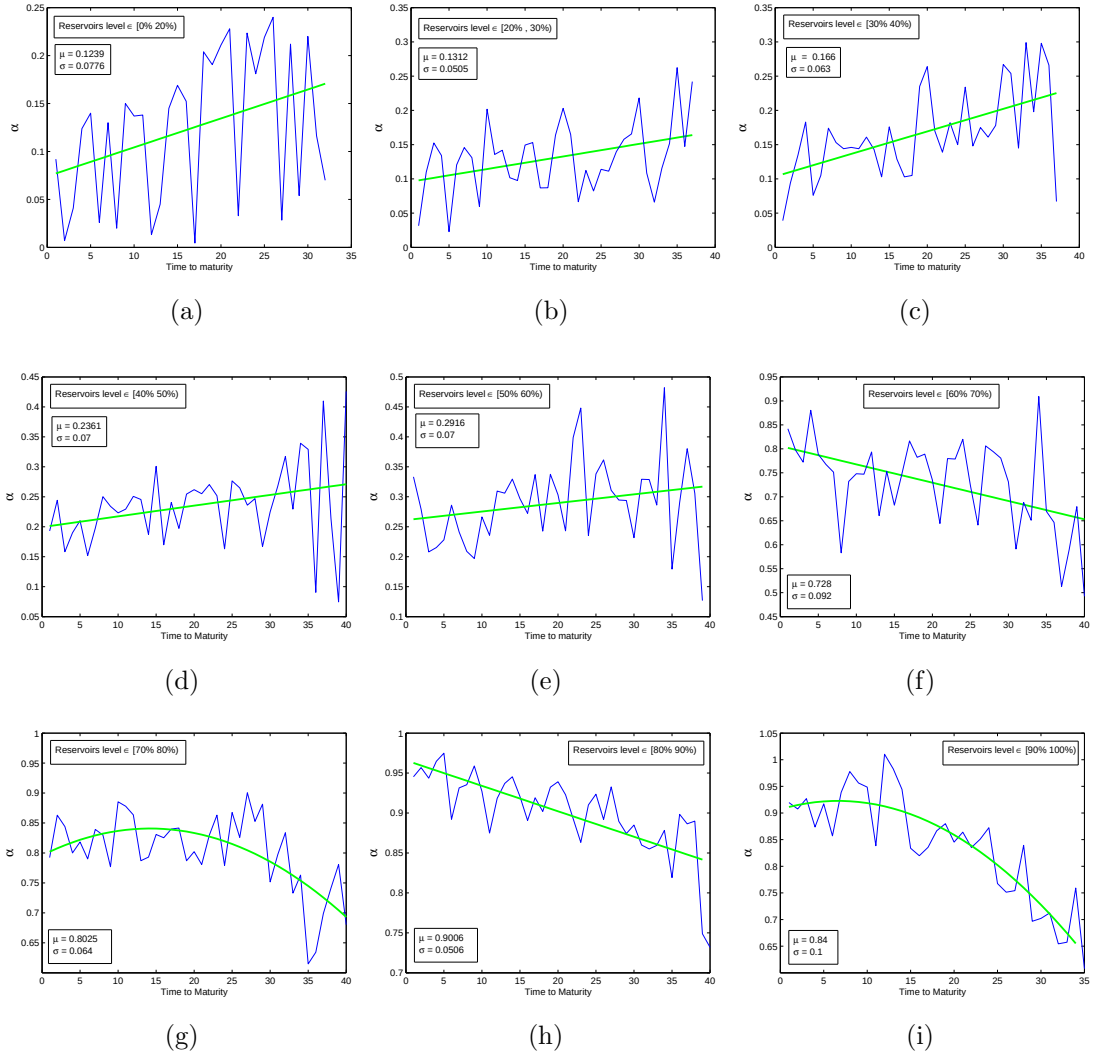

Figure 5.23: α estimate for fixed level of reservoirs as function of the time to maturity expressed in days.

Assuming the proposed pricing model for the futures contract is satisfying, we wonder which implications may have. Maybe the strongest consequence is about the contractual specification of the futures. If it is true that the market futures price takes into account also an optimization of the available water over the entire reservoirs cycle,

the natural conclusion is that a futures contract in the Nord Pool is too expensive for what it offers. The typical week-futures contract enables to fix the electricity spot price during a well-defined week, say a month from now. What the proposed model predicts, is that the producer and in this case the futures seller, agree to sell only at a price which optimizes his revenues over an horizon which is potentially much more longer than the one defined by the futures maturity, that is over the next six months, for instance. Hence, if the seller is selling at a price that for his forecasts is the optimum price for a week futures in the next six months, why we do not let the buyer exercises the futures whenever she prefers during the following six months? It would be more efficient to the buyer, while to the seller little would change as far as he has already optimized the price. This would mean that the strong asymmetry that we face in this market, would be rewarded by an higher degree of freedom, may choosing when to receive the electricity supply underlying the futures contract. This might be an interesting suggestion for further research. We could imagine to issue a new futures type, where $\mathcal{F}_t(\tau, S)$, with $t < S$ and $\tau \leq S - t$, would be the price at time t, of a futures contract of length τ, that is entailing an electricity supply for a period of length τ to be fixed in between t and S. S would represent the end of the water cycle inside of which the futures contract would be issued. This would be a kind of American option on electricity futures, with the crucial difference that the buyer of such a contract should exercise within the final maturity. Obviously some restriction may be thought about the exercise of the futures rights, upon a certain time notice. The issuing of a more flexible futures contract, such as the one suggested, may also provide an answer to why the futures trading in a very hydro-dependent market like the Nord Pool electricity market, is not so much widespread as expected and as observed in other commodity markets. Anyway, this is just a topic which might be worthwhile to investigate and test in further research.

Chapter 6

Conclusion

We have provided an in-depth analysis of Nord Pool electricity price. This market is the oldest and one of the largest European electricity exchange, allowing us to observe a consistently long time series.
Our main contributions are the following:

- we have defined a wavelet-based algorithm, named R_α-WTMM, to automatically detect spikes on a time series. We believe that spikes are one of the most distinguishing features of the electricity commodity, more or less frequent and pronounced in the several markets, but in any case always present. We cannot ignore them if we want to deal with electricity modelling. The starting point is to put it clearly what they are and how to detect them in an as much as possible objective way. Observing that spikes may be seen as a particular sequence of singularities, we modified the WTMM algorithm, used in signal processing to detect singularities, in order to identify only the spikes locations.

- we have proposed a spot price model which enables to reproduce the main features of the observed price trajectory as price-dependent volatility, mean reversion and spikes without adding any jump component. We have chosen a regime-switching configuration, between a diffusion and a non parametric component defined by a double bootstrap procedure. In so doing we have managed to give to the adopted model an high level of freedom in the possible trajectories shapes, although with very few parameters: both positive and negative spikes are allowed for instance, and different length and multiple spikes are

also contemplated. Moreover, thanks to the nice probabilistic properties of our bootstrap, a sensible Markovianity is preserved.

- we have applied the proposed model to the pricing of American options. We have adopted Monte Carlo techniques and starting from the established Monte Carlo Least Square procedure, we should have overcome some difficulties in order to simulate our regime-switching process. By introducing an OrnsteinUhlenbeck Brownian Bridge we manage to consistently generate continuous sample paths for the electricity price, needed to perform backward induction to evaluate American contingent claims. Further, to reduce the high memory storage required by dynamic programming, we have simulated in a backward time-moving direction the underlying process, generalizing this backward simulation technique to any random processes.

- we have provided an extensive empirical analysis of the Futures term structure in the Nord Pool markets aimed to understand the futures risk premium behaviour. We have derived a Futures pricing formula based on reservoirs optimal allocation, given the predominance of the hydropower generated electricity. We have defined each Futures contract as a linear combination of an Asian option and an American option both written on the electricity spot price. The market data support this hypothesis, suggesting interesting economic interpretations.

Appendix

MRPV process: conditional variance calculation

Given the following process

$$P_t = e^{\sigma(W_t - W_s) - \left(\frac{\sigma^2}{2}+k\right)(t-s)} \left(P_s + K\theta \int_s^t e^{-\sigma(W_u - W_s) + \left(\frac{\sigma^2}{2}+k\right)(u-s)} du \right) \tag{6.1}$$

in order to determine the second centered moment with the initial condition P_s we compute the following quantities:

$$\begin{aligned}\mathbb{E}[P_t^2|P_s] = \mathbb{E}\Bigg[& e^{2\sigma(W_t - W_s) - (\sigma^2+2k)(t-s)} P_s^2 + 2K\theta P_s \int_s^t e^{-\sigma(W_u + W_s - 2W_t) + \left(\frac{\sigma^2}{2}+k\right)(u+s-2t)} du \\ & + e^{2\sigma(W_t - W_s) - (\sigma^2+2k)(t-s)} K^2\theta^2 \int_s^t e^{-\sigma(W_u - W_s) + \left(\frac{\sigma^2}{2}+k\right)(u-s)} du \int_s^t e^{-\sigma(W_\mu - W_s) + \left(\frac{\sigma^2}{2}+k\right)(\mu-s)} d\mu \Bigg]\end{aligned} \tag{6.2}$$

Let us note that given the ordering $s < u < t$, $W_u + W_s - 2W_t = 2(W_t - W_u) + W_u - W_s$, represents the sum of two independent intervals of the Wiener process. So, computing the expectations we get

$$\begin{aligned}\mathbb{E}[P_t^2|P_s] = \; & P_s^2 e^{(\sigma^2 - 2K)(t-s)} + 2P_s K\theta e^{\sigma^2 t + K(s-2t)} \int_s^t e^{(K-\sigma^2)u} du + \\ & + \mathbb{E}\left[e^{2\sigma(W_t - W_s) - (\sigma^2+2k)(t-s)} K^2\theta^2 2! \int_s^t \int_s^u e^{-\sigma(W_u + W_\mu - 2W_s) + \left(\frac{\sigma^2}{2}+k\right)(u+\mu-2s)} d\mu du \right] \\ = \; & P_s^2 e^{(\sigma^2 - 2K)(t-s)} + 2P_s \tfrac{K\theta}{K-\sigma^2} e^{-K(t-s)} - 2P_s \tfrac{K\theta}{K-\sigma^2} e^{(\sigma^2-2K)(t-s)} + \\ & \mathbb{E}\left[K^2\theta^2 2! \int_s^t \int_s^u e^{\sigma(2W_t - W_u - W_\mu) + \left(\frac{\sigma^2}{2}+k\right)(u+\mu-2t)} d\mu du \right]\end{aligned} \tag{6.3}$$

The key substitution, widely exploited in similar context by Yor (1992), consists in splitting the domain of integration $[s,t]^2$ in 2! subdomain each of which corresponds to some particular ordering of μ and u, (the set where the two variables are equal has measure 0 and can be safely forgotten). This rearrangement of the mentioned integral has the desirable outcome of making the brownian motion intervals non more overlapping. So now, similarly substituting once again $2W_t - W_u - W_\mu = 2(W_t - W_u) + W_u - W_\mu$, as $\mu < u < t$ we can calculate the expectation left. So the last expectation in (6) is:

$$\begin{array}{l} 2K^2\theta^2 \int_s^t \int_s^u e^{2\sigma^2(t-u)+\frac{\sigma^2}{2}(u-\mu)+\left(\frac{\sigma^2}{2}+k\right)(u+\mu-2t)} d\mu du = \\ 2K^2\theta^2 \int_s^t e^{\sigma^2(t-u)+K(u-2t)} \left(\int_s^u e^{k\mu} d\mu\right) du = \\ 2K\theta^2 \left\{ \int_s^t e^{(\sigma^2-2k)(t-u)} du - \int_s^t e^{\sigma^2(t-u)+K(u+s-2t)} du \right\} = \\ \frac{2K\theta^2}{2k-\sigma^2} - \frac{2K\theta^2}{2k-\sigma^2} e^{(\sigma^2-2k)(t-s)} - \frac{2K\theta^2}{k-\sigma^2} e^{-K(t-s)} + \frac{2K\theta^2}{k-\sigma^2} e^{(\sigma^2-2k)(t-s)} \end{array} \tag{6.4}$$

Substituting this result in (6) we can calculate the conditional variance of the process P_t given P_s

$$\begin{aligned} \mathbb{V}[P_t|P_s] = & \quad \mathbb{E}[P_t^2|P_s] - \mathbb{E}^2[P_t|P_s] \\ = & \quad P_s^2 e^{(\sigma^2-2K)(t-s)} + 2P_s \tfrac{K\theta}{K-\sigma^2} e^{-K(t-s)} - 2P_s \tfrac{K\theta}{K-\sigma^2} e^{(\sigma^2-2K)(t-s)} + \\ & + \tfrac{2K\theta^2}{2k-\sigma^2} - \tfrac{2K\theta^2}{2k-\sigma^2} e^{(\sigma^2-2k)(t-s)} - \tfrac{2K\theta^2}{k-\sigma^2} e^{-K(t-s)} + \tfrac{2K\theta^2}{k-\sigma^2} e^{(\sigma^2-2k)(t-s)} + \\ & - (P_s-\theta)^2 e^{-2K(t-s)} - \theta^2 - 2\theta(P_s-\theta) e^{-K(t-s)} \\ = & \quad e^{(\sigma^2-2K)(t-s)} \left(P_s^2 - \tfrac{2\theta(P_s-\theta)}{1-\frac{\sigma^2}{K}} - \tfrac{\theta^2}{1-\frac{\sigma^2}{2K}} \right) - e^{-2k(t-s)} (P_s-\theta)^2 + e^{-k(t-s)} \tfrac{2\theta(P_s-\theta)}{\frac{K}{\sigma^2}-1} + \tfrac{\theta^2}{\frac{2K}{\sigma^2}-1} \end{aligned}$$

References

Babaud, J., Witkin, A., and Duda, R. (1983). Uniqueness of the Gaussian kernel for scale-space filtering. *IEEE Transactions on Pattern Analysis and Macjine Inteligence* PAMI-8, 26-33.
Barlow, (2002). A Diffusion Model for Electricity Prices. *Mathematical Finance*, 12, 287-298.

Barone-Adesi, G. and Gigli, A. (2003). Managing Electricity Risk. *Economic Notes*, Vol.32, No. 2, 283-294.

Barone-Adesi, G., (2005). The saga of the American put. *Journal of Banking and Finance*, Thirty Years of Continuous-Time Finance, Vol. 29, No. 11, 2909-2918.

Bessembinder, H. and Lemmon, M.L. (2002). Equilibrium Pricing and Optimal Hedging in Electricity Forward Markets. *The Journal of Finance*, 57, 1347-82.

Birnbaum, L., Del Aguila, J. M., Domnguez, G., Lekander, P., (2002). Why Electricity Markets Go Haywire? *McKinsey Quarterly*, 1.

Black, F. (1976). Studies in Stock Price Volatility Changes. American Statistical Association, Proceedings of the *Business and Economic Statistics Section*, pages 177-181.

Bony, J., (1983). Propagation et interaction des singularites pour les solutions des equations au derivees paritelles non-lineaires. Proceeding of the *Internationals congress of Mathematicians*, pp.1133-1147, Warszawa,

Brock, W.A., Dechert, W.D., Scheinkman, J., (1987). A test for independence based on the correlation dimension. Unpublished Manuscript, University of Wisconsin, Madison.

Brock, W.A., Lakonishok, J. and LeBaron, B. (1992). Simple technical trading rules and the stochastic properties of stock returns. *Journal of Finance*, 47 (5), 17311764.

Chan, R.H., Chen, Y., Yeung, K.M., (2004). A memory reduction methods in pricing American options. *Journal of Statistical Computation and Simulation*, Vol.74, No 7, 501-511.

Clment, E., Lamberton, D., Protter, P., (2002). An analysis of a least squares regression method for American option pricing. *Journal Finance and Stochastics*, Vol. 6, No. 4, 1432-1122.

Clewlow, L., Strickland, C., (2000). Energy Derivatives Pricing and Risk Management. Lacima Publications, London.

Conejo, A.J., Plazas, M.A., Espinola, R., Molina, A.B., (2005). Day-ahead electricity price forecasting using the wavelet transform and ARIMA models. *IEEE Transactions on Power Systems*, Vol.20, No.2, 1035- 1042.

Dufresne, D. (1990). The distribution of perpetuity, with applications to risk theory and pension funding. *Scand. Actuarial J.*, 39-79

Dufresne D. (2001). The Integrated Square-Root Process. Research paper 90.

Erzgrber, H., Strozzi, F., Zaldvar, J., Touchette, H., Gutirrez, E., Arrowsmith, D.,K., (2008). Time series analysis and long range correlations of Nordic spot electricity market data. *Statistical Mechanics and its Applications* Vol. 387, No. 26, 6567-6574.
Escribano, Alvaro, J. Ignacio Peaea, and Pablo Villaplana, (2002). Modelling electricity prices: International evidence.
Working paper, Universidad Carlos III de Madrid.

Ethier, R.G., Mount, T.D., (1999). Estimating the volatility of spot prices in restructured electricity markets and the implication for option values. Working Paper, Department of Applied Economics and Management, Cornell University. Ithaca, NY.

Fleten, S.E., Wallace, S.W., (1998). Power scheduling with forward contracts. Proceedings of the Nordic MPS. Molde, Norway.

Geman, H., Roncoroni, A., (2006). Understanding the fine structure of electricity prices. *The Journal of Business*, vol. 79, no. 3 , 1225-1261.

Grassberger, P., Procaccia, I., (1983). Measuring the Strangeness of Strange Attractors. *Physica D*, 9, 189-208.

Green, R.J. (2003). Electricity markets: Challenges for economic research. Proceedings of the Research Symposium on European Electricity Markets (26 September), The Hague, Netherlands.

Gjolberg, O. and T. Johnsen (2001). Electricity futures: Inventories and price relationships at Nord Pool. Discussion Paper IOR/UMB D-16/2001

Huisman R., de Jong C. (2003). Option pricing for power prices with spikes. *Energy Power Risk Management*, 7.11, 1216.

Huisman, R, Mahieu, R.J., (2003). Regime jumps in electricity prices . *Energy Economics*, Vol. 25, No. 5, 425-434.

Hummel, B. Moniot, R. (1989). Reconstruction from zero-crossings in scale-space. *IEEE Transactions on Acoustics, Speech, and Signal Processing* , Vol.37, No. 12.

Hurst, H.E., (1951). Long-term storage capacity of reservoirs. *Transactions of the American Society of Civil Engineers*, 116, 770-799.

Jaffard, S. (1991). Pointwise smoothness, 2-microlocalization and wavelet coefficients. *Publication Matemàtiques*, 35, 155168.

Johnson, B. Barz, G. (1999). Selecting stochastic process for modelling electricity prices. Energy modelling and the management of uncertainty. London, Risk Publications.

Kaminski, V. (1997). The challenge of pricing and risk managing electricity derivatives. P. Barber (Ed.) The U.S. power market: Reconstructing and risk management. 149-171. London, Risk Publications.

Kanzler, L., (1999). Very fast and correctly sized estimation of the BDS statistic. Department of Economics, University of Oxford.

Koenderinck, J.,J. (1984). The structure of images. *Biological Cybernatics*, Vol. 50, No. 5, 363-370.

Krapels, E.N. (2000). Electricity Trading and Hedging. Risk Publications.

Longstaffz, F.A., Schwartz, E.S., (2001). Valuing American options by simulation: a simple least-squares approach. *Review of Financial Studies*, Vol. 14, No. 1, 113-147.

Lucia, J.J., Schwartz, E.S., (2002). Electricity prices and power derivatives: evidence from the Nordic power exchange. *Review of Derivatives Research* 5, 550.

Lucia, J. J., and Torro, H. (2007). Short-term electricity futures prices: Evidence on the time-varying risk premium. Unpublished manuscript, University of Valencia, Spain)

Malamud, B.D., Turcotte, D.L., (1999). Self-affine time series: measures of weak and strong persistence. *Journal of Statistical Planning and Inference* Vol.80, No. 1-2, 173-196.

Mallat, S., Hwang, W.L. (1992). Singularity detection and processing with wavelets. *IEEE Transactions on Information Theory* , Vol.38, No. 2, 617-643.

Mallat, S. (1999). A Wavelet Tour of Signal Processing. Academic Press, 2nd edition.

Merton, R.C., (1976). Option pricing when underlying stock returns are discontinous. *Journal of Financial Economics* 3, 125144.

Meyer, Y., (1989). La 2-microlocalisation. Preprint

Muzy, J.F., Barcy, E., Arneodo, A. (1994). The Multifractal Formalism revisited with wavelets. *International Journal of Bifurcation and Chaos*, Vol. 4, No. 2, 245-302.

Pirrong, C. and M. Jermakyan (1999). Valuing Power and Weather Derivatves on a Mesh Using Finite Difference Methods. Energy Modelling and the Management of Uncertainty, Risk Publications.

Pirrong, C. and M. Jermakyan (2000). The Price of Power: the Valuation of Power and Weather Derivatives. WP, Olin School of Business, Washington University.

Rogers, L.C.G., Williams, D., (2000). Diffusions, Markov Processes and Martingales. Cambridge Mathematical Library, Vol. 2.

Schwartz, E., (1997). The stochastic behavior of commodity prices: implications for valuation and hedging. *Journal of Finance* 52, 923-973.

Simonsen,I., Hansen, A., Nes, O. (1998). Determination of the Hurst exponent by use of wavelet transforms. *Physical Review E* 58, 2779-2787.

Skantze, P., A. Gubina and M. Ilic (2000). Bid-based Stochastic Model for Electricity Prices: the Impact of Fundamental Drivers on Market Dynamics. Report 00-04, Energy Laboratory, MIT.

Skantze, P. and M. D. Ilic (2001). Valuation, Hedging and Speculation in Competitive Electricity Markets: a Fundamental Approach. Kluwer Academic Publishers

Struzik, Z.R., Siebes, A.P.J.M., (2002) *Physica A: Statistical Mechanics and its Applications*. Vol. 309, No. 3-4, 388-402.

Tesfatsion, L., (2006). Agent-Based Computational Economics: A Constructive Approach to Economic Theory. Handbook of computational economics. Agent-Based Computational Economics, vol. 2, 831880, North-Holland.

Vahvilinen, I., Pyykknen, T., (2005). Stochastic factor model for electricity spot price the case of the Nordic market. *Energy Economics*, Vol. 27, No. 2, 351367.

Veit, D.J., Weidlich, A., (2008). A critical survey of agent-based wholesale electricity market models. *Energy Economics*, Vol. 30, No. 4, 1728-1759.

Villaplana, P., (2003). Pricing power derivatives: A two-factor jump-diffusion approach. Working Paper 03-18, Department of Industrial Economics, University Carlos III, Madrid.

Villaplana, P., (2004). A Two-state Variables Model for Electricity Prices. Third World Congress of the Bachelier Finance Society, Chicago.

Yor, M., (1992). On Certain Exponential Functionals of Real-Valued Brownian Motion. *Journal of Applied Probability*, 29, 202-208.

Yuille, A., Poggio, T. (1986). Scaling theorems for zero-crossings. *IEEE Transactions on Pattern Analysis and Machine Intelligence*, 8.